

11.7.3 FAULT MODEL

(1) Fault Model of the Indian Ocean Earthquake and Tsunami

Firstly, the reliability of various fault models was checked by comparing them with the actual tide observation data.

Fault models of the 2004 Indian Ocean Tsunami are proposed by several organizations as shown in Table 11.7.4. The model of the Tohoku University [Tohoku Univ. (1)] is selected for this study. The parameters and outline of the Tohoku University model are shown in Table 11.7.5 and Figure 11.7.8, respectively. It has been found out that the tidal records in Sri Lanka and Maldives agreed with the model's simulation data.

Table 11.7.4 Fault Models

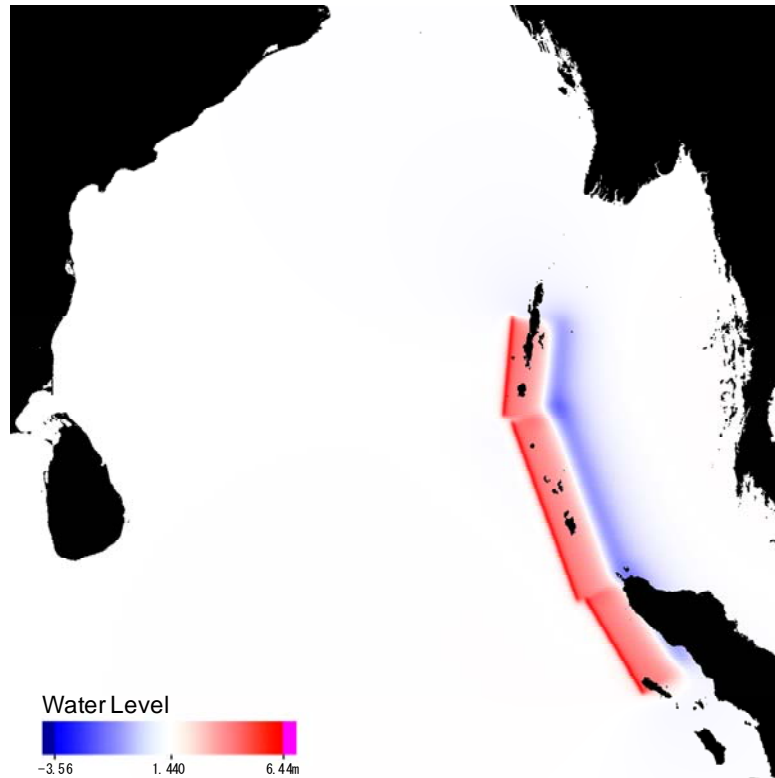
Organization	Fault Segment Numbers	Fault Slip Amount (m)	Fault Length (km)	Fault Width (km)
Tohoku Univ.(1)	3	11	1,200	150
JAMSTEC	14	0.6 ~ 29.7	1,400	150
AIST	22	0.0 ~ 24.6	2,200	100
Akita Univ.	14	8.9	980	240
Tohoku Univ.(2)	2	11	900	150
Kyoto Univ.	1	13.9	560	150

Source: JICA Project Team

Table 11.7.5 Parameters of Fault Model of Tohoku University

Segment	1	2	3
Latitude	2.5	5.0	10.0
Longitude	95.75	94.0	92.0
L (km)	330	570	300
W (km)	150	150	150
Dislocation (m)	11.0	11.0	11.0
Depth (km)	7.0	7.0	7.0
Strike	329	340	5
Dip	15	15	15
Slip	110	110	110

Source: Tohoku University, Japan



Source: JICA Project Team

Figure 11.7.8 Outline of the Tohoku University (1) Fault Model

(2) Fault Model with Consideration of the Northern Part Structure Line

Two cases have been considered in the fault model (see Figure 11.7.9 and Figure 11.7.10). The characteristics of each case study has been summarized below.

1) Case 1: Including the aftershock area only of the Northern Part Structure Line (Figure 11.7.9 and Table 11.7.6)

The activity area of earthquake is the aftershock area of the 2004 Indian Ocean Earthquake at the Northern Part Structure Line. Though the strain energy has not accumulated at the boundary of the plates since the 2004 Indian Ocean Earthquake, it is expected that the faults in this area become active.

2) Case 2: Including the whole area of the Northern Part Structure Line (Figure 11.7.10 and Table 11.7.7)

The activity area of earthquake is the whole area of the Northern Part Structure Line. The activity area is expanded further north from that of Case 1. In the expanded area, it is considered that the possibility of earthquake occurrence is comparatively low, as this area was not an aftershock area of the 2004 Indian Ocean Earthquake. However, since the strain energy at the boundary of plates has been accumulating, earthquakes could occur in lesser probability. Furthermore, since the expanded area is close to Myanmar, the area is added as the activity area.

Table 11.7.6 Fault Model Parameters of Case 1

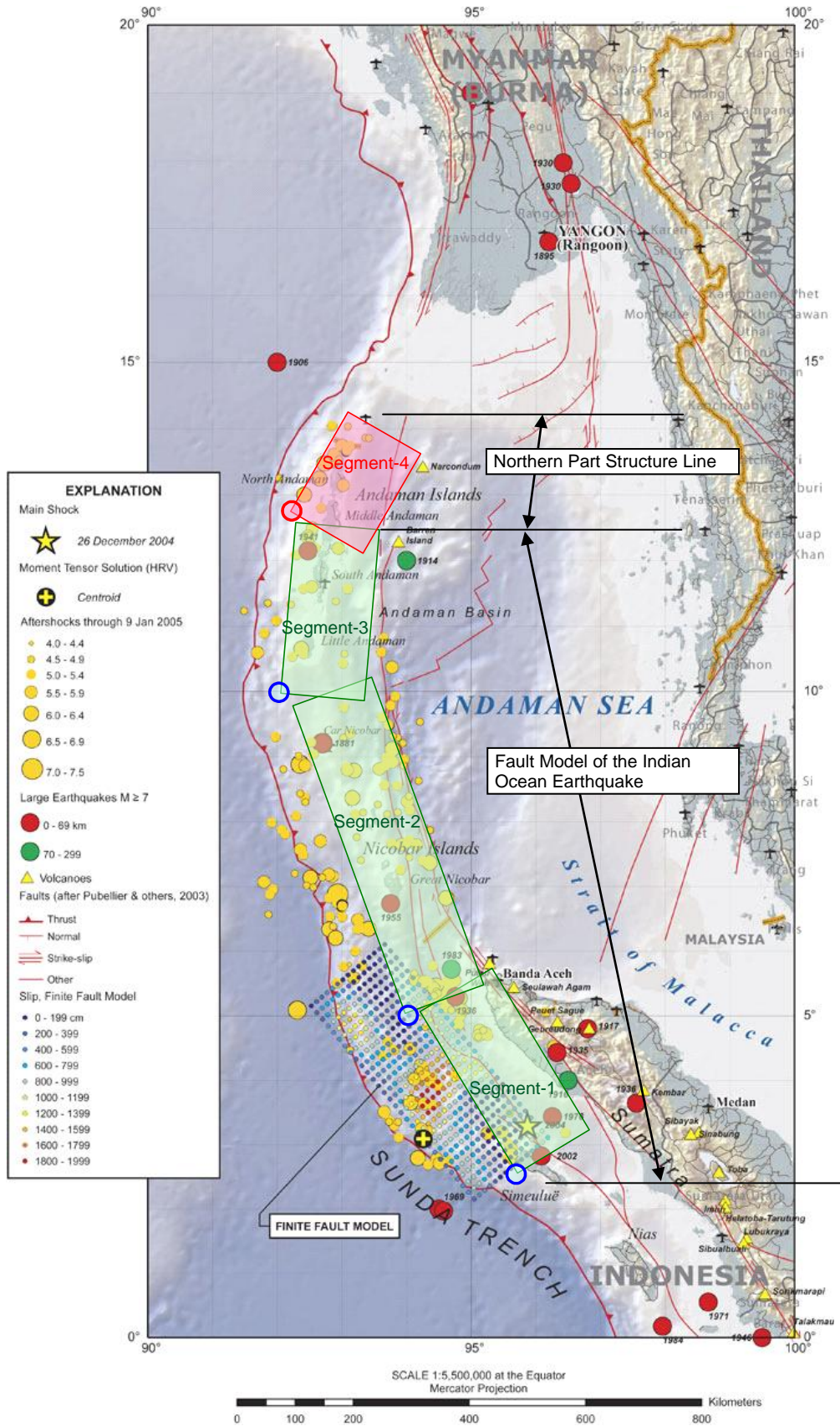
	Latitude	Longitude	L (km)	W (km)	δ (°)	Strike (°)
1 st	2.50	95.75	330	150	15	329
2 nd	5.00	94.00	570	150	15	340
3 rd	10.00	92.00	300	150	15	5
4 th	12.75	92.25	200	150	15	30

Source: JICA Project Team

Table 11.7.7 Fault Model Parameters of Case 2

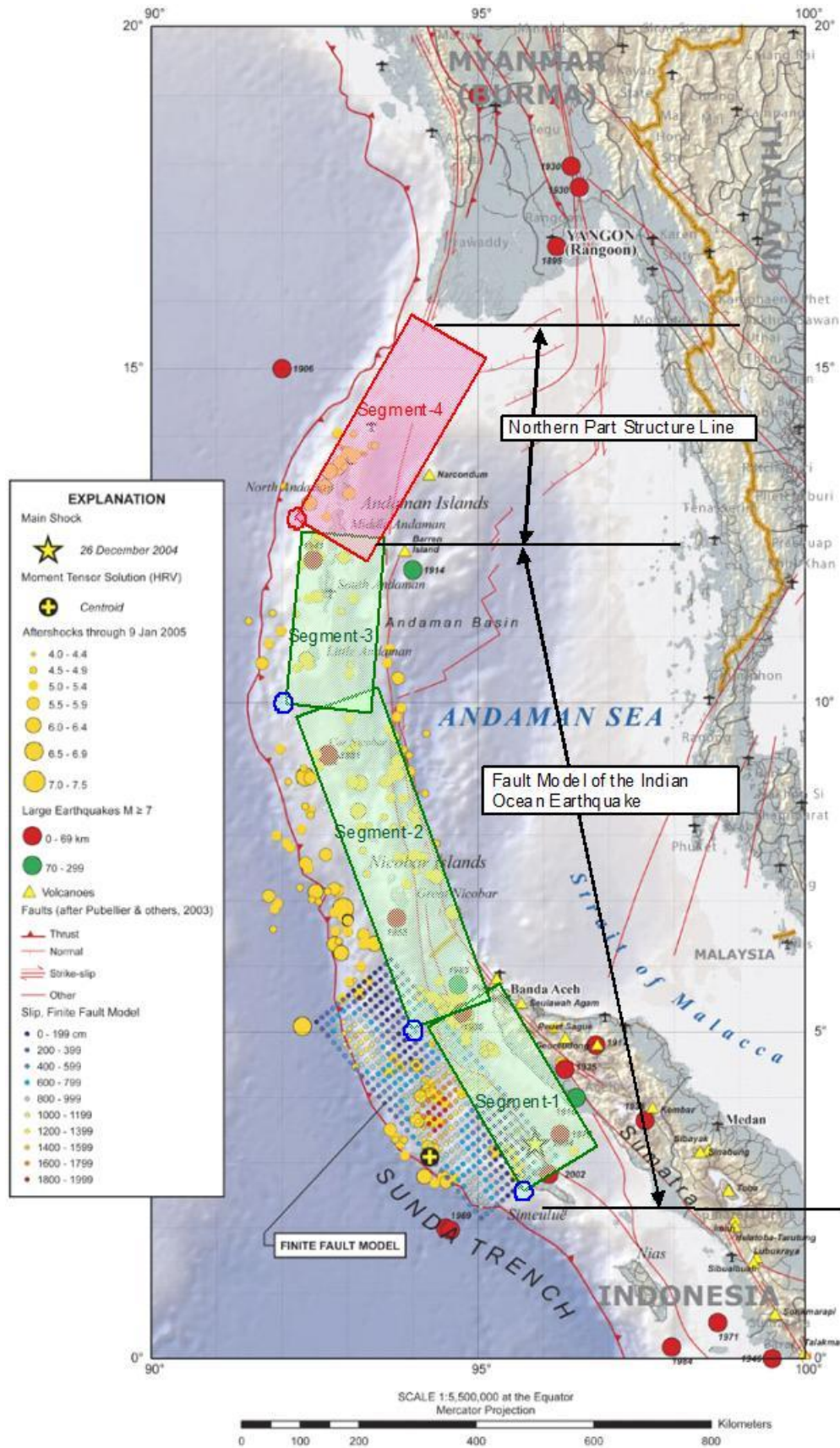
	Latitude	Longitude	L (km)	W (km)	δ (°)	Strike (°)
1 st	2.50	95.75	330	150	15	329
2 nd	5.00	94.00	570	150	15	340
3 rd	10.00	92.00	300	150	15	5
4 th	12.75	92.25	400	150	15	30

Source: JICA Project Team



Source: USGS (<http://walrus.wr.usgs.gov/tsunami/sumatraEQ/seismo.html>), edited by the JICA Project Team

Figure 11.7.9 Fault Model Including the Aftershock Area in the Northern Part Structure Line



Source: USGS (<http://walrus.wr.usgs.gov/tsunami/sumatraEQ/seismo.html>), edited by the JICA Project Team

Figure 11.7.10 Fault Model Including the Whole Area in the Northern Part Structure Line

11.7.4 TSUNAMI SIMULATION

(1) Fault Conditions

Table 11.7.8 shows the fault parameters in case of considering the distribution of aftershock of the north part geological structure line. The first, second, and third fault plates were defined by Tohoku University in Japan, and the fourth parameter are defined in this study. In order to compare the results by the difference of the calculation conditions, several numerical conditions were assumed. Table 11.7.9 shows the fault conditions for estimating the tsunami height around Myanmar.

Table 11.7.8 Fault Parameters in Case of Considering Distribution of Aftershock of the North Part Geological Structure Line

	Latitude	Longitude	L (km)	W (km)	δ (°)	Strike (°)
1 st	2.50	95.75	330	150	15	329
2 nd	5.00	94.00	570	150	15	340
3 rd	10.00	92.00	300	150	15	5
4 th	12.75	92.25	200	150	15	30

Source: JICA Project Team

Table 11.7.9 Fault Conditions for Tsunami Simulation

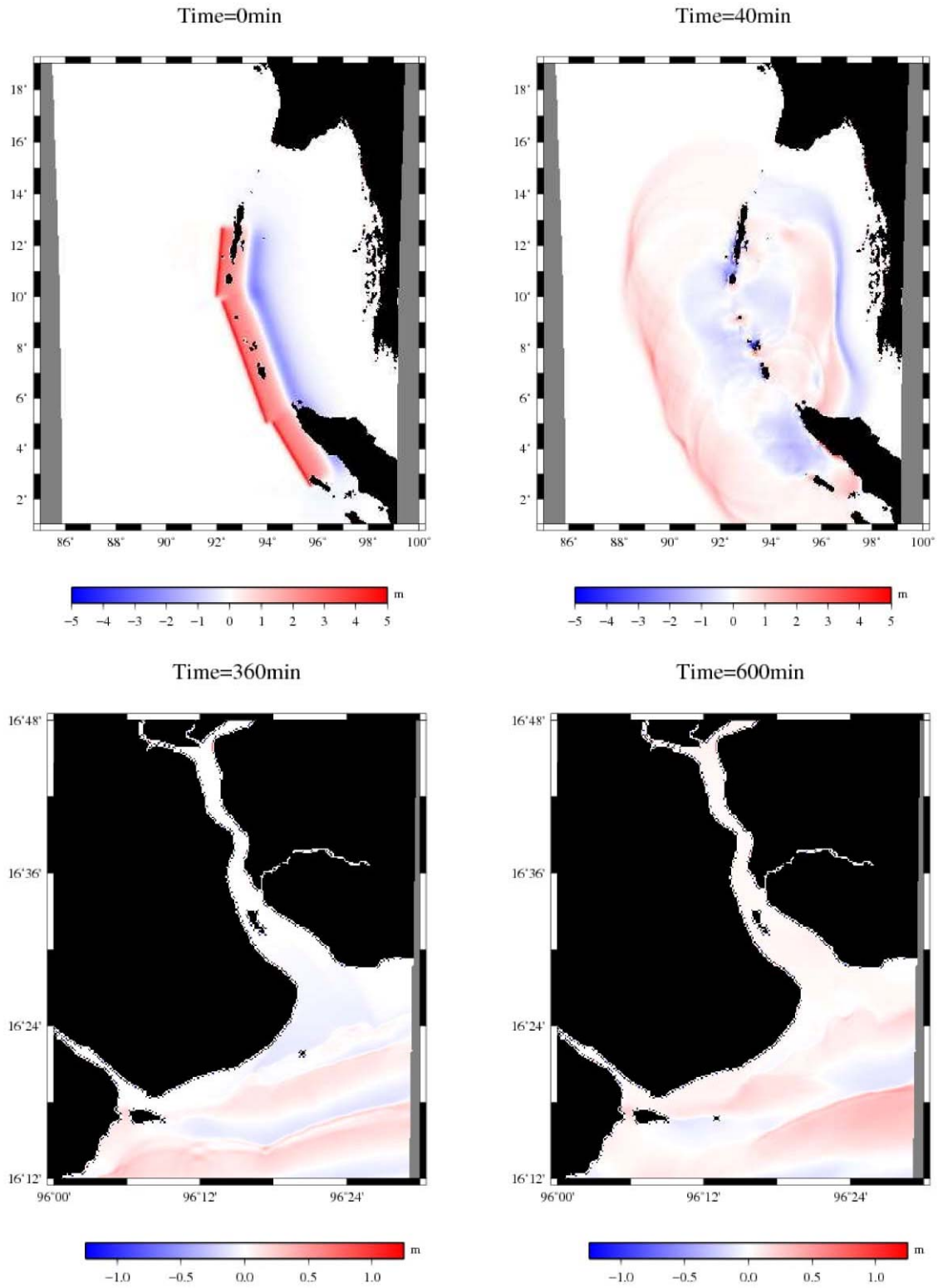
Case	Assumed Fault		Dislocation (m)	Tide Level (m)
	Sumatra + after Shock Area	North Part of Plate		
1	with consideration	X	11	0 (M. S. L)
2		L = 400 km		
3		L = 200 km		
4	without consideration	L = 400 km	13	
5				
6				
7				
8	without consideration			

Note: Sumatra + aftershock area = 1st, 2nd, 3rd segment, North part of plate = 4th segment

Source: JICA Project Team

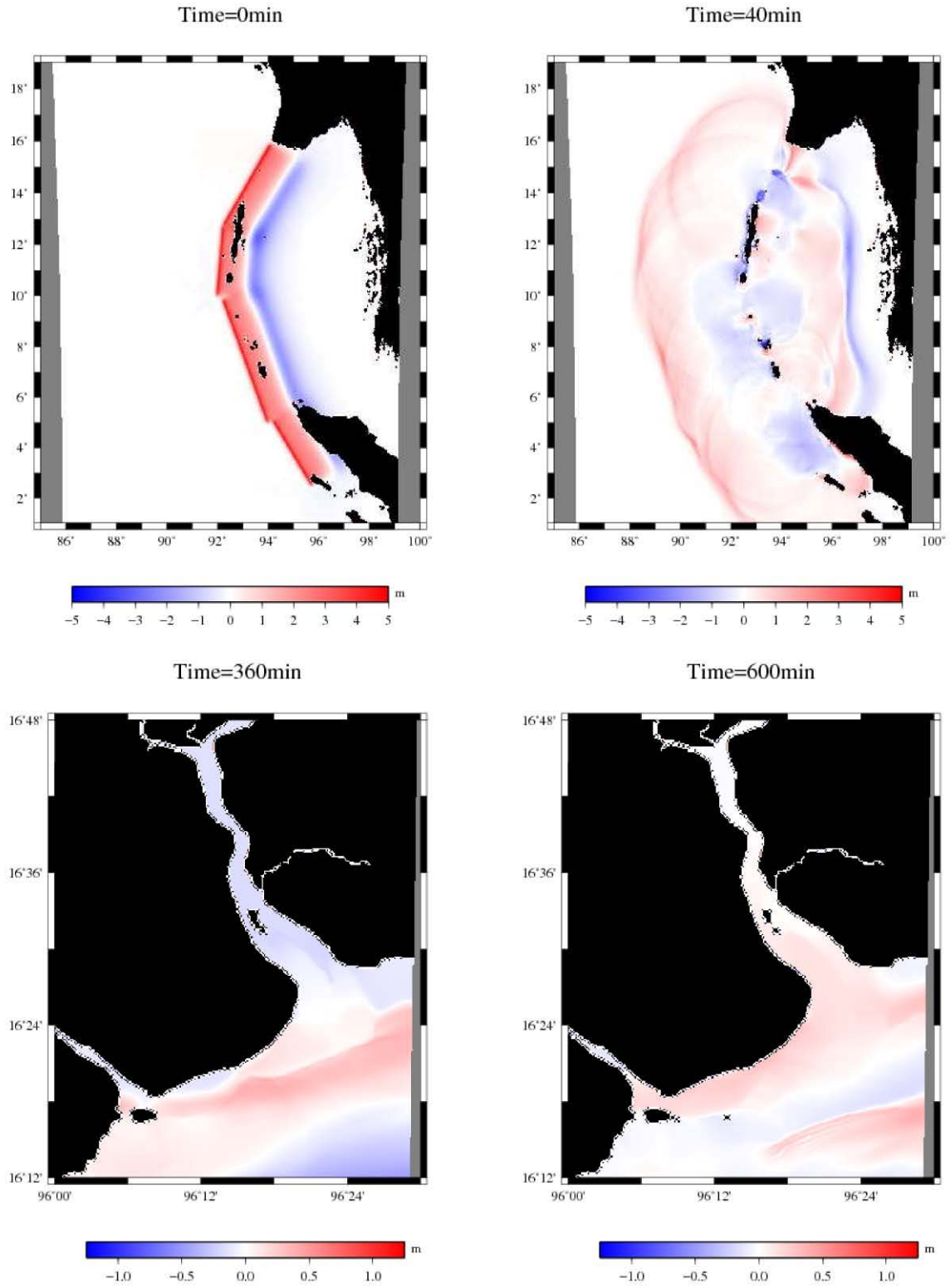
(2) Simulation Results

Figure 11.7.11 to Figure 11.7.18 show the tsunami height distribution of calculation domain 1 and domain 3 in case of initial condition (time = 0), and after 40, 360, and 400 minutes. It can be seen that the results in case with consideration of the north part plate (fourth plate) has a large impact in Myanmar. From these results, Case 7 and Case 8 (in case that the tide is 3 m and the north plate is considered) have the hugest impacts in the Yangon River. Figure 11.7.19 shows the tsunami time history by tsunami simulation in Myanmar. According to this figure, the maximum tsunami height around the Yangon River is about 0.6 m, and the arrival time at the Yangon River of a tsunami of maximum height is about 11 hours. In comparison, in the coastal area around Ayeyarwady Division, the maximum tsunami height is more than 4 m and the arrival time is about 1 hour.



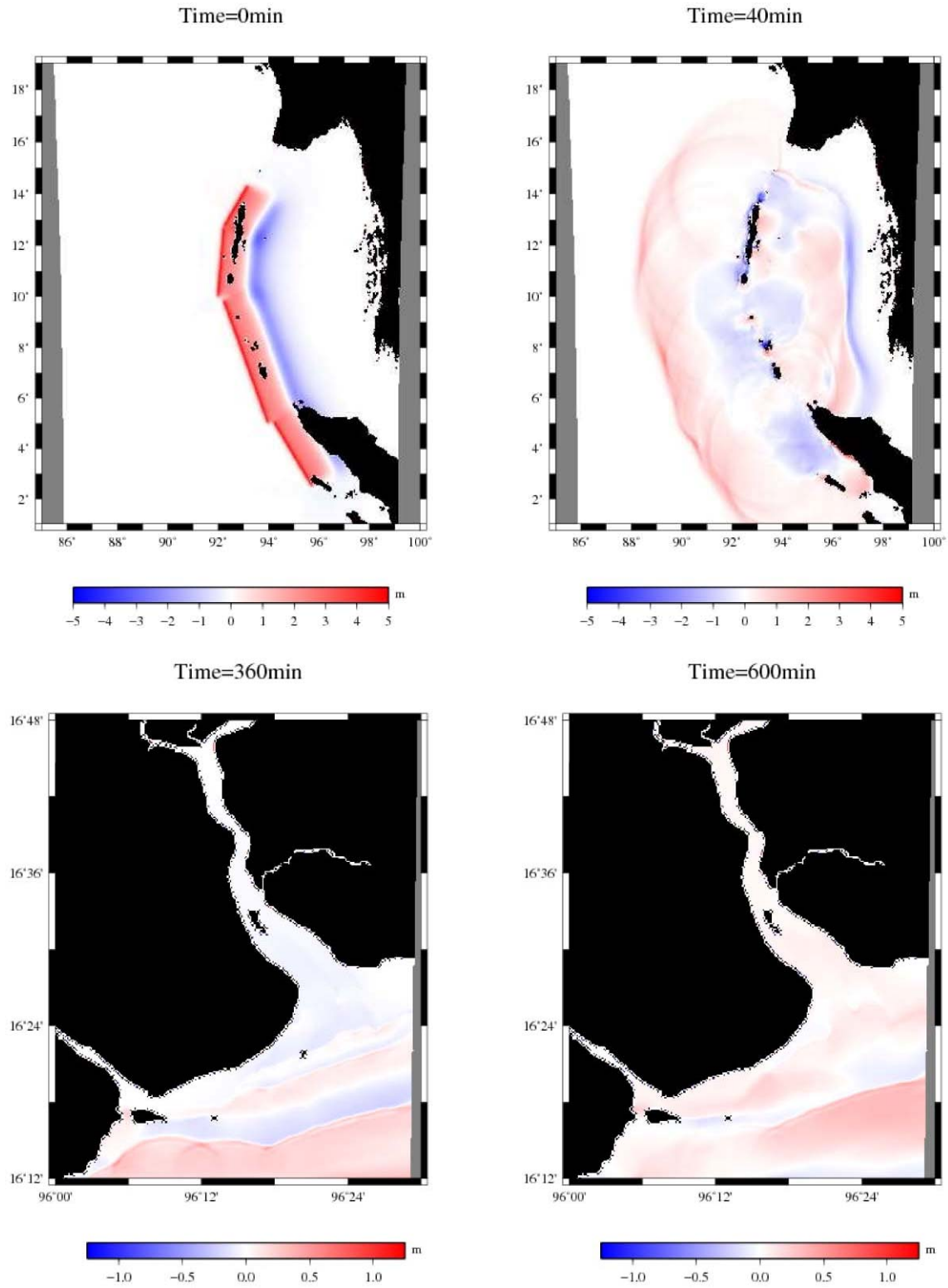
Source: JICA Project Team

Figure 11.7.11 Results of Tsunami Simulation, Domain 1 (Case 1)



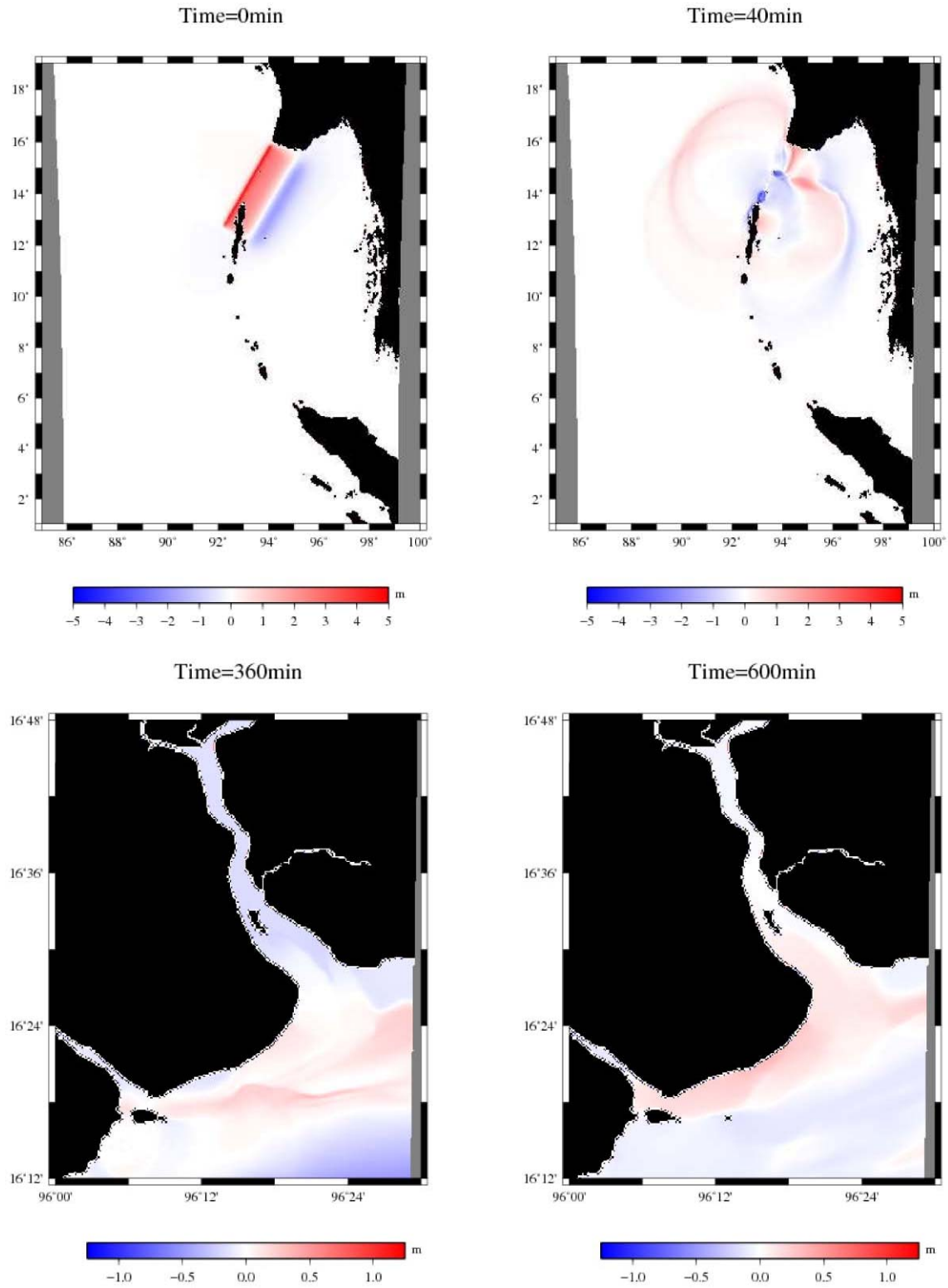
Source: JICA Project Team

Figure 11.7.12 Results of Tsunami Simulation, Domain 1 (Case 2)



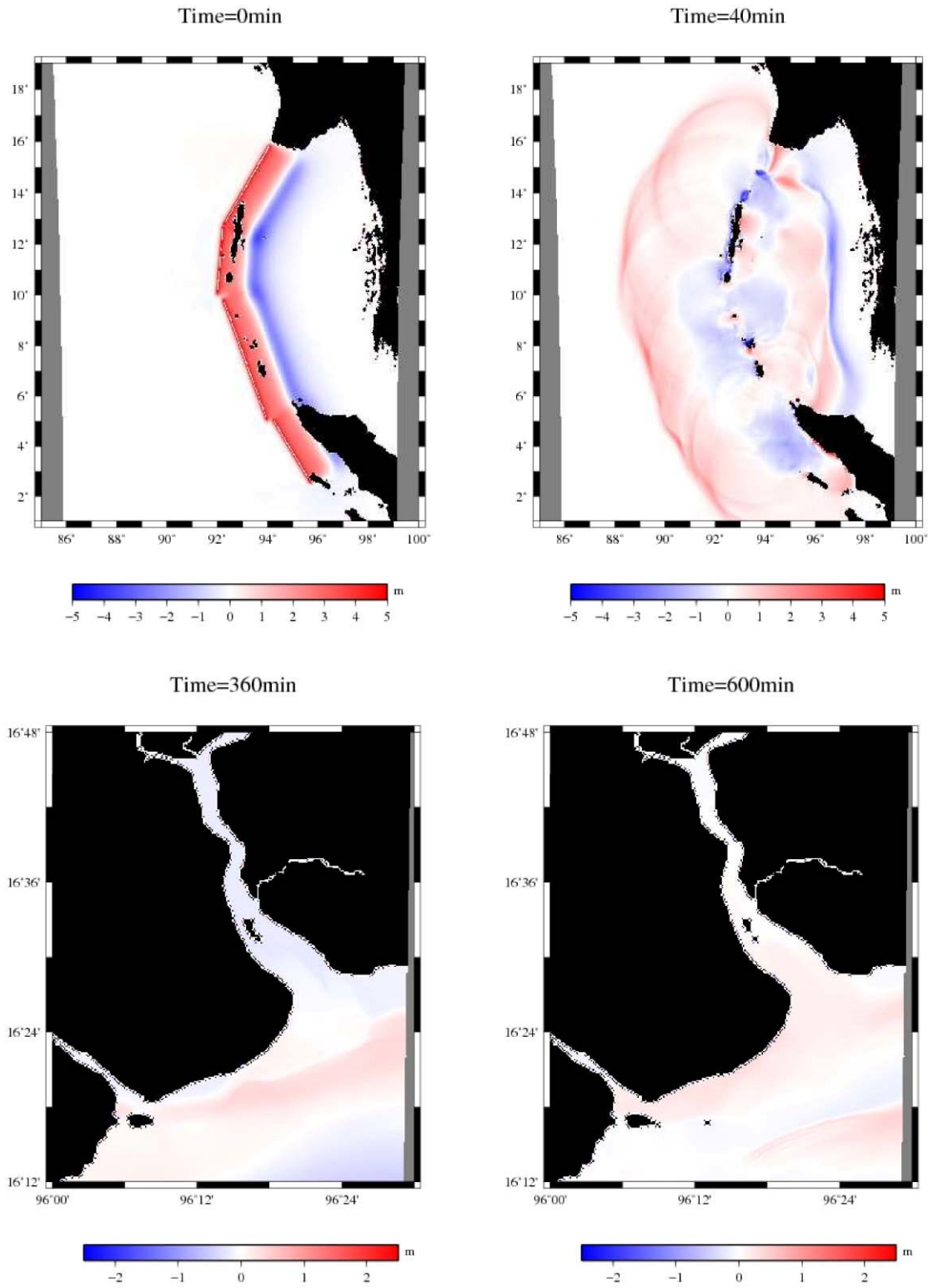
Source: JICA Project Team

Figure 11.7.13 Results of Tsunami Simulation, Domain 1 (Case 3)



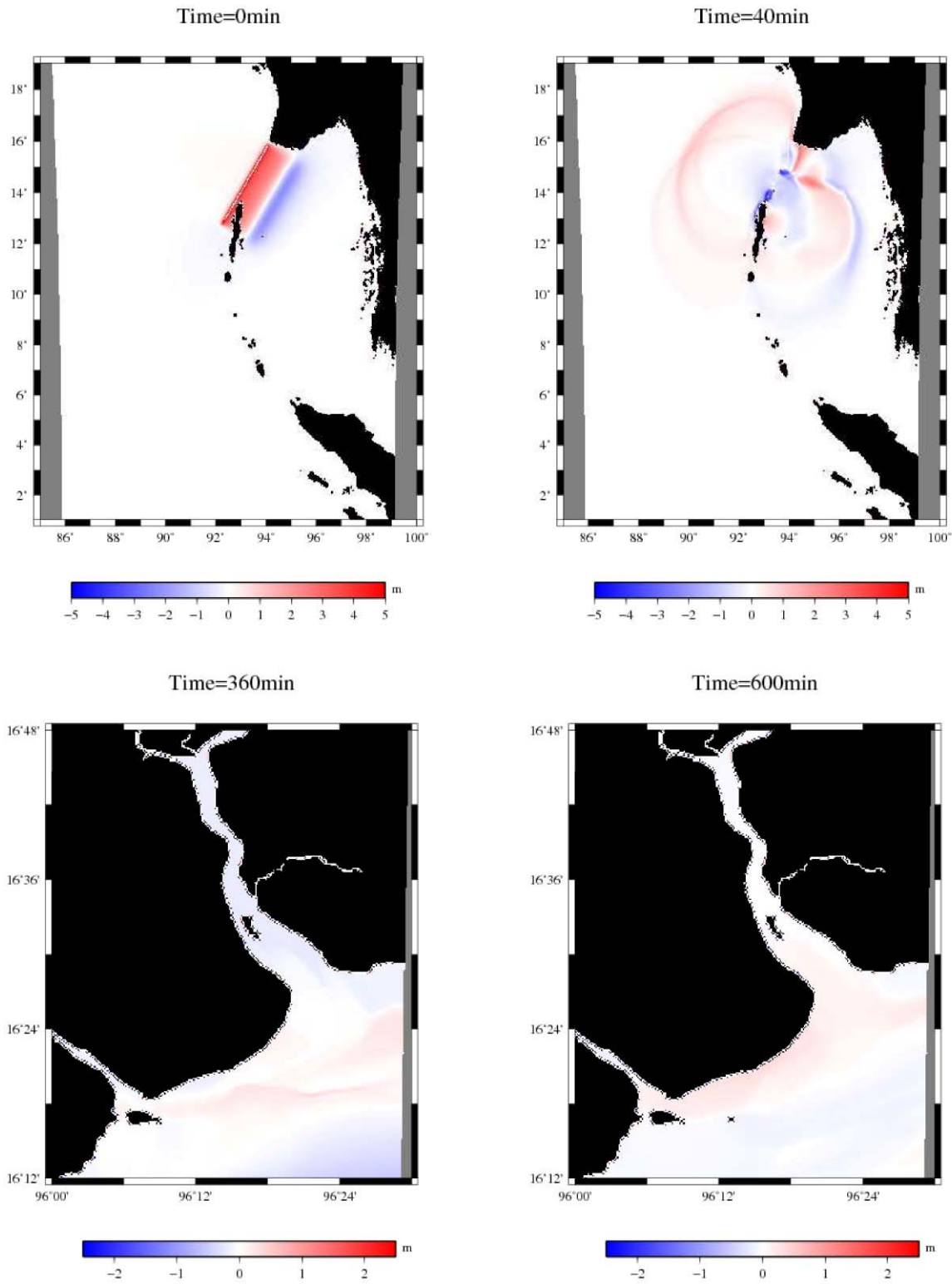
Source: JICA Project Team

Figure 11.7.14 Results of Tsunami Simulation, Domain 1 (Case 4)



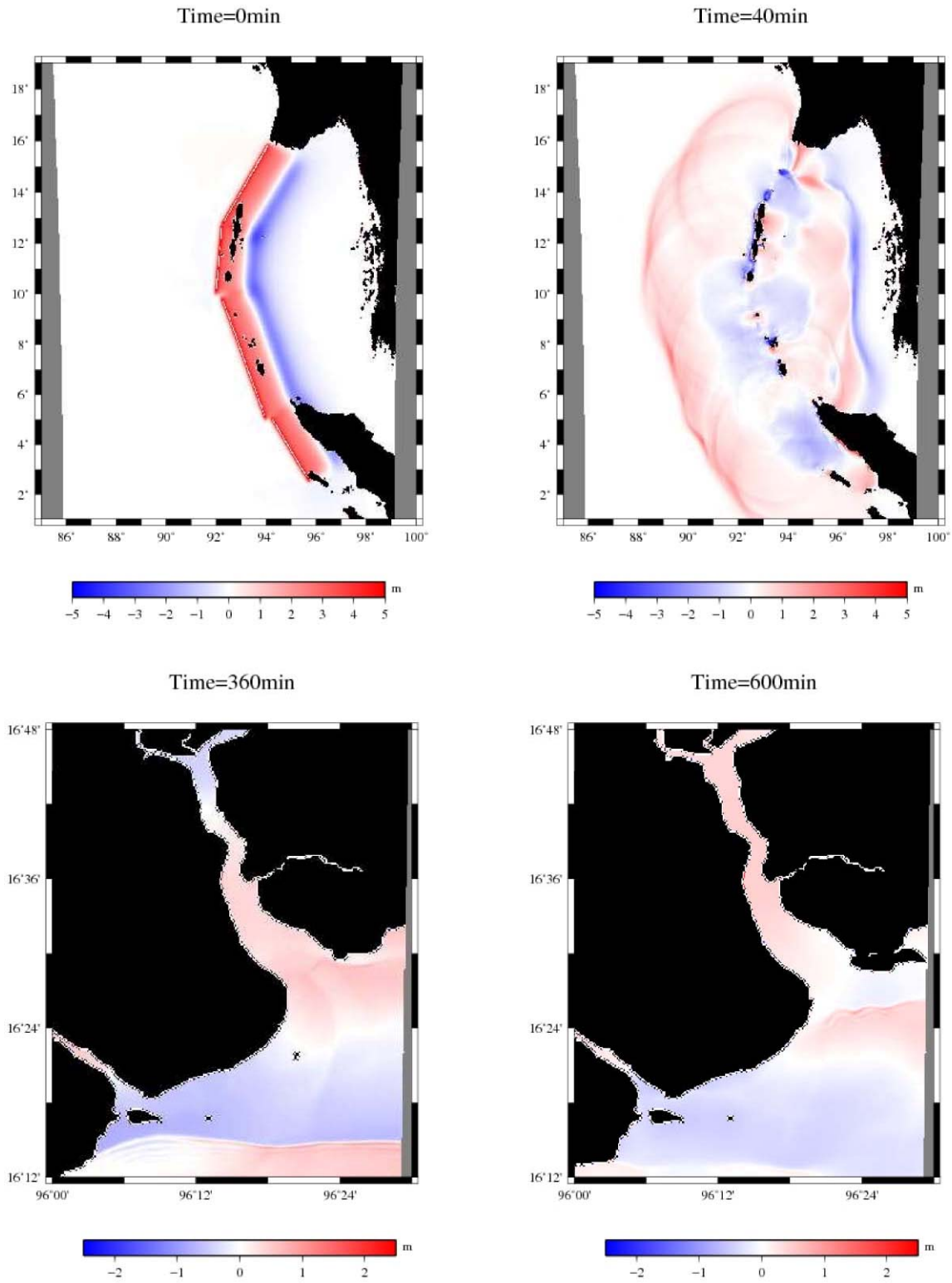
Source: JICA Project Team

Figure 11.7.15 Results of Tsunami Simulation, Domain 1 (Case 5)



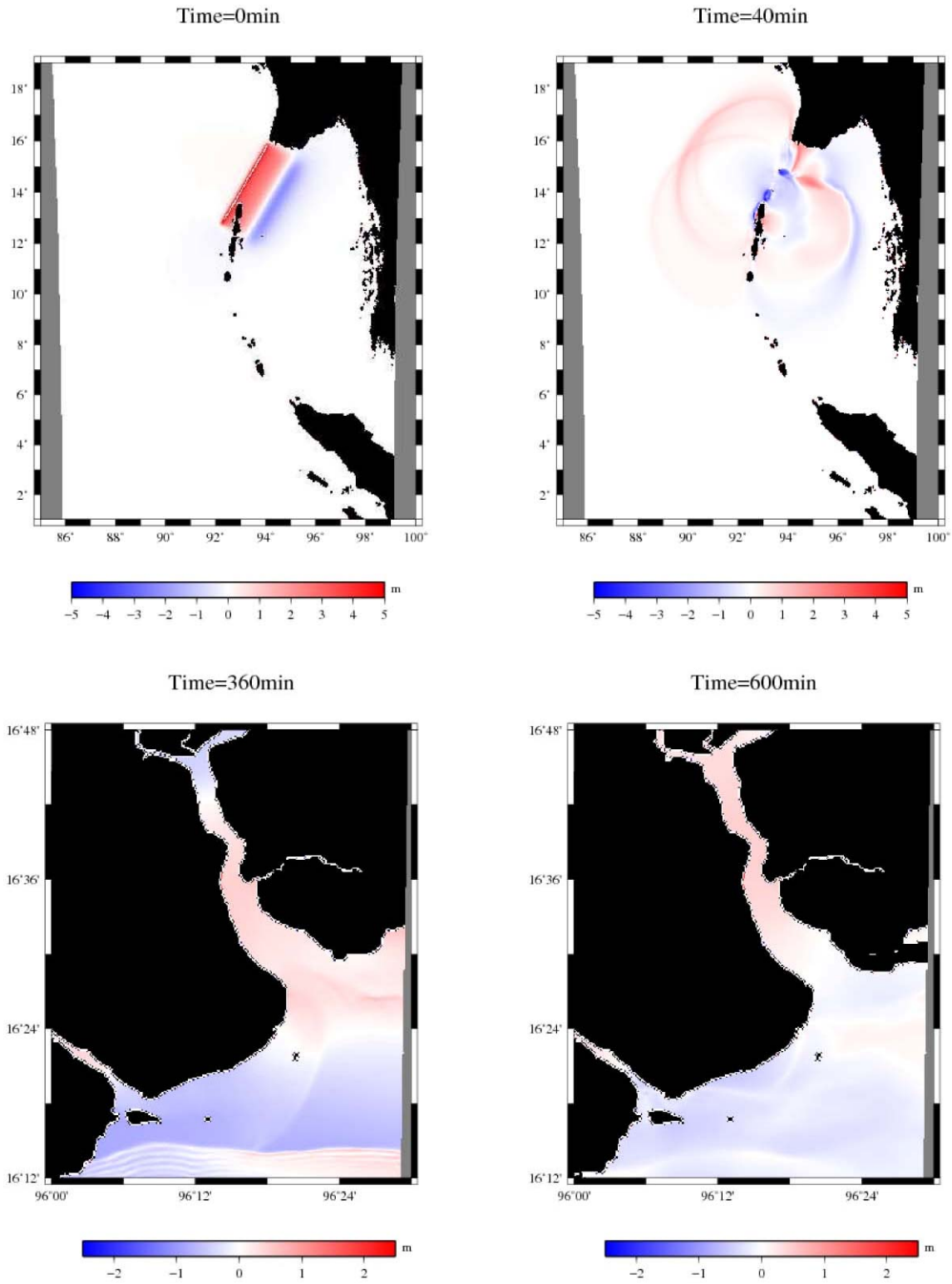
Source: JICA Project Team

Figure 11.7.16 Results of Tsunami Simulation, Domain 1 (Case 6)



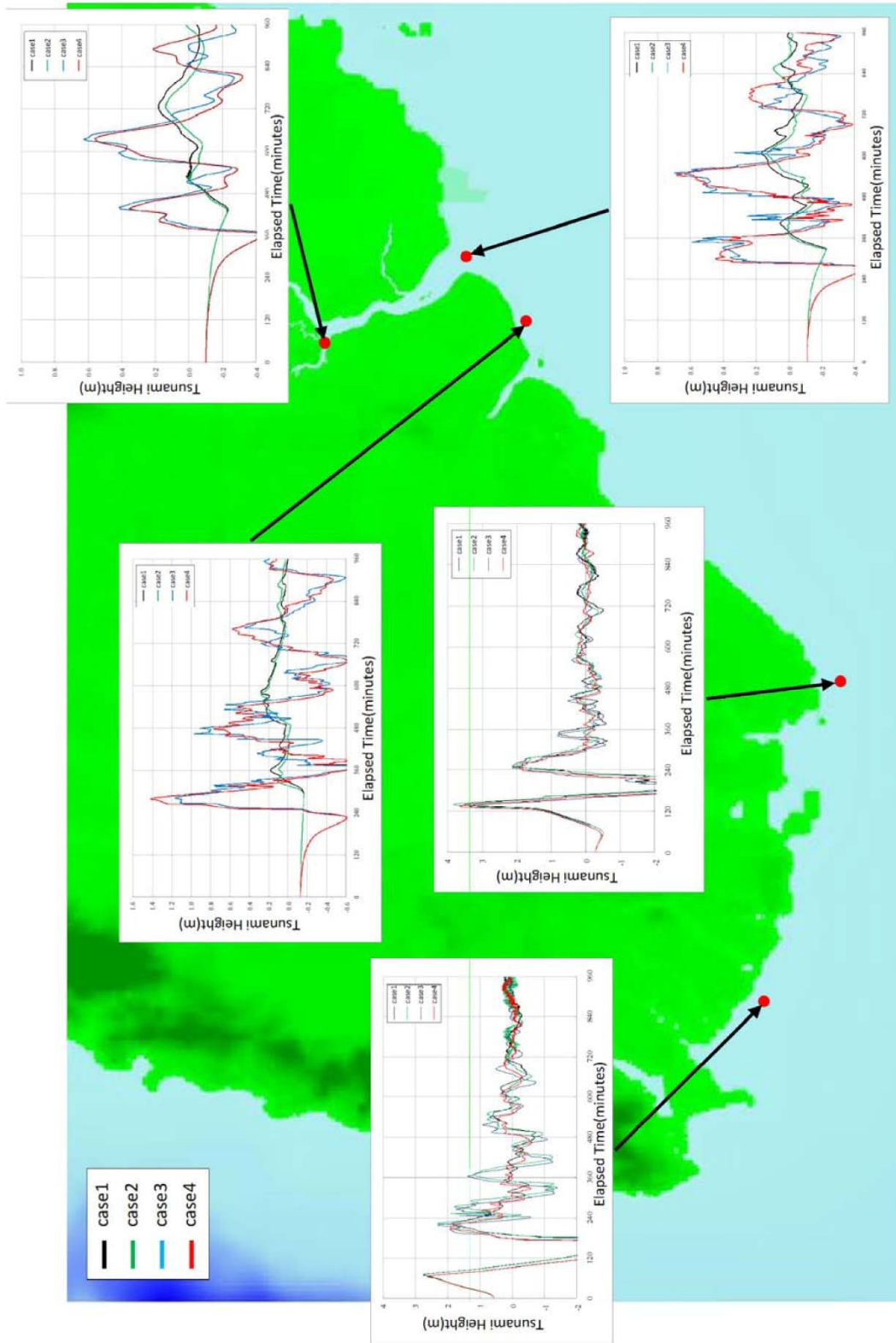
Source: JICA Project Team

Figure 11.7.17 Results of Tsunami Simulation, Domain 1 (Case 7)



Source: JICA Project Team

Figure 11.7.18 Results of Tsunami Simulation, Domain 1 (Case 8)



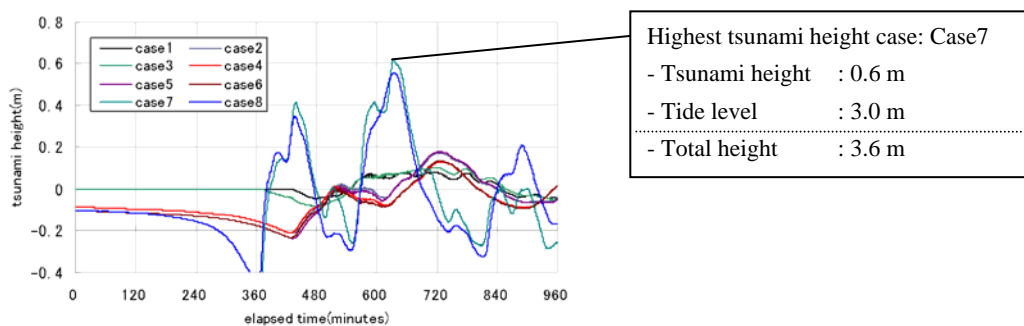
Source: JICA Project Team

Figure 11.7.19 Tsunami Time History by Tsunami Simulation in Myanmar

11.7.5 TSUNAMI DAMAGE ESTIMATION

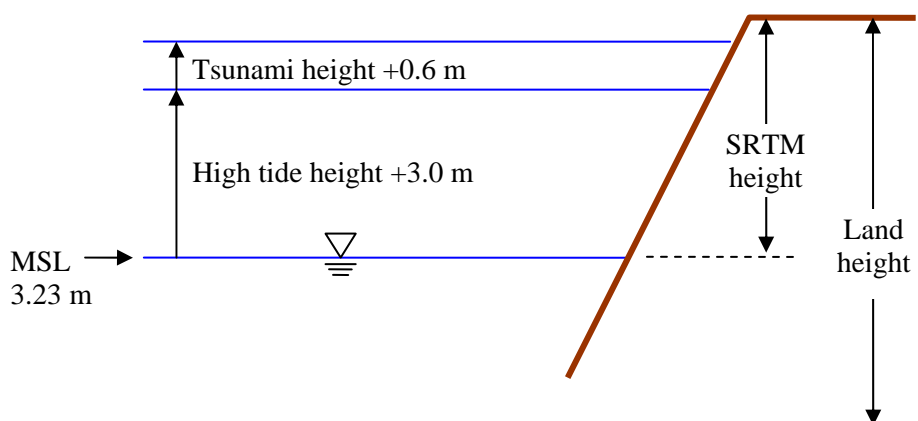
(1) Tsunami Height Condition

The results of the tsunami simulation in Yangon Port is shown in Figure 11.7.20. The sketched graph of highest sea level, which is the sum of the tsunami height and high tide, is shown in Figure 11.7.21. According to the results of tide level observation, the tide level changes about 0 m to 6 m. Assuming that the mean sea level is 3.0 m, the high tide level is 3 m from mean sea level. The summation of high tide level (+3.0 m) and maximum tsunami height (+0.6 m) from mean sea level is the highest sea level by tsunami (+3.6 m). The inundation area was calculated from this height.



Source: JICA Project Team

Figure 11.7.20 Results of the Tsunami Simulation in Yangon Port

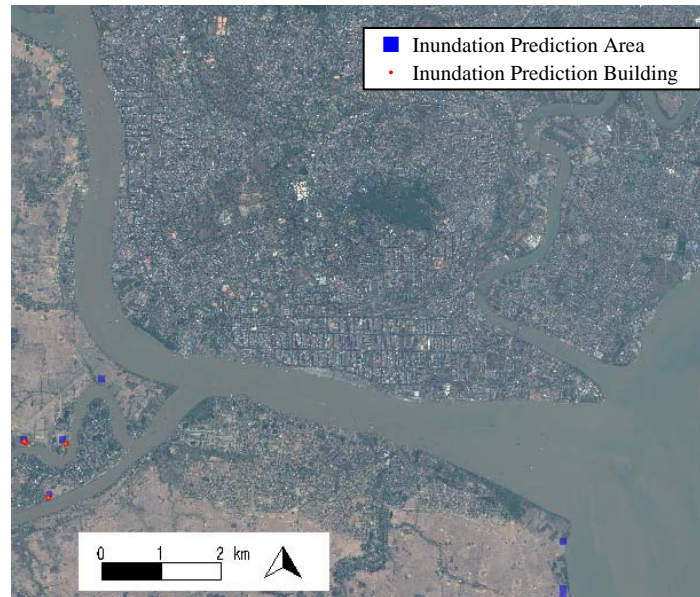


Source: JICA Project Team

Figure 11.7.21 Conceptual Diagram of Highest Sea Level

(2) Inundated Buildings in Yangon Port

The location of inundated buildings in Yangon Port is shown in Figure 11.7.22. Four buildings were inundated.



Source: JICA Project Team

Figure 11.7.22 Inundated Buildings in Yangon Port

(3) Damage Rate of Buildings

The JICA Project Team estimated direct damage using mesh data and inundation depth.

Several methods to estimate direct damage are created based on the building damage by tsunamis in Japan, Sri Lanka, and Indonesia. In case of Japan, when inundation depth becomes more than 2 m, a building will completely collapse. In other cases, when inundation depth becomes more than 2 m, the probability of complete collapse rises sharply. Inundation depth of 2 m is the threshold of large damage and small damage.

The JICA Project Team applied the method used in Japan. Damage rate of building by inundation depth is shown in Table 11.7.10. There are four buildings in the area in which inundation depth is 0.5 m to 1.0 m. Those areas should be considered as high risk areas.

Table 11.7.10 Estimation of Building Damage by Tsunami in Yangon Port

Inundation Depth	Wooden House		Non Wooden House		Inundated Building
	Damage Classification	Damage Rate	Damage Classification	Damage Rate	
0.5 ~ 1 m*	Slight Damage	20.5%	Slight Damage	20.5%	4
1 ~ 2 m	Major Damage	38.2%	Slight Damage	20.5%	0
Over 2 m	Destroyed	100.0%	Slight Damage	20.5%	0
Total					4

*: The topographic data applied in the analysis is in the format of 1 m interval of elevation. The elevation data of less than 0.5 m was counted as 0.5-1 m.

Source: JICA Project Team

<Reference: Case Study of Sri Lanka>

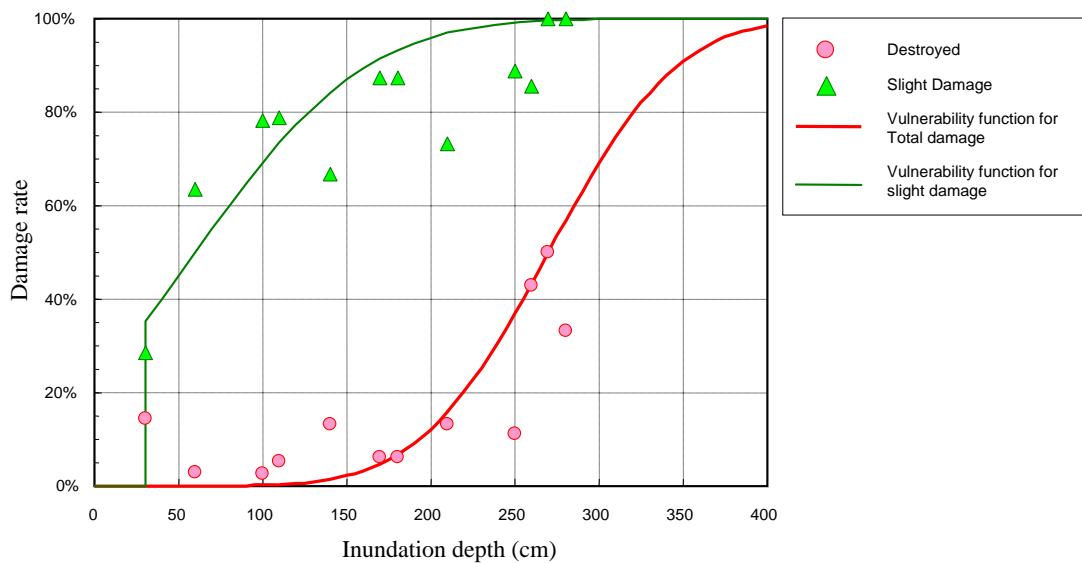
Building damage rate by tsunami was estimated referring to the case study of Sri Lanka (Kentaro KIMURA, Kazuhisa IWAMI and Seich SATO, “Verification of tsunami wave source model and formulation of vulnerability function for buildings based on the investigation of actual damage due to the Sumatran earthquake and tsunami” , Coastal Engineering Committee, Vol. 53, pp.301-305, 2006). Formulation of vulnerability function for buildings is shown in Table 11.7.11. About 70% of inundated buildings are damaged.

Table 11.7.11 Formulation of Vulnerability Function for Buildings

$P(x) = \frac{1}{\sigma\sqrt{2\pi}} \int_{30}^x \exp\left\{-\frac{1}{2}\left(\frac{x-\mu}{\sigma}\right)^2\right\} dx$	$P(x)$: building damage rate x : inundation depth (m) μ : Destroyed : 2.7 m Slight damage : 0.6 m σ : Destroyed : 0.6 m Slight damage : 0.8 m
--	--

Table 11.7.12 Buildings Damage Rate

Inundation Depth	Inundation Facility	Damage Rate (%)	
		Destroyed	Slight Damage
0 m ~ 1 m	4	0.2	69.1
1 m ~ 2 m	0	12.2	96.0
2 m ~ 3 m	0	69.1	99.9
Over 3 m	0	93.3	100.0



(4) Rate of Human Loss

As for the human loss function, there are also several cases in Japan, Sri Lanka, and Indonesia.

In case of Japan, the death toll was estimated from the death rate, which was set according to the tsunami height and then corrected by the tsunami arrival time and people’s awareness of disaster prevention. In other countries, the death rate was set only by the tsunami height.

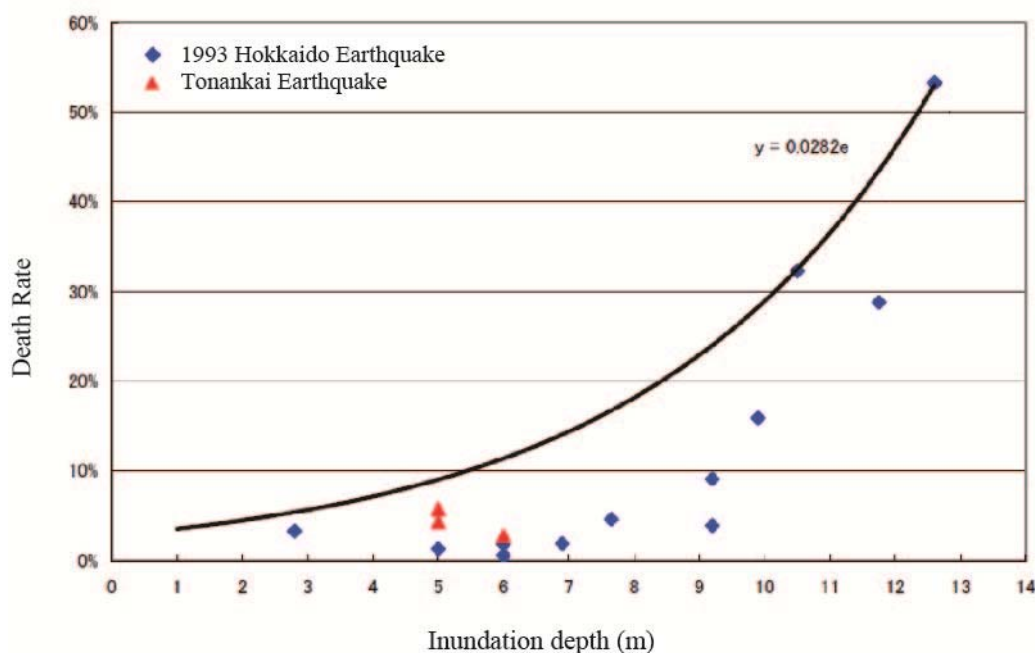
In case of Yangon Port, it takes more than six hours for the arrival of tsunami from the occurrence of earthquake, so there is enough time for evacuation. The JICA Project Team applied the cases in Japan wherein the tsunami arrival time is taken into consideration.

Death rates arranged by inundation depth are shown in Table 11.7.13 and Figure 11.7.23. Death rate of people who live in inundated buildings is 0%. This death rate is corrected by the tsunami arrival time and people’s awareness of disaster prevention. However, when the tsunami arrival time is 60 minutes or longer, human loss would not occur as shown in Figure 11.7.24 below. Human loss in Yangon Port can be minimized if the tsunami warning and evacuation are carried out thoroughly.

Table 11.7.13 Death Rate

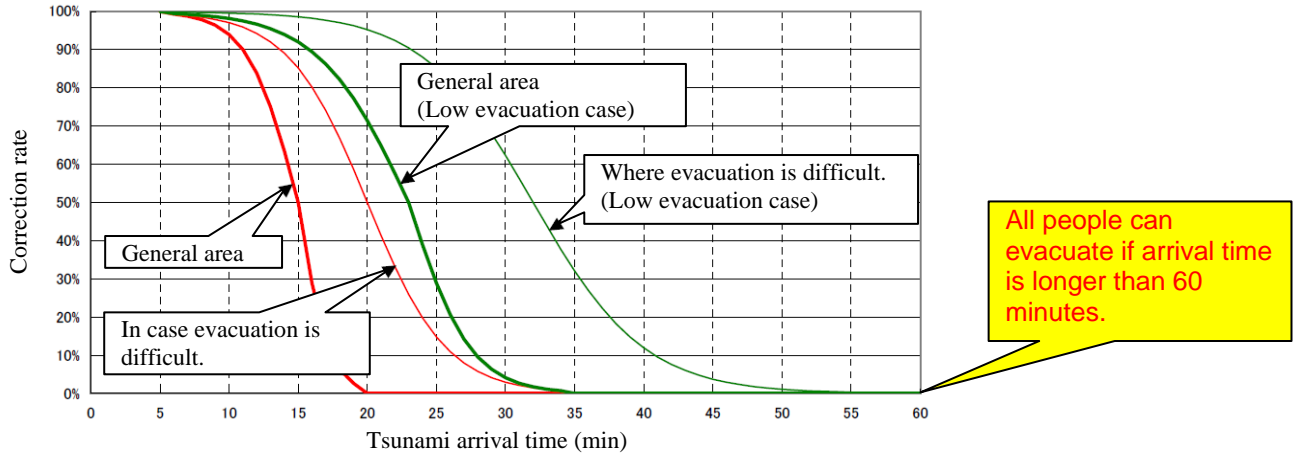
Inundation Depth	Inundation Building	Death Rate
0 m – 1 m	4	0%

Source: JICA Project Team



Source: JICA Project Team

Figure 11.7.23 Death Rate and Inundation Depth



Source: Cabinet Office, Government of Japan

Figure 11.7.24 Correction Rate and Tsunami Arrival Time

<Reference: Case study of Sri Lanka>

Death rate by tsunami was estimated referring to the case study of Sri Lanka (Kentaro KIMURA, Kazuhisa IWAMI and Seich SATO, “Verification of tsunami wave source model and formulation of vulnerability function for buildings based on the investigation of actual damage due to the Sumatran earthquake and tsunami” , Coastal Engineering committee, Vol.53, pp.301-305, 2006). The formulation for death rate estimation is shown in Table 11.7.14, Table 11.7.15, and Figure 11.7.25. About 15% of people who live in inundation buildings are dead.

Table 11.7.14 Formulation for Death Rate Estimation

Formulation for Death Rate Estimation	
Case study of Sri Lanka	$Y = 0.029e^{0.225X} + 0.112$ <p>X : inundation depth (m) Y : death rate (%)</p>

Table 11.7.15 Death Rate

Inundation Depth	Inundation Building	Death Rate
0 m ~ 1 m	4	14.8%
1 m ~ 2 m	0	15.7%
2 m ~ 3 m	0	16.9%
Over 3 m	0	17.7%

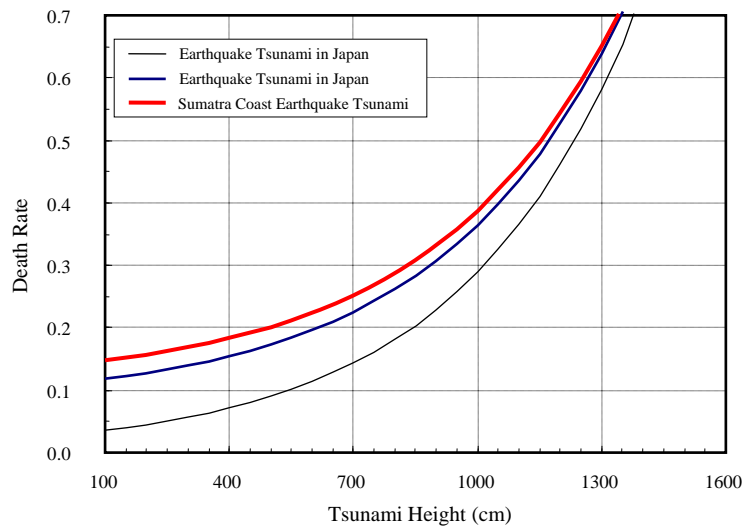


Figure 11.7.25 Death Rate and Tsunami Height

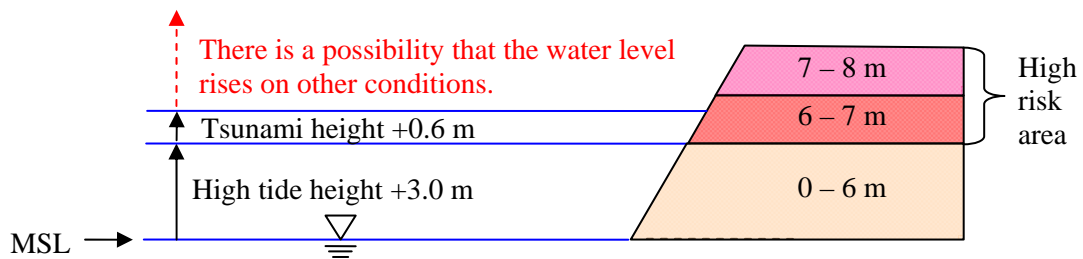
11.7.6 RISK OF TSUNAMI DISASTER IN YANGON PORT

(1) Tsunami Features

A tsunami cannot come into the Yangon River easily because its river mouth is shallow. However, the fluid force of a tsunami is larger than a storm surge because the flow velocity of a tsunami is fast. By this strong fluid force, tsunami inundation could cause severe damage even if inundation depth is not so deep.

(2) Yangon Port Features

There is low elevation area on the bank of the Yangon River. In such areas, the risk increases when the water level rises due to high tide or other conditions as shown in Figure 11.7.26.

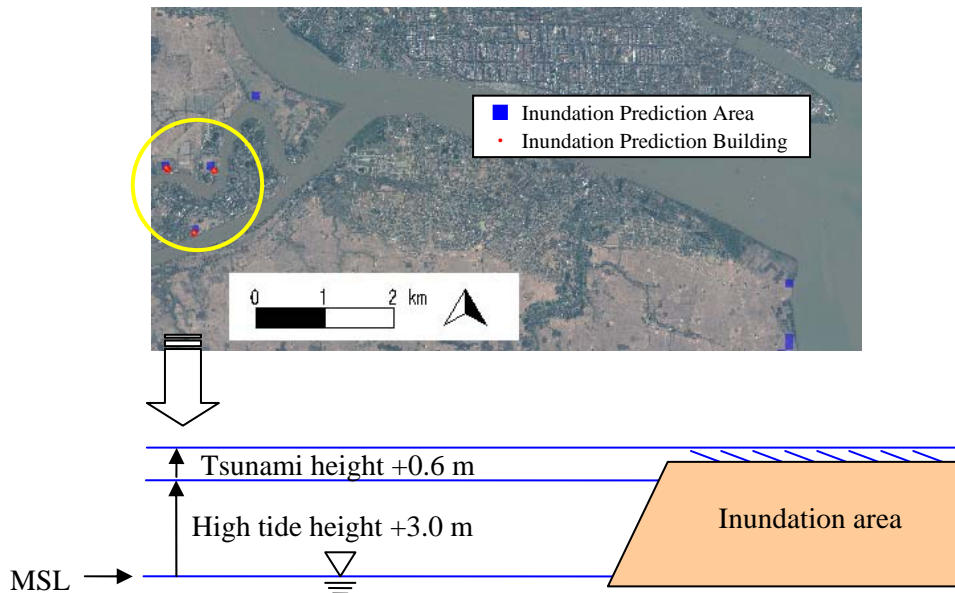


Source: JICA Project Team

Figure 11.7.26 High Risk Area Diagram

(3) Areas Judged as Inundation Area

The elevation of the area estimated as inundation area is almost equal to the high tide level. Such areas need attention because the possibility of inundation is high when the water level rises even a little at high tide.



Source: JICA Project Team

Figure 11.7.27 Areas Judged as Inundation Area

(4) Safe Evacuation Limit

The threshold level for vehicle damage and evacuation action in relation to the current and depth was set by Suga (1995) (Kyozo SUGA, "Flood of the Tone River, handed down history of valley", Sankaido, pp.217). Even if the tsunami height is low, cars start to float a little and safe evacuation becomes difficult.

Table 11.7.16 Conditions of Vehicle Damage

Inundation Depth (m)	Inundation Condition	Degree of Dangerous
0.1	Half tire	Braking effectiveness is lost
0.5	20c m over door step	The car comes to float a little
0.7	Half door	Difficult to open the door
Over 0.7	20 cm over door	The risk of drift is high

Source: Suga, 1995

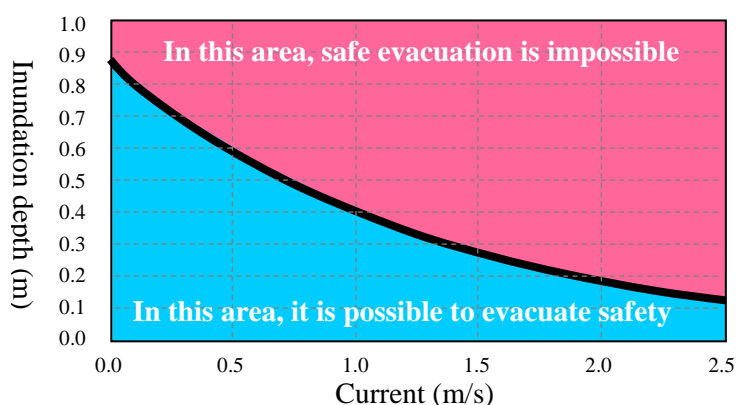
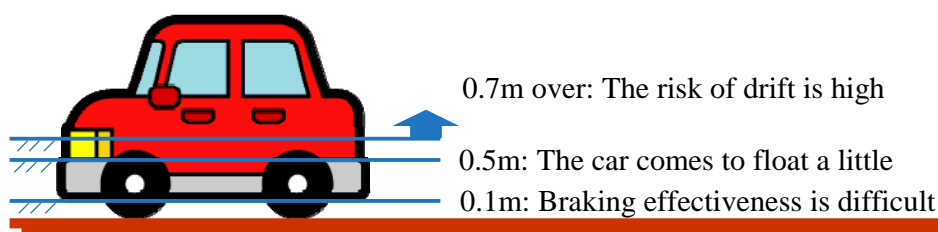


Figure 11.7.28 Relation between the Safe Evacuation Limit and Current and Depth

11.7.7 TSUNAMI HAZARD MAP OF YANGON

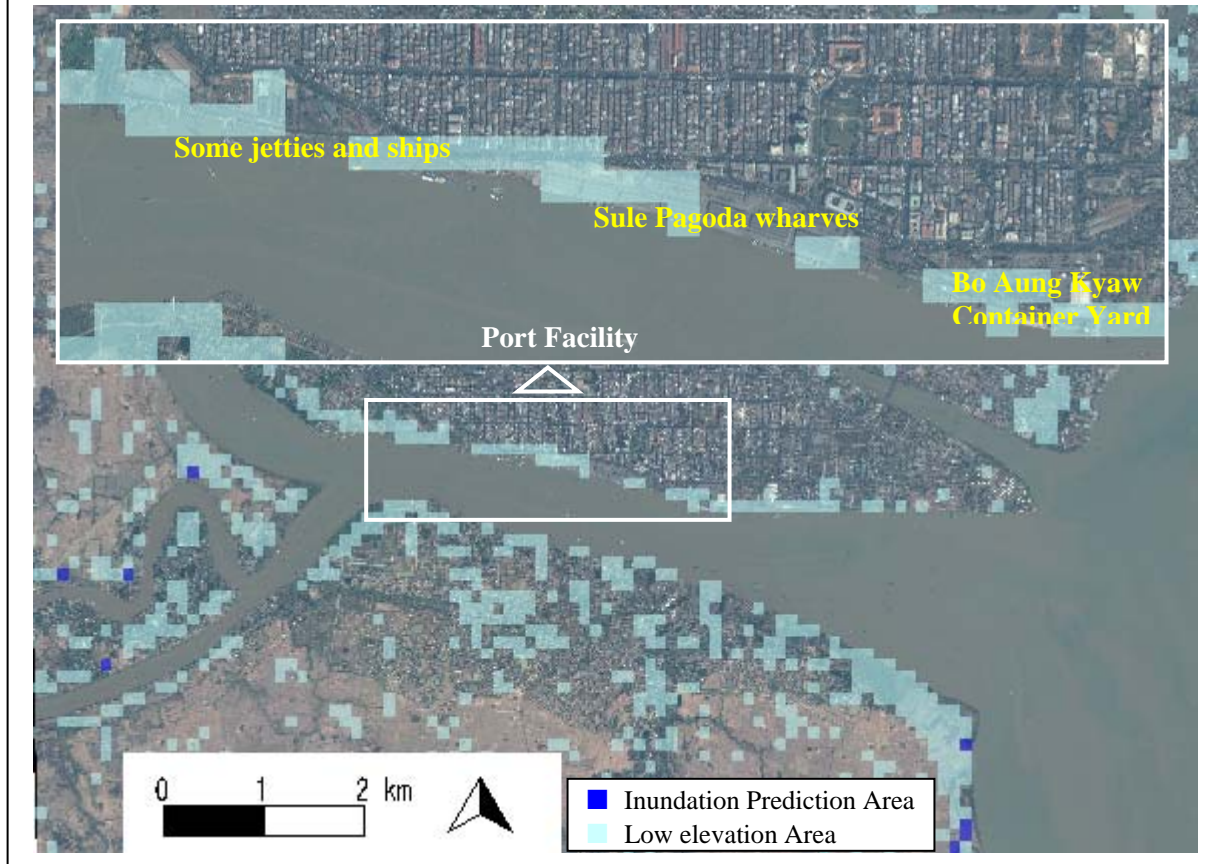
The tsunami hazard map of Yangon is shown in Figure 11.7.29.

There is not so large inundation in case a tsunami occurs from the Indian Ocean. However, the inundation risk is high in areas of low elevation in the Yangon River side.

TSUNAMI HAZARD MAP OF YANGON

This map is intended to identify the dangerous areas in case a tsunami occurs.

There is not so large inundation in case a tsunami occurs from the Indian Ocean. However, the inundation risk is high in areas of low elevation in the Yangon River side (■ area).



Source: JICA Project Team

Figure 11.7.29 Tsunami Hazard Map of Yangon

11.7.8 IMPORTANT POINTS ON EARTHQUAKES AND TSUNAMIS IN MYANMAR

(1) Earthquake in Myanmar

Myanmar is adjacent to the subduction boundary of the Indian Plate and Eurasian Plate. In 2004 when the Indian Ocean Tsunami occurred, most of this subduction boundary, 1,200 km in length, was moved while the other subduction boundaries near Myanmar (northern tectonic line) were not active. In the future, however, the northern tectonic line would also move when deformation accumulates. Thus, the JICA Project Team assumes that such a severe case where both the structures, subduction boundary of the Indian Ocean Tsunami and northern tectonic line, will move at the same time.

There have been many earthquakes in Myanmar in the past. Though most of the earthquakes occurred in the northern or eastern parts of Myanmar, which are adjacent to the plate boundary and active faults, the southern part of Myanmar, including Yangon, was also affected by the Rangoon Earthquake (1970) and some others. Plate activity and fault movement are repetitive at roughly regular intervals, so it is highly possible that Yangon will be severely damaged by a nearby earthquake. Furthermore, there would be

huge earthquakes in the northern or eastern parts of Myanmar, which are adjacent to the plate boundary and active faults.

(2) Tsunami in Myanmar

The tsunami simulations were carried out in various cases. In the simulation case of the Indian Ocean Tsunami, the tsunami height is not so high in Myanmar. In the simulation case with the Northern Part Structure Line, the tsunami causes large impacts in Myanmar.

It is predicted that the maximum tsunami height in the Yangon River is about 0.6 m. The effect of tsunami in the Yangon River is not so large. In case of high tide, however, there is a possibility of inundation. In case of high tide, the arrival time to Myanmar becomes shorter than in case of the mean sea level. This is because the tsunami wave velocity becomes faster in case of high tide.

In Ayeyarwady Division, the tsunami height is estimated up to 3 m to 4 m. It is much larger than in the Yangon Port area. The arrival time of tsunami is short because the distance from the northern fault is short. The Yangon Port area is relatively strong and Ayeyarwady Division is weak against a tsunami attack.

From this study, it can be seen that the tsunami damage is relatively small around Yangon because of low tsunami height and long arrival time. However, in case that people do not evacuate in advance, human loss will become severe. Even if the tsunami height is small, the velocity and energy of tsunamis are high enough to cause human loss.

In order to raise people's awareness of disaster prevention, it is necessary to enlighten people about tsunami damage.

11.7.9 COUNTERMEASURES

It would take a long time and much amount of money to rehabilitate port facilities damaged by an earthquake. Thus, seismic assessment taking in consideration degradation level is recommended. According to the seismic assessment, maintenance and reinforcement must be appropriately done if needed.

It is impossible to know when an earthquake will occur. It may occur before maintenance and reinforcement of port facilities are finished. In preparation for such case, it is recommended to draw up a BCP after a disaster in order to maintain a minimum of port functions.

Though Yangon Port is relatively strong against a tsunami attack, further study on damage by tsunami and countermeasures is need for the port facilities.

In Ayeyarwady Division, further investigation is needed about tsunami propagation and damage estimation in future works. It is also necessary to study disaster prevention (e.g., tsunami warning system) and the countermeasure plan (e.g., tsunami evacuation tower). In Ayeyarwady Division, an early alarm system for tsunamis should be installed to secure the evacuation time because the arrival time of the tsunami is short.

In order to evacuate quickly, enhancement of the awareness for disaster prevention is important. It is necessary to hold regular seminars on disaster prevention and enlighten people the details of damage estimation and the location of evacuation areas.

The following measures are necessary in Ayeyarwady Division since potential tsunami damage is large therein:

Durability is improved if port facilities are made from RC.

Introduce a tsunami warning system to transmit information on tsunami occurrence quickly.

Create a hazard map and set the evacuation area.

High place that can become evacuation areas are set up.

Improvement of disaster awareness (holding of regular disaster prevention seminars).

It is necessary to execute tsunami simulation in Ayeyarwady Division when the abovementioned measures are examined, and to estimate the height of the tsunami, flood area, and damage caused by the tsunami.

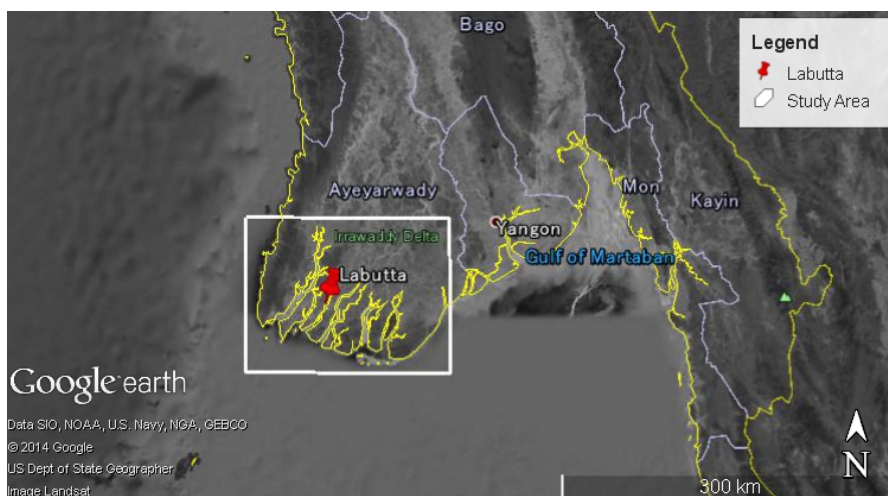
11.8 STORM SURGE AND TSUNAMI SIMULATION IN DELTA AREA

11.8.1 OBJECTIVE OF STUDY

Myanmar lies on an earthquake belt with fault lines like the famous Sagaing Fault extending from north to south of Myanmar. There is the Indo-Australia/Eurasia Plate Boundary, a part of which caused the Indian Ocean Tsunami on 26 December 2004, lying along the west coast of the Myanmar. It was identified in Section 11.7 that the area of the Northern Part Structure Line was not the aftershock area of the 2004 Indian Ocean Earthquake, and the strain energy at the boundary of plates would have been accumulated. There is a slight possibility that a catastrophic earthquake could occur in the future.

Tsunami simulation was conducted and was described in Section 11.7, and concluded that inundation depth in the Yangon Port area was not so high, while the delta area received a tsunami of several meters' height a short time after the occurrence of an earthquake. Therefore, the tsunami and storm surge simulations in the delta area were conducted in this section for damage estimations.

The objective of the study is to conduct tsunami and storm surge simulations in the delta area, where the results will be used for the improvement of Maritime Disaster Prevention Programme and preparedness of stakeholders.



Source: JICA Project Team

Figure 11.8.1 Study Area

11.8.2 DATA COLLECTION

(1) Data Collection of Cyclones and Earthquakes around Delta Area

Data on cyclones and earthquakes around the delta area were collected for the tsunami and storm surge simulations. Topographic data for building the simulation model was also collected. The list of collected data is shown in Table 11.8.1.

Table 11.8.1 List of Collected Data

Category	Collected Data
Topography data	<ul style="list-style-type: none"> • Bathymetry feature • Land feature • Land use
Condition of tsunami simulation	<ul style="list-style-type: none"> • Earthquake database (USGS) • Fault models (Japan)
Condition of storm surge simulation	<ul style="list-style-type: none"> • Cyclone tracks (JTWC) • Numerical simulation outputs (MRI/JMA)
Damage inflicted by tsunami	<ul style="list-style-type: none"> • Pictures of the delta area, which show buildings damaged by the tsunami caused by the 2004 Indian Ocean Earthquake

Source: JICA Project Team

(2) Data Collection of Damages by Cyclone Nargis in Delta Area

The pictures showing the damages by Cyclone Nargis in delta area are shown below.



Source: JICA Project Team

Figure 11.8.2 Damage of Delta Area by Cyclone Nargis

(3) Data Collection of Tsunami Damages in Delta Area

The tsunami caused by the 2004 Indian Ocean Earthquake reached the delta area of Myanmar, and caused damages. Detailed information on inundation depth and area is very limited. The damages caused by the tsunami in the village of Aling Hlaing located in the eastern part of the delta area were reported as shown in Figure 11.8.3. It is clear that houses were partly damaged, and inundation depth was more than one meter.



Source: Nippon Koei Co., Ltd

Figure 11.8.3 Pictures of Houses Damaged by Tsunami caused by
2004 Indian Ocean Earthquake in Delta Area

(4) Topographic Data Collection

Data for the topography model is shown in Table 11.8.2.

Table 11.8.2 Data for Topography Model

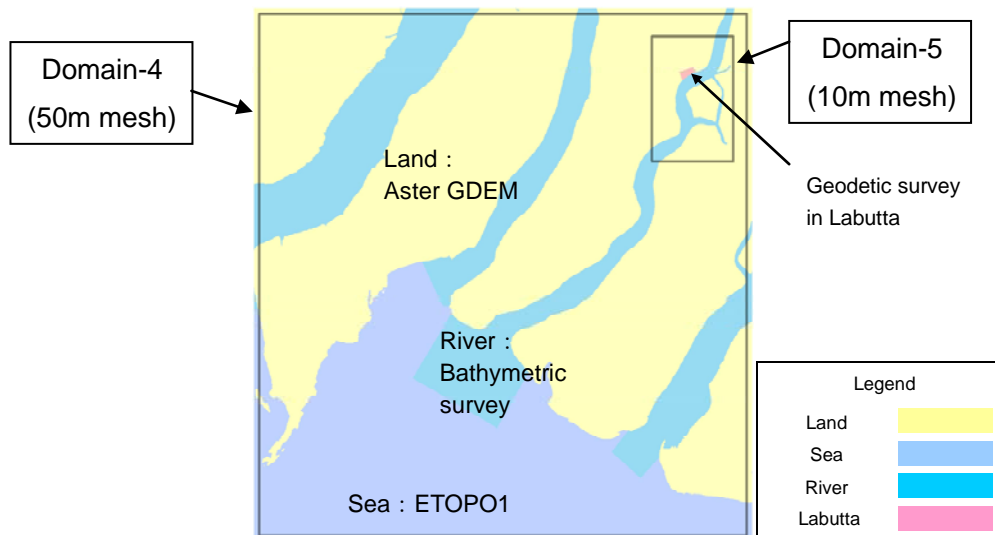
Computation Domain	Mesh Size	Land	River	Sea	Town of Labutta
1	1,800 m	ETOPO1			
2	600 m				
3	200 m				
4	50 m	Aster GDEM	Bathymetry survey by JICA Project Team	ETOPO1	Geodetic survey by JICA Project Team
5	10 m				

Source: JICA Project Team

ETOPO11 is the 1 arc-minute global relief model of earth's surface that contains digital elevation data. The advantage of ETOPO1 is that it contains a wide area of data and bathymetry features. ETOPO1 was applied for the 1,800 m and 600 m model.

Aster Global Digital Elevation Map (GDEM) is the detailed digital elevation data of 30 m mesh size. The advantage of Aster GDEM is accuracy of elevation. Aster GDEM was applied for the 200?m, 50 m and, 10 m models. It is noted that user registration and application form to National Aeronautics and Space Administration, Government of United States (NASA) or Ministry of Economy, Trade and Industry, Government of Japan (METI) are required, if the data is used for commercial purpose.

The topography model of 200 m, 50 m and, 10 m were made by Aster GDEM and the geodetic survey outputs by JICA Project Team. Spatial compositions of 50 m and 10 m models are shown in Figure 11.8.4.



Source: JICA Project Team




Figure 11.8.4 Composition of 50 m and 10 m Mesh Topography Models




11.8.3 SITE SURVEY OF CYCLONE NARGIS AND 2004 INDIAN OCEAN EARTHQUAKE TSUNAMI

The extent of inundation and damages by the Cyclone Nargis and the 2004 Indian Ocean Earthquake were surveyed in the town of Labutta and the Ywe River, which are the representative town and river in Delta area; respectively. The results of the site and interview surveys were used to verify the accuracy of outputs of the tsunami and storm surge simulations.

The records of interview survey are described below with their approximate locations in Figure 11.8.5 and Figure 11.8.6.

- 1) Around the jetty in Labutta (No. 15 in Figure 11.8.6), the water level exceeded the revetments during the onslaught of Cyclone Nargis. The inundation started at 15:00 and continued until midnight. In the 2004 Indian Ocean Earthquake Tsunami, inundation did not occur, but the water level almost reached the crown of revetments.
- 2) In the town center of Labutta (around No.13 in Figure 11.8.6), the buildings located almost four blocks away from the jetty were inundated during Cyclone Nargis. The inundation depth was between 0.1 m and 1.0 m.
- 3) Upstream of Labutta, the storm surge ran up the small rivers during Cyclone Nargis. Buildings were inundated and damaged.
- 4) In the mouth of Ywe River (No.5 in Figure 11.8.5), the inundation depth was 8 feet (2.44 m) during Cyclone Nargis. People evacuated to higher grounds, but inundation still reached up to neck height.
- 5) In the town center of Labutta (around No.13 in Figure 11.8.6), there was no damage on the buildings during Cyclone Nargis. In the settlements located west or east of Labutta, approximately 30 buildings had collapsed.
- 6) Around the market of Labutta (around No.13 in Figure 11.8.6), about two buildings were damaged in the 2004 Indian Ocean Earthquake Tsunami.
- 7) In the area from the river mouth of Labutta to the settlement at the downstream of Labutta (No.4 in Figure 11.8.5), almost all buildings collapsed because of Cyclone Nargis. Few buildings remained standing and people used them as evacuation buildings.








No.	1	2	3 (Sluice Gate)
Cyclone Nargis	Inundation: 0 m	Inundation: 6 ft (1.83 m)	Inundation: 1 m over dike
2004 Indian Ocean Earthquake and Tsunami	No information	No information	Inundation: 0.5 m in houses in front of sluice gate. The tsunami reached the crown of sluice gate.
Picture			

No.	4	5	6
Cyclone Nargis	Inundation: 1 m	Inundation: 8 ft (2.44 m)	Inundation: 0.75 m over dike
2004 Indian Ocean Earthquake and Tsunami	No information	No information	No information
Picture			



Source: JICA Project Team

Figure 11.8.5 Result of Site Survey (1/2)

No.	11	12	13
Cyclone Nargis	Inundation: 0.3 – 0.4 m	Inundation: 0.1 – 0.15 m	Inundation: 1 m
2004 Indian Ocean Earthquake and Tsunami	No information	No information	No information
Picture			
No.	14	15	16
Cyclone Nargis	Inundation: 4 ft (1.22 m)	Inundation: 1 ft (0.3 m)	Inundation: 0m
2004 Indian Ocean Earthquake and Tsunami	No information	Inundation: 0 m Waves almost reached crown of dike.	No information
Picture			
No.	17		
Cyclone Nargis	Inundation: 6 feet (1.83 m)		
2004 Indian Ocean Earthquake and Tsunami	No information		
Picture			



Source: JICA Project Team

Figure 11.8.6 Result of Site Survey (2/2)

11.8.4 GEODETIC SURVEY

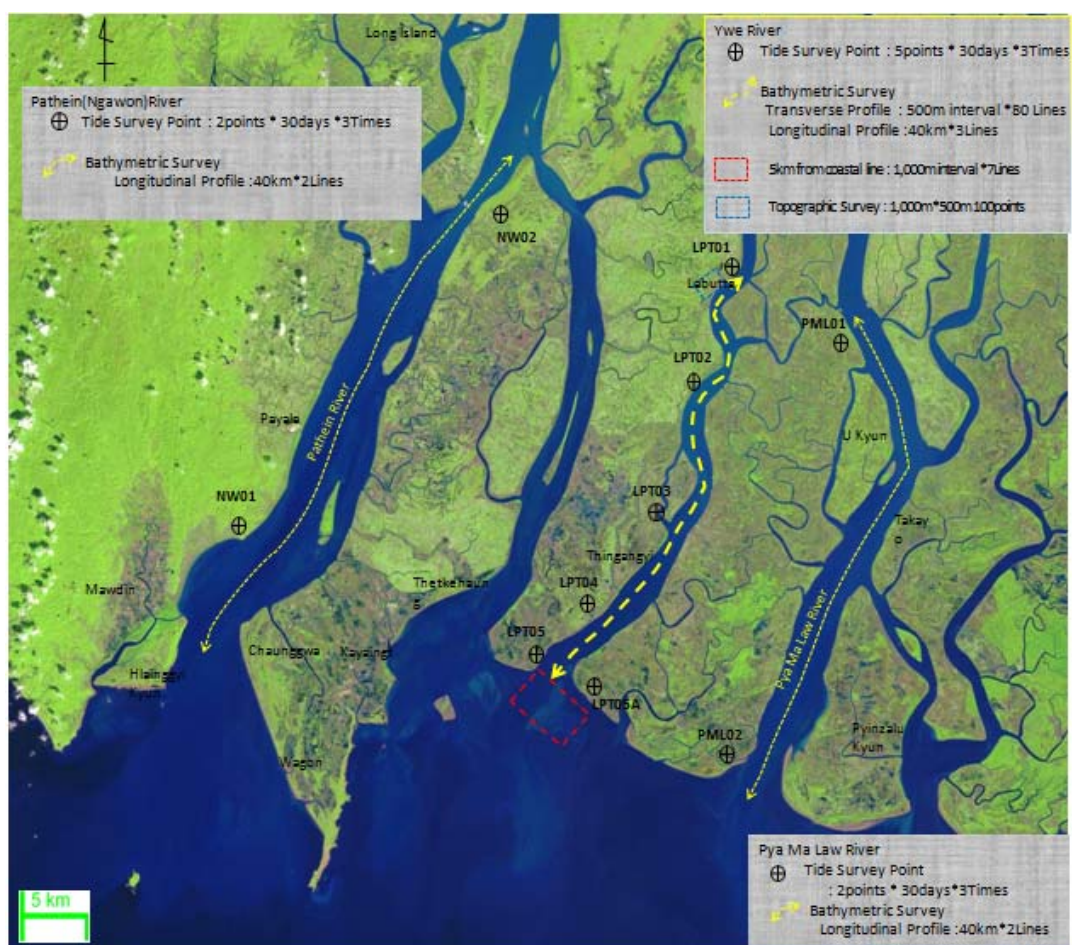
(1) Summary of the Survey

1) Objective of the Survey

Objective of the survey was to obtain the basic data necessary for setting condition of river channel, water level and terrain in town area for the storm surge and tsunami simulation. The survey conducted included the topography of Labutta, tide level and bathymetry of the Ywe River, Pathein River (Ngawon) and Pya Ma Law River which were main rivers in the delta area.

2) Survey Area

Figure 11.8.7 shows activity areas of each survey.



Background image: Landsat-8

Source: JICA Project Team

Figure 11.8.7 Survey Points

3) Items of the Survey

Table 11.8.3 and Table 11.8.4 show items, numbers, etc.

Table 11.8.3 Summary of the Survey (1/2)

Items	Numbers of Survey	Measurement Area	Remarks
Tide survey Measurement of control point	- two times at 13 points + one time at 11 points	Existing control point : two points Ywe River: five points of tenkm interval for 40 km from river-mouth Pathein River: two points at edge of river mouth and 40 km upstream from river mouth Pya Ma Law River: two points at edge of river mouth and 40 km upstream from river mouth Labutta town: two points	- Control point (known point) : No.0742 and No.0729 - The zero gauge elevations of tide staff/boards were obtained by leveling to the nearest control points. - Control points of each river were used as base station of RTK GPS ³ and DGPS ⁴ for bathymetric survey. - Control point in town area was used for topographic survey.
Tidal observation (Staff Gauge) Tidal observation (Automatic Tide Gauge)	- three times at nine points for 30 days - two times at two points for 30 days	Near the control points of each river Setting water pressure type of automatic tide gauge at LPT01 and LPT04 in the Ywe River	- Visual observation at ten minute intervals - Setting at staff gauge in both points - Automatic observation at ten minute intervals
Bathymetric Survey Bathymetric Survey (River) Ywe River	Cross section: 80 survey lines at 500 m intervals Longitudinal profile: three survey lines at right, center, left bank	- four zones at ten km intervals, totalling 40 km	- Bathymetric survey was implemented at RTK GPS base station which was set at control point - Control point at river mouth and upstream were set as base station and bathymetric survey was implemented by DGPS
Pathein River	Longitudinal profile: two survey lines at left and right bank	- 40 km range from river mouth to upstream	- Tide correction was dependent on results of tidal observation.
Pya Ma Law River	Longitudinal : two survey lines at left and right shore	- 40 km range from river mouth to upstream	

Source: JICA Project Team

Table 11.8.4 Summary of the Survey (2/2)

Items	Numbers of Survey	Measurement Area	Remarks
Bathymetric Survey (Coastal area) Ywe River mouth	five km of offshore: seven survey lines at 1 km intervals.	- six km intervals east and west from center of river mouth - Offshore: 5 km	- Control point at river mouth was set as base station and bathymetric survey was implemented by RTK GPS
Topographic survey in Labutta	Observation points: 100 points	- Town center - Along the river bank: 1,000 m - Inland : 500 m	- Coordinates and altitude were surveyed by traverse based on control point of Labutta area. - Photography of main intersection was taken for basic data simulation

³ Real Time Kinematic Global Positioning System

⁴ Differential Global Positioning System

	2012				2013		
	1st Survey		2nd Survey		3rd Survey		
	Feb	Mar	Aug	Sep	Jan	Feb	Mar
Tide Survey	GPS Survey ↔ Ywe River Observation ↔ Patheingyi River and Pya Ma Law River Observation ↔		GPS Survey ↔		GPS Survey ↔	Ywe River, Patheingyi River and Pya Ma Law River Observation ↔	
Bathymetric Survey	Ywe River and Coastal Area ↔ Patheingyi River and Pya Ma Law River ↔						
Topographic Survey						Lubutta City ↔	

Source: JICA Project Team

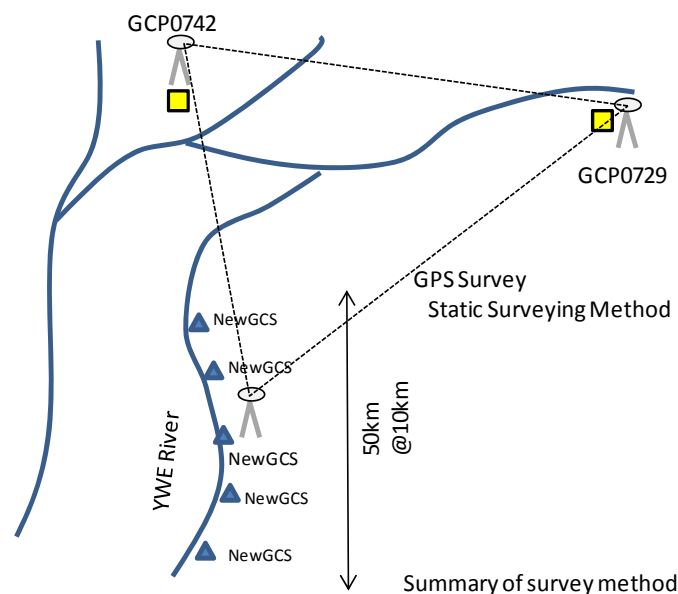
Figure 11.8.8 Schedule of the Survey

(2) Contents of the Survey

1) First Water Level Survey

(a) Measurement of Control Point

Static Global Positioning System (hereafter called Static GPS) was used in this survey for the setting of control points that were required for water level survey and bathymetric survey. New control points were set from two existing control points. A total of 11 control points consisting of two points in the Patheingyi River, five points in the Ywe River, two points in the Pya Ma Law River and two points in Lubutta area. Concrete pile was set in each new control point. Measurement of control points were implemented using the procedure shown in the Figure 11.8.9. Coordinate and altitude of new control points were obtained. Based on these control points, elevation of staff gauge which were used for tidal observation were obtained by leveling.



Source: JICA Project Team

Figure 11.8.9 Summary of Measuring Control points

(b) Tidal Observation (Staff Gauge)

Staff gauges for tidal observation were set in each river around new control points. The zero gauge elevations of tide staffs/boards were obtained by leveling to the nearest control points. Observation was implemented for 30 days which was recorded by staff gauge for ten minute intervals. The observers measured water levels at ten minute intervals, and recorded those for 30 days.

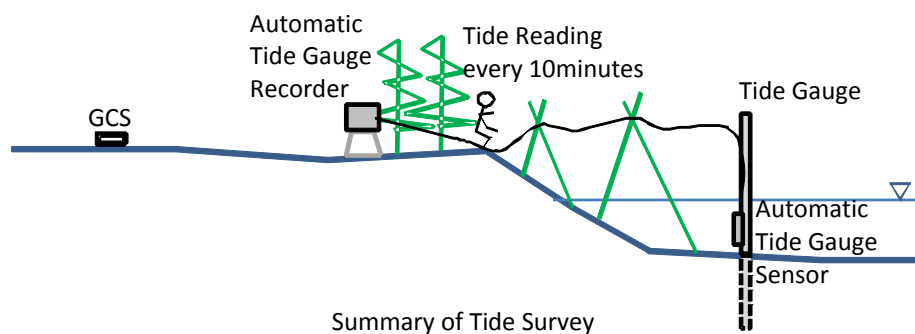


Source: JICA Project Team

Figure 11.8.10 Setting Staff gauges

(3) Tidal Observation (Automatic Tide Gauge)

Tidal observation was implemented for 30 days by using water pressure-type automatic tide gauges. The observation was implemented in parallel with visual observation of staff gauges at upstream (LPT01) and river mouth (LPT04) in the Ywe River. The sensor of the automatic tide gauge was set on the staff gauge. At LPT01, the recorder was set on land in which the cable was pressed over the river bank using bamboo piers. At LPT04, to keep the water depth, setting point of staff gauges was far from the river bank. Therefore the recorder was set on a boat which was fixed near the staff gauge. The interval of water level recording was set at ten minutes. At the starting time of the observation, the zero gauge elevation was calibrated with the staff gauge.



Source: JICA Project Team

Figure 11.8.11 Summary of Tidal Observation

(4) Second Water Level Survey

The objective of the second survey was to implement tidal survey in a rainy season. The survey was implemented for 30 days which was of the same duration as the first survey. The control points installed in the first survey were checked with the existing national control points by Static GPS, using the same procedure as the first survey. LPT05 in the Ywe River could not be observed due to river flooding. Alternatively, LPT05A was set at the opposite side of the river. In addition, flow velocity at LPT04 in the Ywe River was increased because of the flood. Therefore, the point of staff gauge and automatic tide gauge were moved to the tributary.



Source: JICA Project Team

Figure 11.8.12 Point of Tidal Observation

(5) Third Water Level Survey

The objective of the third survey was to confirm the fluctuation of water level in a dry season. Before the start of the water level survey, the control points which were used in the second survey were checked by Static GPS. The third survey was done in order to get the water level survey by using staff gauges. Staff gauges were set in the same points as in the second survey. The survey was implemented for 30 days and accurately took the records of the water levels with staff gauges at 10 minute intervals.



Source: JICA Project Team

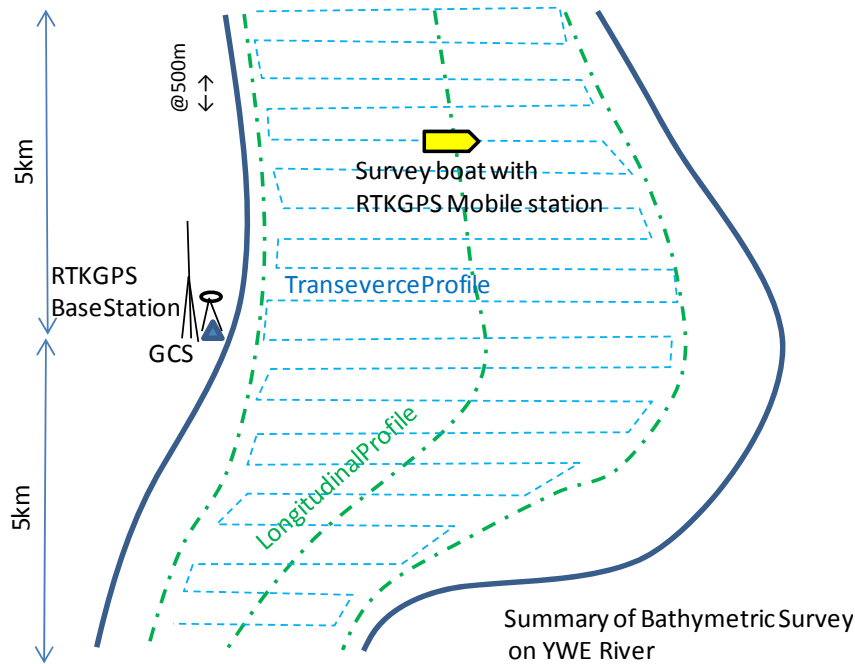
Figure 11.8.13 Setting Staff Gauges and Survey of Control Points

(6) Bathymetric Survey

The bathymetric survey was implemented at the three main rivers to set the condition of river cross section for simulation of storm surge and tsunami. Surveying all rivers in delta area were not realistic considering the timeline of the study, therefore; only cross section and longitudinal profile survey were implemented in the Ywe River. Only the profile surveys were conducted in the Patheingyi River and the Pyaw Oon River, and cross sections of the two rivers were estimated from the pattern of the Ywe River.

1) Cross Section and Longitudinal Profile Survey in the Ywe River

The base stations for RTK GPS were set at the nearest control points, and the coordinate and elevation of the boat for echo sounding were obtained. The cross-sectional survey in the Ywe River was implemented by setting 80 sections at 500m intervals from river-mouth to 40 km upstream. Cross-section survey was implemented on block of each new control points. Profile survey was set in three survey lines which were right, center and left side in the river channel, and bathymetric surveying was implemented in each block.

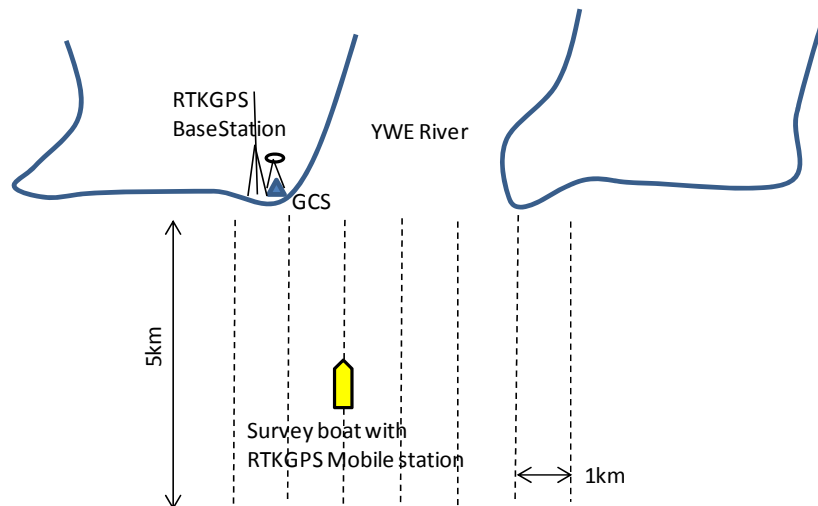


Source: JICA Project Team

Figure 11.8.14 Summary of Bathymetric Survey using RTK GPS in the Ywe River

2) Bathymetric Survey of River Mouth of the Ywe River

The bathymetric survey was implemented in a total of seven survey lines perpendicular to the coastline at 1 km intervals with width of 5 km from the coastline as shown in Figure 11.8.15. The water depth was measured using an echo sounder, and the coordinates and elevation of the boat was obtained by RTK GPS.

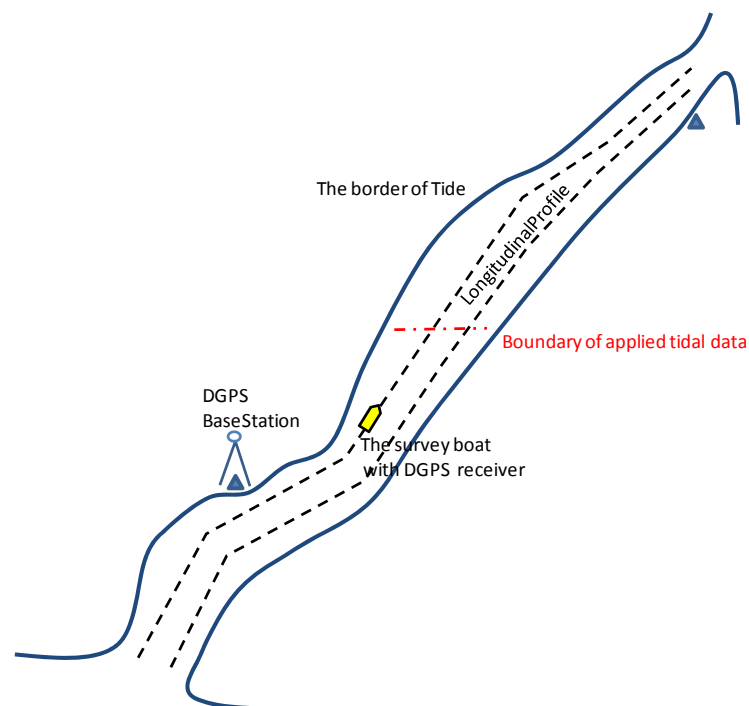


Source: JICA Project Team

Figure 11.8.15 Summary of Bathymetric Survey in River-mouth of the Ywe River

3) Longitudinal Profile Survey of the Patheingyi River and the Pya Ma Law River

The longitudinal profile survey was implemented from river mouth to 40 km upstream of the Patheingyi River and the Pya Ma Law River. The profile survey had two survey lines at the left and right sides of the river channel. The position of the boat was measured by DGPS of which the base station was set at the control points, and the water levels were measured by using an echo sounder. The measured depths were the observed tide levels at the control points upstream or downstream.



Source: JICA Project Team

Figure 11.8.16 Summary of Longitudinal Profile Survey in the Patheingyi River and the Pya Ma Law River

(7) Topographic Survey in Labutta Area

The topographic survey was implemented in Labutta for simulation of storm surge and tsunami. The traverse survey was mainly conducted at intersections of major streets based on the control points, installed by the GPS survey. Coordinates and altitude were obtained for the main intersections and traverse points, and results of the survey were plotted on the map. In addition, to check situation of surrounding buildings at the main intersections, photographs were taken from four sides of the intersections.



Source: JICA Project Team

Figure 11.8.17 Area of Topographic Survey in Labutta Town



Source: JICA Project Team

Figure 11.8.18 Photos of Topographic Survey and Intersection

11.8.5 TIDE OBSERVATION IN DELTA

(1) Summary of the Observation

1) Objective of the Observation

Tidal observations were conducted on the Ywe River flowing through the western part of Ayeyarwaddy Delta, the Patheingyi River flowing through the west side of the Ywe River, and the Pya Ma Law River flowing through the eastern side of the Ywe River. The characteristics of the tide levels were analyzed based on the observation data, and the tide level conditions for calculation of tsunami and high tide were obtained from the result of the harmonic analysis.

2) Observation Points

Five observation points in the Ywe River were established at 5-10 km intervals for approximately 30 km from the river mouth to Labutta in the Ywe River. In the Patheingyi River and the Pya Ma Law River, two observation points were set near the river mouth and at about 30 km upstream from the river mouth. Therefore, the observation points were nine in total.



Source: JICA Project Team

Figure 11.8.19 Location of Observation Points

Table 11.8.5 Coordinates of Observation Points

River Name	Latitude	Longitude	Easting	Northing	Elev. (MSL/Orho.)	Description
Ywe River	16°08'59.62017"N	94°46'14.39141"E	689329.882	1786329.909	2.220	LPT-01/No. 1
	16°04'43.33973"N	94°43'10.07734"E	683919.668	1786329.909	2.010	LPT-02
	16°00'41.83288"N	94°41'47.91365"E	681538.583	1786329.909	1.850	LPT-03
	15°57'29.43618"N	94°37'26.19832"E	673804.267	1786329.909	2.400	LPT-04/No. 4
Patheingyi River	15°56'19.16564"N	94°34'56.61385"E	669372.617	1762792.375	1.991	LPT-05
	16°03'27.47971"N	94°23'52.57087"E	649537.072	1775815.125	1.140	NW-01
Pya Ma Law River	16°13'08.20707"N	94°35'52.43776"E	670793.126	1793819.577	1.550	NW-02
	16°06'13.06557"N	94°50'19.41759"E	696655.305	1781273.810	1.620	PML-01
	15°52'08.46647"N	94°43'07.1102"E	684023.919	1755201.867	1.910	PML-02

Note: No. 1 and No. 4 indicates the location where a automatic water-level gauge was set to observe, in addition to the visual observation

Source: JICA Project Team

(b) Observation Method

In the visual observation, the leveling rod was fixed as shown in the photograph below at a place which did not appear even at spring tide, and the water levels were recorded at intervals of 10 min.

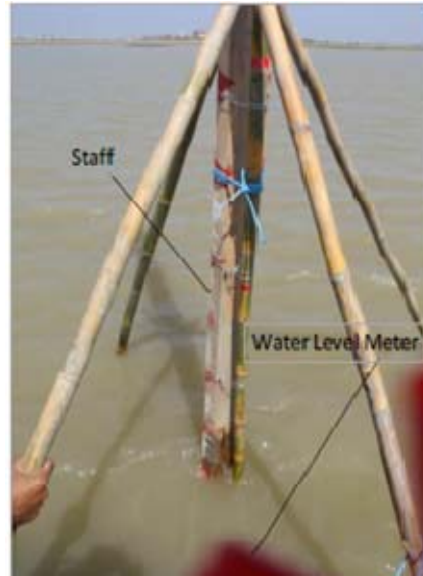
In No.1 where an automatic water level gauge was installed, a temporary jetty was installed and the water level sensor was fixed to its pier. In addition, the recording unit was fixed to a stable place near the jetty, and the data was recorded automatically.

Also, in No.4 using a water-level gauge, the water level sensor was fixed to the tide staff/board. The waterproof recording unit was installed in the boat moored to the staff/board, and the data was automatically recorded.



Source: JICA Project Team

Figure 11.8.20 Situation of the Observation Points



Source: JICA Project Team

Figure 11.8.21 Equipment installed at LPT-04 and No.4



Source: JICA Project Team

Figure 11.8.22 Recording of Water Level by Transit at Intervals of Ten Minutes

(2) Observation Results

1) Compendium of the Observation Data

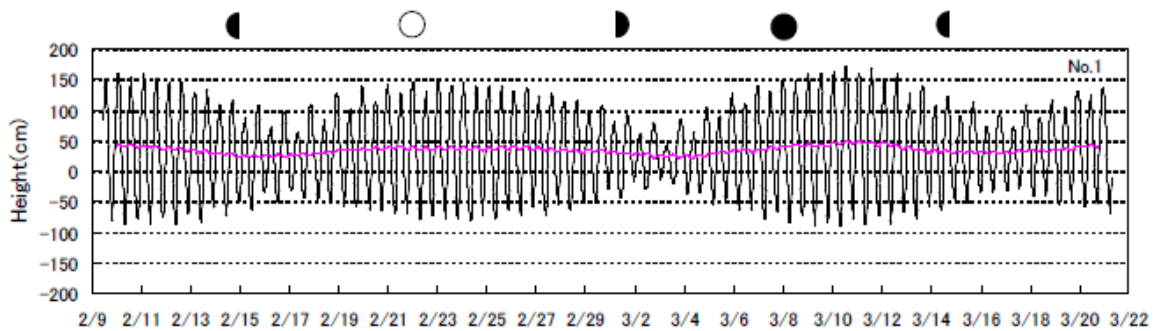
The difference in tide levels of 10 to 20 cm was identified between two times of the observation data collected in the dry season. Mean water level in the rainy season was higher than that in the dry season by the rising of the river. For example, the difference in mean tide levels between the first round of the dry season and the rainy season was 40 cm at LPT-05 in the Ywe River, while about 10-20 cm at other points in the Ywe River and 15 cm at PML-02 in the Pya Ma Law River. There were mostly no differences at two points in the Patheingyi River.

In all results, a similar tendency of data was identified. The tide level observation data collected in the first round of the dry season is shown in Figure 11.8.23 as a typical case.

The tidal curve indicated regular movement, and the tidal change fluctuation corresponded to the phase of the moon. Therefore, it was identified that the water level fluctuation at the coastal area did not change until at least Labutta in the upper reaches of the Ywe River.

In addition, the peak at the spring tide after full moon (O) appeared in one day, while the peak after new moon (●) was seen in two to three days.

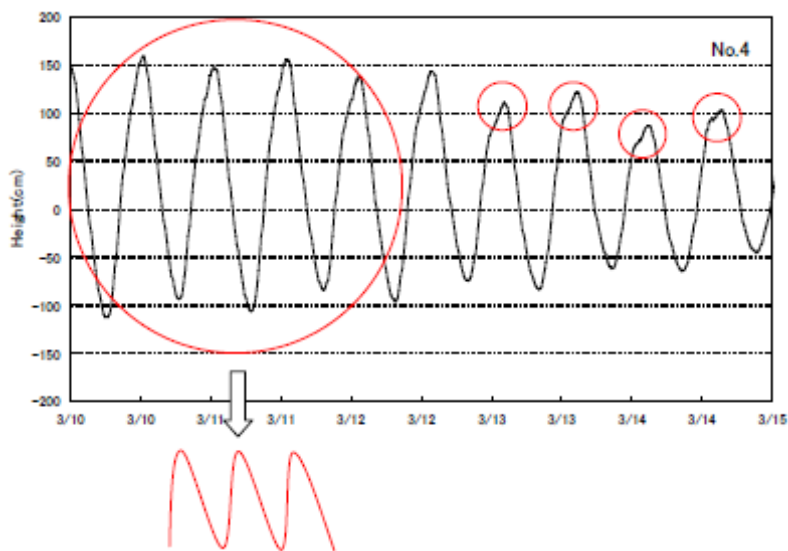
As shown in Figure 11.8.24 of the enlarged waveform, the upward speed of rising tide was faster than downward speed of ebbing tide, and the stage hydrograph lacked symmetry. Moreover, the upward speed of water level decreased discontinuously around the peak of the rising tide, and the tendency for the waveform of water level to deviate from the tide curve was identified.



Note: First Round of the Dry Season (No.1, measurement by automatic water level gauge)

Source: JICA Project Team

Figure 11.8.23 Typical Example of Observation Result



Note: (No.4 [measurement by automatic water level gauge], example of the first round of the dry season)

Source: JICA Project Team

Figure 11.8.24 Diagram of Wave Distortion

2) Characteristics of Tide Levels

(a) Tide Levels and Tidal Ranges

Table 11.8.7 to Table 11.8.9 show the organized data of tide levels and tidal ranges by comparing the highest and lowest values. Maximum tidal range in all observation points was over 2 m. In addition, tidal range in the rainy season tended to be slightly larger than that in the dry season.

Some observation points in the Ywe River recorded more than 2.7 m of tidal range. The tendency that the tidal ranges become larger when the observation points get closer to the river mouth was not identified.

The average interval between high tides was 12.4 hr in all observation points and in all periods. Namely, half-diurnal tide pattern was identified.

Table 11.8.7 Tide Levels and Tidal Ranges (First Round of the Dry Season)

		Ywe River							Pya Ma Law River		Pathein River	
		No. 1	No. 4	LPT-01	LPT-02	LPT-03	LPT-04	LPT-05	MPL-01	PML-02	NW-01	NW-02
Tidel Level (cm)	High	170	179	181	170	179	173	170	158	152	105	138
	Low	-89	-94	-108	-96	-83	-93	-136	-113	-117	-125	-114
Tidal Ranges (cm)	Max.	259	273	267	249	246	264	277	265	269	230	247
	Min.	56	40	55	53	52	40	153	55	51	51	74
	Ave.	181	169	185	180	178	172	213	181	169	148	172
Interval between high tides (hr)		12.44	12.44	12.43	12.44	12.43	12.44	12.44	12.44	12.40	12.42	12.42

Source: JICA Project Team

Table 11.8.8 Tide Levels and Tidal Ranges (Rainy Season)

		Ywe River							Pya Ma Law River		Pathein River	
		No. 1	No. 4	LPT-01	LPT-02	LPT-03	LPT-04	LPT-05	MPL-01	PML-02	NW-01	NW-02
Tidel Level (cm)	High	183	164	185	183	189	181	181	181	168	131	165
	Low	-83	-83	-92	-94	-96	-93	-96	-91	-109	-121	-82
Tidal Ranges (cm)	Max.	266	247	276	277	285	264	277	272	278	244	247
	Min.	68	55	82	66	65	55	51	66	46	61	69
	Ave.	193	165	199	193	198	183	185	190	183	166	181
Interval between high tides (hr)		12.42	12.42	12.42	12.42	12.42	12.44	12.44	12.44	12.40	12.42	12.42

Source: JICA Project Team

Table 11.8.9 Tide Levels and Tidal Ranges (Second Round of the Dry Season)

		Ywe River					Pya Ma Law River		Pathein River	
		LPT-01	LPT-02	LPT-03	LPT-04	LPT-05	MPL-01	PML-02	NW-01	NW-02
Tidel Level (cm)	High	156	142	153	146	143	151	135	89	128
	Low	-107	-104	-100	-100	-102	-92	-107	-126	-104
Tidal Ranges (cm)	Max.	257	246	245	243	245	238	242	211	220
	Min.	54	42	66	35	33	44	50	34	43
	Ave.	186	174	174	166	167	176	165	147	163
Interval between high tides (hr)		12.41	12.41	12.40	12.41	12.41	12.41	12.44	12.42	12.40

Source: JICA Project Team

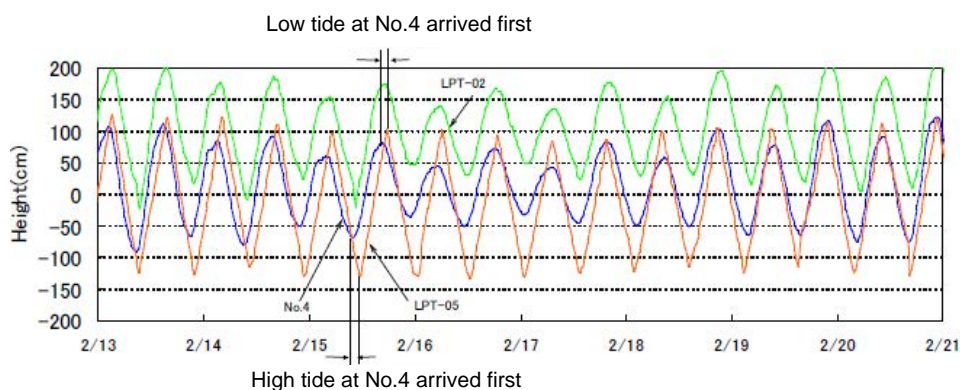
(b) Characteristics of Tide Cycle

As shown in Table 11.8.7 to Table 11.8.9 described above, the average interval of the high tide was about 12.4 h in any observation points. Moreover, the next predominant component was the diurnal tide of 24 hr, while periodic component of 6 hr and 4 hr were also identified.

(c) Characteristics of Tidal Times

Figure 11.8.25 shows the tidal times at high tide and at low tide in each point of the Ywe River, comparing with tidal times at LPT-05 (05A) located in the river mouth. The blue line shows the tidal times at LPT-04 (No. 4) near LPT-05, and the red line, blue line, and green line is the order of distance from the river mouth.

Since tides are propagation of long waves, tidal times are expected to become late in the upper stream, shifting to the upper side in the graph of Figure 11.8.25. However, while the neap tide was approaching in the first round of the dry season, the tides at the upstream of LPT-05 tended to arrive earlier (negative value) than that at LPT-05. When the waveform became asymmetrical in shape that occurred easily at LPT-05, the tidal times tended to reverse as shown in Figure 11.8.25. On the other hand, in the rainy season and the second round of the dry season when the observation point was shifted to LPT-05A, the tendency for the tidal times to arrive late in the upper stream was constantly identified.



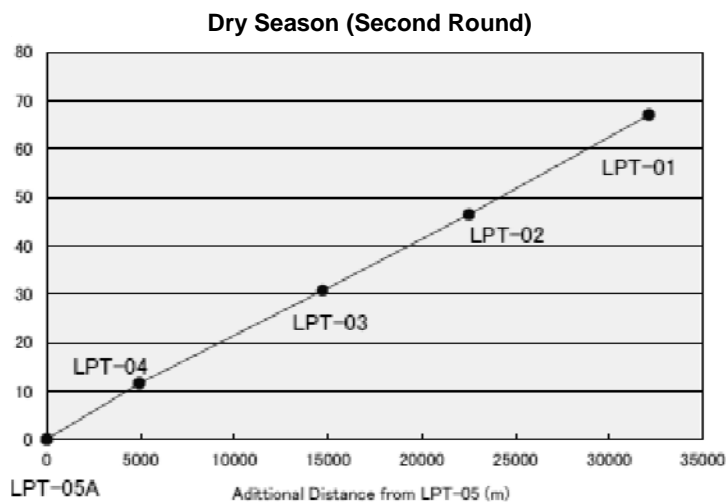
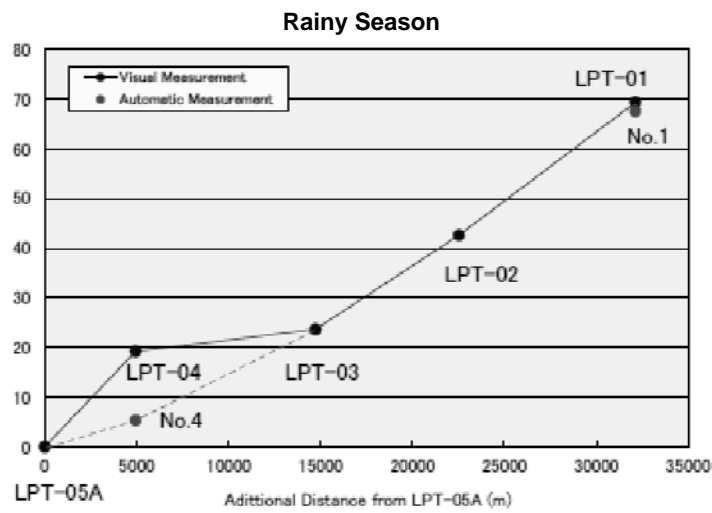
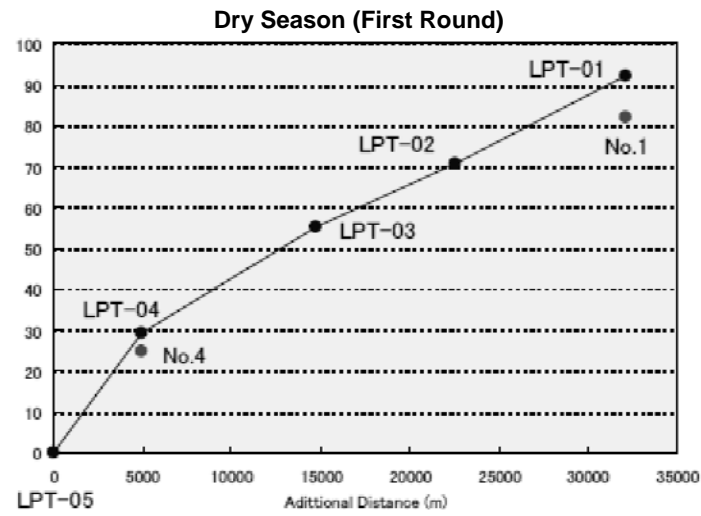
Source: JICA Project Team

Figure 11.8.25 Example of Comparison of Tide Curves

The observation point at the mouth of the Ywe River was changed to LPT-05A on the left river bank in the rainy season and in the second round of the dry season. In LPT-05A, tidal times tended to arrive late in the upper stream and the reversed trend was hardly observed. The gaps of tidal times between the river mouth and Labutta were about 50-100 min.

In the Pya Ma Law River, PML-01 was the observation point at the upper stream, and the time of high tides and low tides lag as much as 80 min on average behind those at PML-02. Similarly, in the Pathein River, the time of high tides and low tides at NW-02, the point in the upstream, lag as much as 80 min behind those at NW-01.

Figure 11.8.26 shows the average value of tidal time delay from LPT-05 (LPT-05A) the observation point at the mouth of the Ywe River, calculated from the observation data four days before or after the spring tide. About 90 min of tidal time delay was observed at LPT-01 located in Labutta in the first round of the dry season. Therefore, the average delay rate of the tidal time was 3 min/km. On the other hand, in the rainy season and the second round of the dry season after the observation point was shifted to LPT-05A, since the tidal time delay at LPT-01 was about 70 min, the average delay rate of the tidal time was 2 min/km.



Note: The horizontal axis shows accumulation of the distances between observation points.

Source: JICA Project Team

Figure 11.8.26 Distribution of Tidal Time Delay from LPT-05 (LPT-05A),
Observation Point at the Mouth of the Ywe River

(3) Harmonic Analysis

1) Calculation of Harmonic Constants

Harmonic analysis of 29 component tides were conducted by using the data collected during the period indicated by the arrows in Table 11.8.6. The results of analysis are shown in Table 11.8.10 to Table 11.8.12. Neap high high water (NHHW), the average highest water level at full and new moon is the value obtained by adding the mean water level A0 to M2+S2+K1+O1, while neap lowest low water (NLLW), the average lowest water level at full and new moon is the value obtained by subtracting M2+S2+K1+O1 from the mean water level A0.

Half diurnal tide was predominant in all periods and in all observation points.

Table 11.8.10 List of Harmonic Constants (Dry Season: First Round)

	No. 1	No. 4	LPT-01	LPT-02	LPT-03	LPT-04	LPT-05	PML-01	PML-02	NW-01	NW-02
M2 + S2 + K1 + O1	126.6	123.3	127.20	120.1	114.1	121.4	130.4	140.5	118.0	87.5	108.5
N.H.H.W.	161.1	160.6	161.7	154.0	153.1	159.0	140.4	154.6	136.2	78.3	118.9
N.L.L.W.	-92.1	-86.0	-92.7	-86.2	-75.1	-83.8	-120.4	-126.4	-99.8	-96.7	-98.1
(K1 + O1)/(M2 + S2)	0.20	0.19	0.18	0.21	0.15	0.17	0.09	0.18	0.17	0.05	0.21

Source: JICA Project Team

Table 11.8.11 List of Harmonic Constants (Rainy Season)

	No. 1	No. 4	LPT-01	LPT-02	LPT-03	LPT-04	LPT-05	PML-01	PML-02	NW-01	NW-02
M2 + S2 + K1 + O1	142.1	117.2	145.60	146.1	138.0	136.0	136.8	137.2	141.0	116.2	127.1
N.H.H.W.	199.0	166.5	199.8	194.6	189.3	184.8	185.9	187.6	180.4	133.4	172.8
N.L.L.W.	-85.2	-67.9	-91.4	-97.6	-86.7	-87.2	-87.7	-86.8	-101.6	-99.0	-81.4
(K1 + O1)/(M2 + S2)	0.17	0.22	0.19	0.17	0.22	0.17	0.16	0.18	0.16	0.17	0.19

Source: JICA Project Team

Table 11.8.12 List of Harmonic Constants (Dry Season: Second Round)

	LPT-01	LPT-02	LPT-03	LPT-04	LPT-05A	PML-01	PML-02	NW-01	NW-02
M2 + S2 + K1 + O1	151.80	137.8	144.9	131.7	127.4	145.3	139.5	107.7	134.6
N.H.H.W.	176.6	160.9	173.9	159.8	152.9	173.1	160.8	98.8	148.5
N.L.L.W.	-127.0	-114.7	-115.9	-103.6	-101.9	-117.5	-118.2	-116.6	-120.7
(K1 + O1)/(M2 + S2)	0.14	0.16	0.14	0.16	0.18	0.16	0.25	0.19	0.16

Source: JICA Project Team

(4) Characteristics of Tide Around the Ywe River

Tidal characteristics obtained from the results of the three periods of observation, twice in the dry season and once in the rainy season, were summarized as follows:

1) Mean water level in the rainy/dry season

The difference of the mean water levels between the rainy season (when the river was rising) and the dry season was about 40 cm at the highest area. However, since the mean water levels at some points

differed between the first round of the dry season and the second round of the dry season, it is thought that water level in the rainy season would also vary in height from year to year.

2) Water level fluctuation

Water level fluctuation at each observation point responded to the oceanic tide fluctuation corresponding to the phase of the moon. This means that the Ywe River, including the uppermost stream in the observational range, were strongly subject to the influence of the tide.

3) Waveform distortion

Tidal waveform had an asymmetric curve which was often seen at the river mouth, and the tidal curve at low tide deviated from the astronomical tidal curve. This deviation made up the difference of about 20-30 min in tidal times from the predicted values.

4) Tidal range (Tidal variation)

The tidal range was small from the river mouth to the uppermost stream in the survey area. Moreover, the difference between the dry season and rainy season was not big, either. The tidal range in both the dry season and rainy season was about 2 m.

5) Characteristics of tide cycle

The result of spectral analysis showed that half-diurnal tide was predominant in all periods and in all observation points, which coincided with the result of the harmonic analysis.

6) Gap of tidal times

Tidal times arrived late in the upper stream. In case of the Ywe River, the delay rate of the tidal time was 2-3 min/km toward the upstream site. However, the gap of the tidal times between the river mouth and Labutta varied to some extent from 50 to 100 min.

7) Result of harmonic constants

M2 and S2 component tides were predominant in almost all periods and in almost all observation points. The difference between the predicted tide levels based on the harmonic constants obtained from the analysis result and observational tide levels were within 25 cm in all cases.

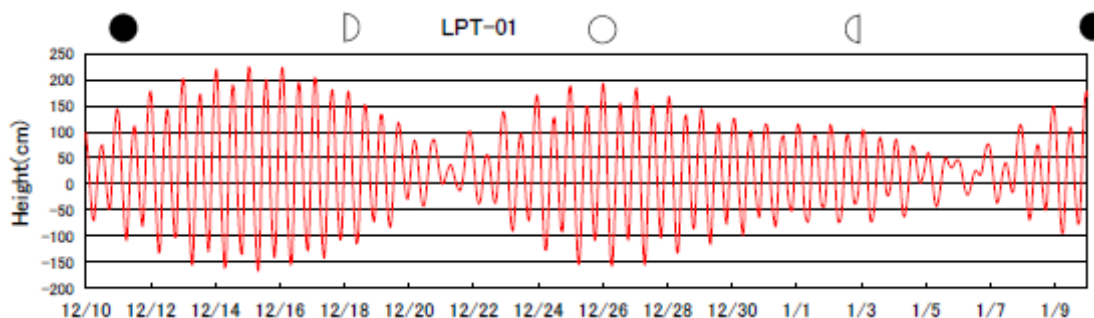
(5) Prediction of Tide Levels in Case of Disaster

A three-day astronomical tide at each observation point was predicted when the Indian Ocean Earthquake and Tsunami (December 26, 2004) and Cyclone Nargis (May 2, 2008) occurred.

1) 2004 Indian Ocean Earthquake and Tsunami

Since the Indian Ocean Earthquake occurred in December in the dry season, tide levels were predicted based on the harmonic constants calculated by using observation data collected in the second round of the dry season. The result is shown in the figure below.

When the earthquake occurred, it was at the spring time, and it was estimated that tide levels went up by about 2m in Labutta (LPT-01).



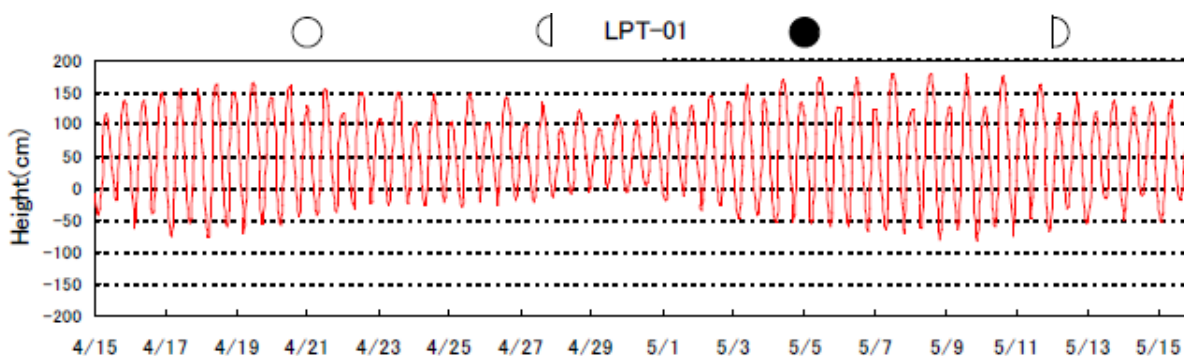
Source: JICA Project Team

Figure 11.8.27 Predicted Tide Level During the 2004 Indian Ocean Earthquake

2) Cyclone Nargis

Since the storm surges caused by Cyclone Nargis occurred in May in the beginning of the rainy season, tide levels were predicted based on the harmonic constants calculated by using observation data in the rainy season. The result is shown in the figure below.

Since the storm surges occurred between the neap tide and spring tide, the high water level was estimated to be 50 cm lower than that at the spring tide, although it varied with location.



Source: JICA Project Team

Figure 11.8.28 Predicted Tide Level during Cyclone Nargis

11.8.6 TOPOGRAPHY MODEL OF THE DELTA AREA

The topography model of the delta area was prepared and used in the simulations of both the storm surge analysis and tsunami analysis.

(1) Calculation Domain

The nesting method was applied in the storm surge and tsunami simulation. In the nesting method, several calculation domains with different mesh size can be combined, and the integrated calculation from wide calculation domain (large mesh size) to narrow calculation domain (small mesh size) become possible. The five-step nesting model was applied.

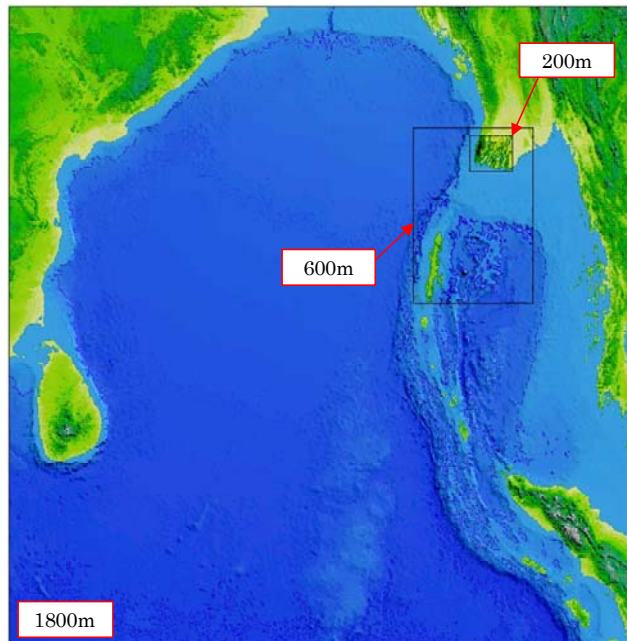
Domain 1 (1800 m mesh):	The area of the Bay of Bengal and the Andaman Sea
Domain 2 (600 m mesh):	The area from the epicenter to the delta area
Domain 3 (200 m mesh):	The delta area
Domain 4 (50 m mesh):	The area from the river mouth of the Ywe River to the town of Labutta

Domain 5 (10 m mesh): The area around the town of Labutta

The area of each domain is shown in Figure 11.8.29 and Figure 11.8.30.

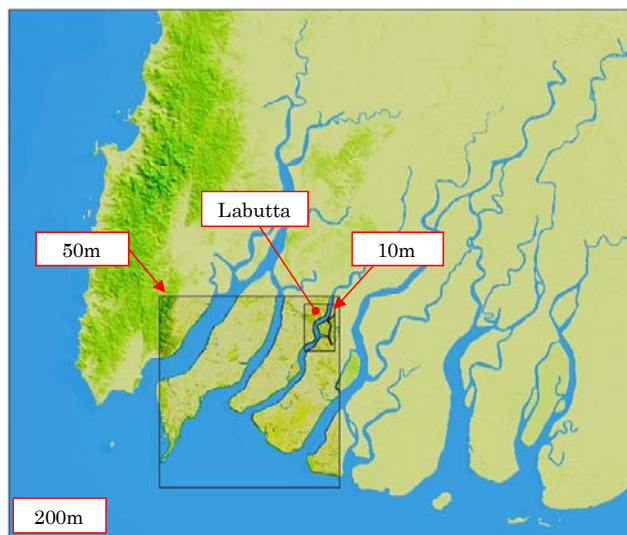
(2) Land Elevation

Land elevation data of Domains 3, 4, and 5 were prepared with the geodetic survey data (for Labutta) and the Aster GDEM (for the whole area except for Labutta). There were differences in elevation between Aster GDEM and the geodetic survey data, and the elevation of Aster GDEM was adjusted.



Source: Prepared by the JICA Project Team based on data of ETOPO1

Figure 11.8.29 Calculation Domains 1, 2, and 3



Source: Prepared by the JICA Project Team based on data of ETOPO1

Figure 11.8.30 Calculation Domains 3, 4, and 5

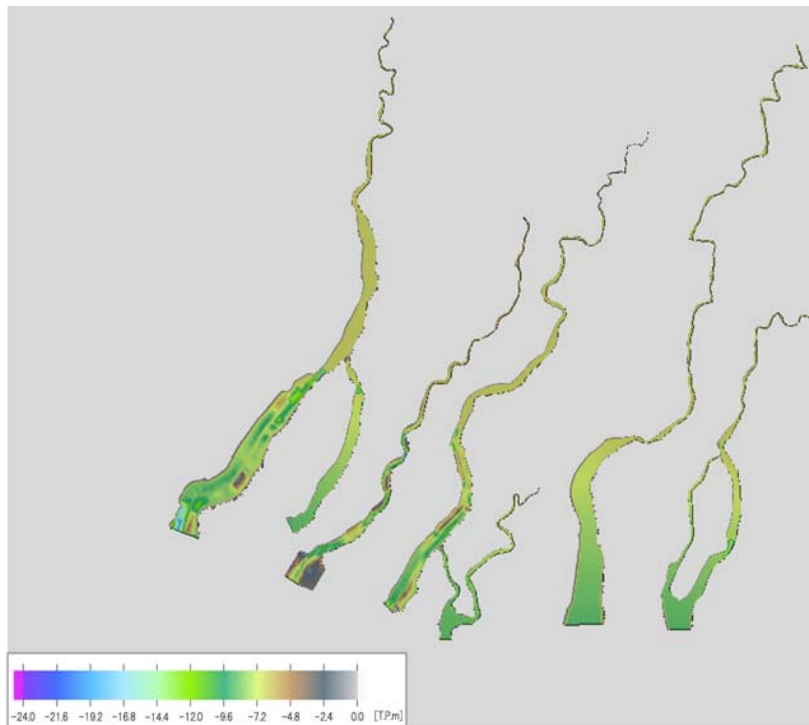
(3) Bathymetric Feature

There are differences in elevation between ETOPO1 and the geodetic survey data on the river mouths. The differences were corrected by interpolation of both data following the procedure described below:

- 1) The boundary of land and sea was defined. Some parts of neritic zone were recognized as land in ETOPO1. Therefore, the coastal line of ETOPO1 was changed as -1 m in water depth.
- 2) The differences of the geodetic survey data and ETOPO1 in the river mouths were checked. The ETOPO1 data around the edge of the geodetic data was deleted. The deleted portions were interpolated with ETOPO1 and the geodetic survey data.

(4) River Feature

The data on river features was generated from the river cross section and profile survey outputs. Details are described in the Appendix.



Source: JICA Project Team

Figure 11.8.31 River Feature

(5) Causeway

The roads marked in red line shown in Figure 11.8.32 are constructed as causeway at higher elevation of approximately 1.0 m from the surrounding area. These causeway roads prevent inundation of inland areas in case of tsunamis and storm surges. Therefore, the roads were considered in the topographic model as line features with height of +1 m of mesh elevation.



Source: JICA Project Team

Figure 11.8.32 Causeway

(6) Classification of Land Use and Roughness Coefficient

1) Collection of Land Use Data

Land use data was collected for setting of roughness coefficient as shown in Figure 11.8.33. The collected land use data did not cover the west portion of the study area. The missing land use data was filled in by using satellite imagery analysis. The details of the satellite imagery analysis are described in the Appendix.

2) Reclassification of Land Use Data and Setting of Roughness Coefficient

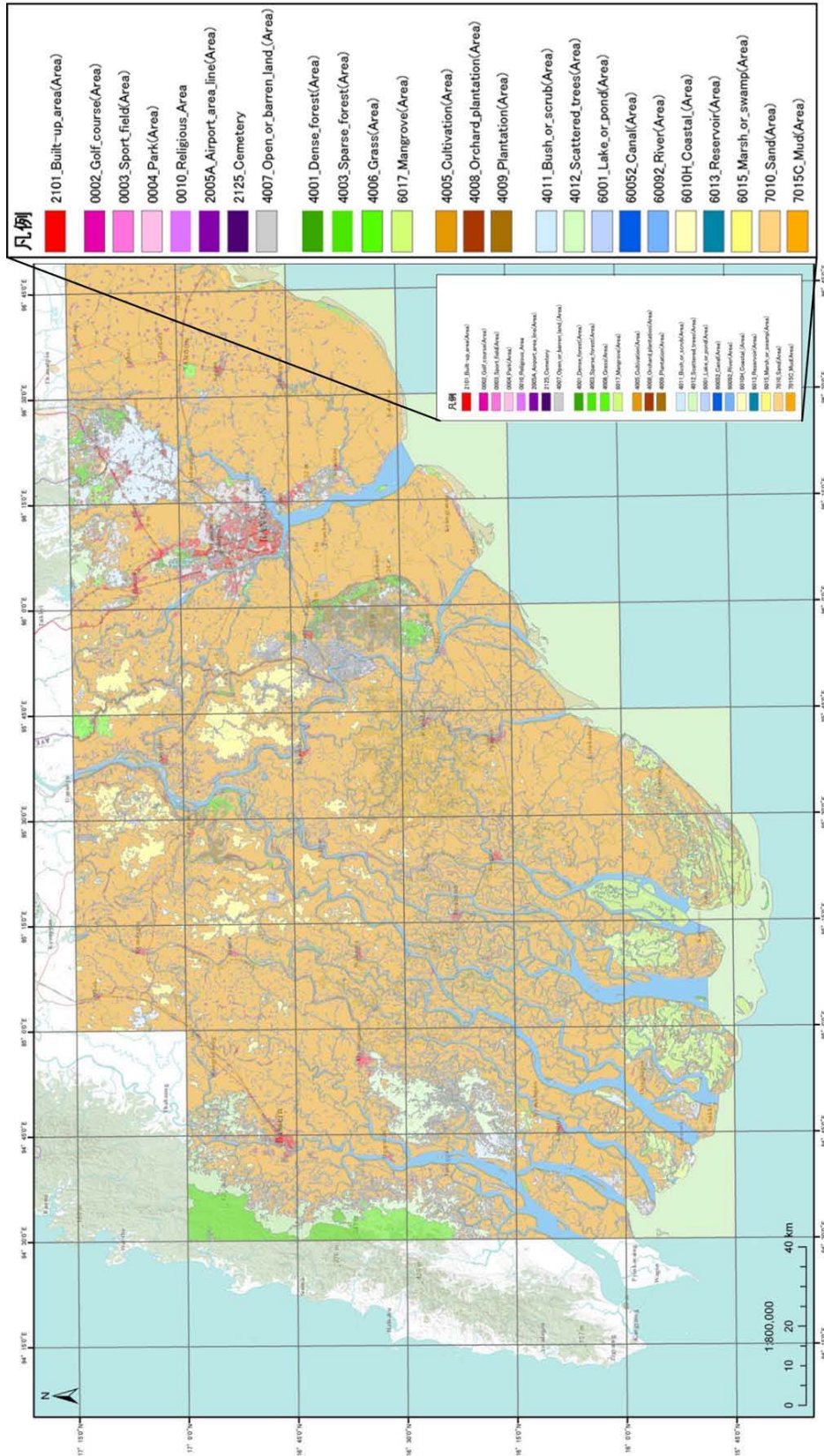
The collected land use dataset was reclassified to set the roughness coefficient. The reclassification table is shown in Table 11.8.13. The roughness coefficients were set considering the references listed below:

- | | |
|--------------|--|
| Reference 1) | Komura, Imamura, and Syuto, Tsunami Simulation and Damage Estimation with GIS, Coastal Engineering Journal of Japan, Vol. 45, pp.356-360, 1998 |
| Reference 2) | Expert Panel of Tonankai and Nankai Earthquake, Center Disaster Prevention Council of Cabinet Office of Japan, Documents of 26th meeting, Appendix No.6, p.6-2, 2006 |

Table 11.8.13 Classification of Roughness Coefficient

Classification	Roughness Coefficient	Land Use
Water body	0.025	Lake or pond, canal, river, coast, reservoir, marsh or swamp, sand, mud
Agricultural land	0.020	Cultivation, orchard plantation, plantation
Forest	0.030	Dense forest, sparse forest, grass, bush or scrub, scattered trees, mangrove
Built-up area	0.060	Built-up area
Other land use	0.025	Golf course, sports field, park, religious sites, airport, cemetery, open or barren land

Source: JICA Project Team

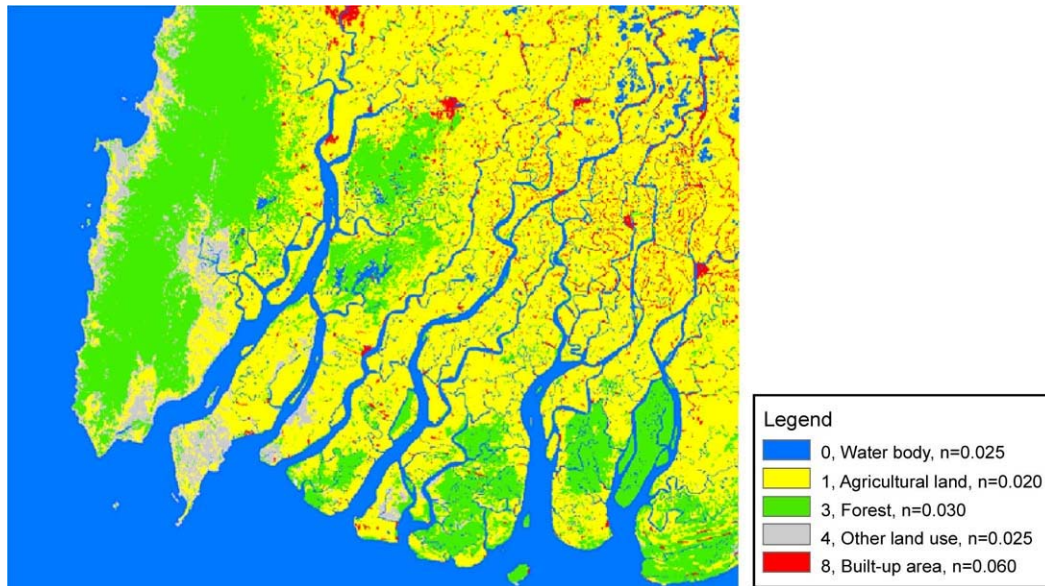


Source: The Establishment of Geographic Database for the National Rehabilitation and Development Programme in the Union of Myanmar, JICA, August 2004

Figure 11.8.33 Collected Land Use Data

3) Roughness Coefficient Map

The prepared roughness coefficient map is shown in Figure 11.8.34.



Source: JICA Project Team

Figure 11.8.34 Roughness Coefficient Map (Domain 3, 200 m Mesh)

11.8.7 STORM SURGE SIMULATION IN THE DELTA AREA

The storm surge simulation was conducted to simulate water level changes when cyclones hit the delta area. The studied cases were: 1) Cyclone Nargis, which inflicted the severest damage in the delta area, and 2) sensitivity analysis of water levels to cyclone traveling routes.

(1) Simulation Case

The simulation cases are shown in Table 11.8.14. Case 1 is for Cyclone Nargis, and Case 2 and Case 3 are for the sensitivity analysis of water levels to cyclone traveling routes.

Table 11.8.14 Storm Surge Simulation Case

Case	Route of Cyclone	Sea Level Pressure
1	Cyclone Nargis	Cyclone Nargis
2	Cyclone Nargis + 1 degree	Cyclone Nargis
3	Cyclone Nargis – 1 degree	Cyclone Nargis

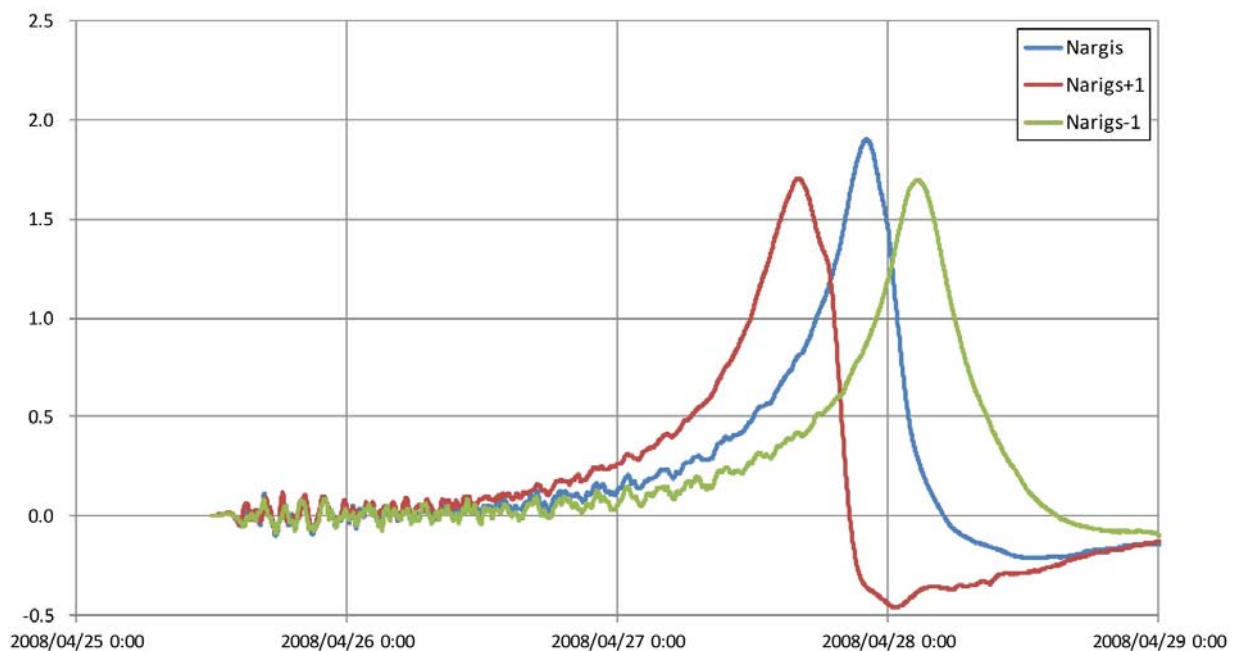
Source: JICA Project Team

(2) Simulation Result

The simulations of Cases 1, 2, and 3 were conducted, and the worst case was Case 1 of the simulation of Cyclone Nargis, which showed the maximum water level in the Ywe River. The water level chart of the three cases is shown in Figure 11.8.35, and the water level and wind maps of the three cases are shown in Figure 11.8.36.

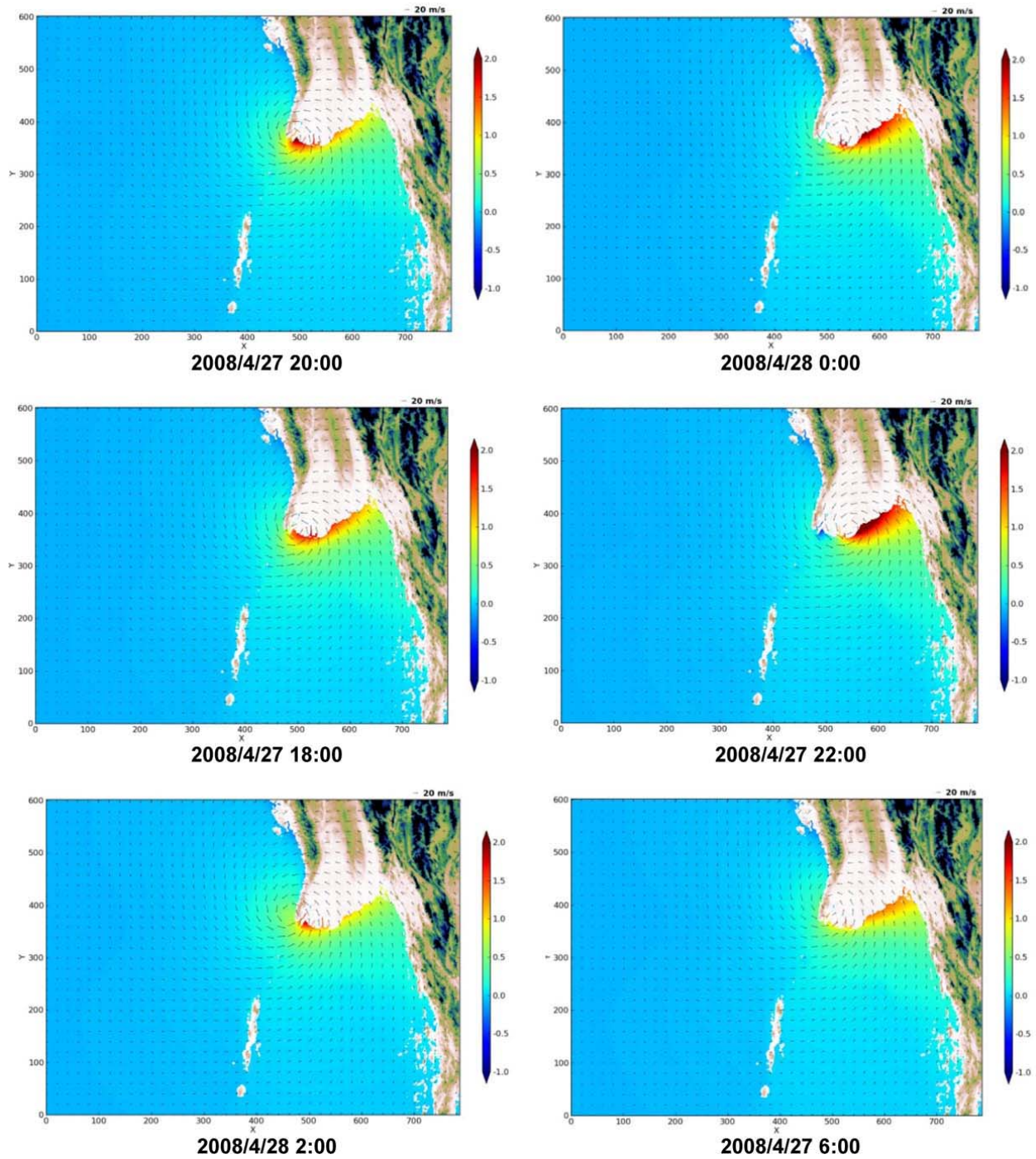
The detailed water level and wind map of the worst case (Case 1) is shown in Figure 11.8.37. The water level rise due to the storm surge was more than 2 m around the Ywe River and the Thet Ke Thaug River. In addition, the storm surge runs upstream. However, the simulated water levels were lower than the actual water level obtained by the interview survey. The reasons for the differences between the simulation and actual were estimated as follows:

- 1) The simulated deviation of water level in Case 1 was about 2 m. On the other hand, the inundation depth around the Ywe River was about 8 ft according to the interview survey. The simulated deviation is the height from astronomical tide level, and the inundation depth is the height from the ground level. Considering the difference of definition of heights, the difference of the simulation outputs (deviation) and records (inundation) are understandable.
- 2) The effects of ocean waves may be significant. If the ocean waves reached the coastline without damping, both the ocean wave and the storm surge would jointly cause the inundation.



Source: JICA Project Team

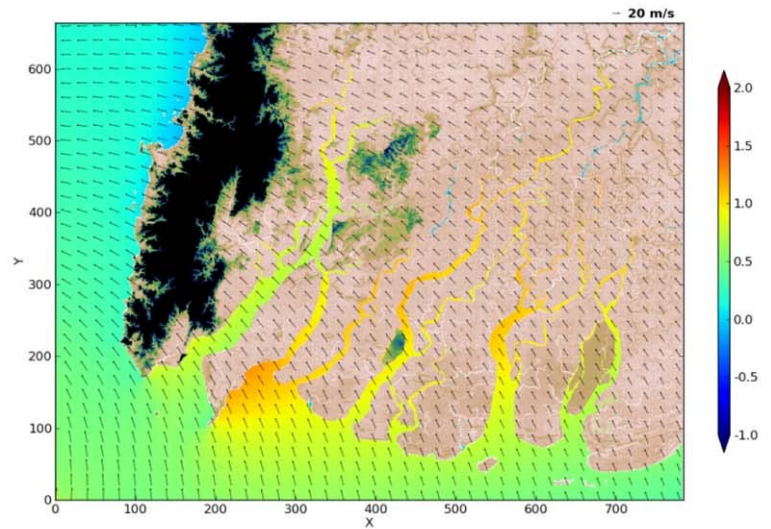
Figure 11.8.35 Deviation of Simulated Water Level at the Ywe River Mouth (Cases 1, 2, and 3)



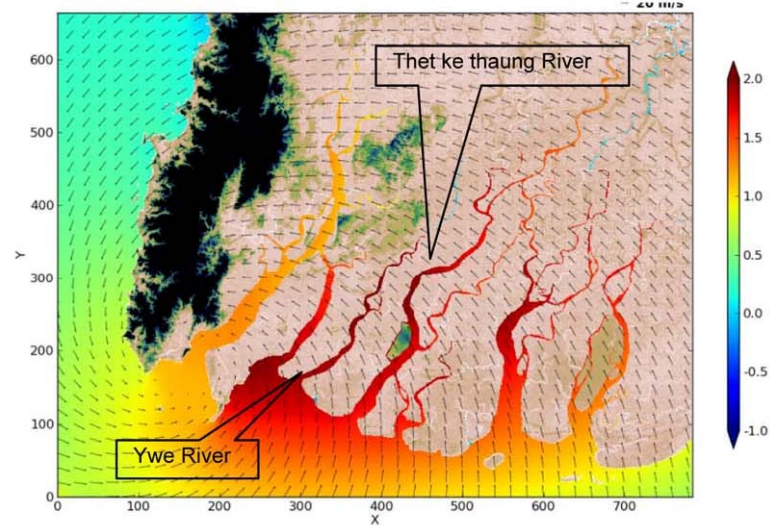
Note: Upper: Cyclone Nargis, Middle: Cyclone Nargis +1° Traveling Route, Lower: Cyclone Nargis -1° Traveling Route

Source: JICA Project Team

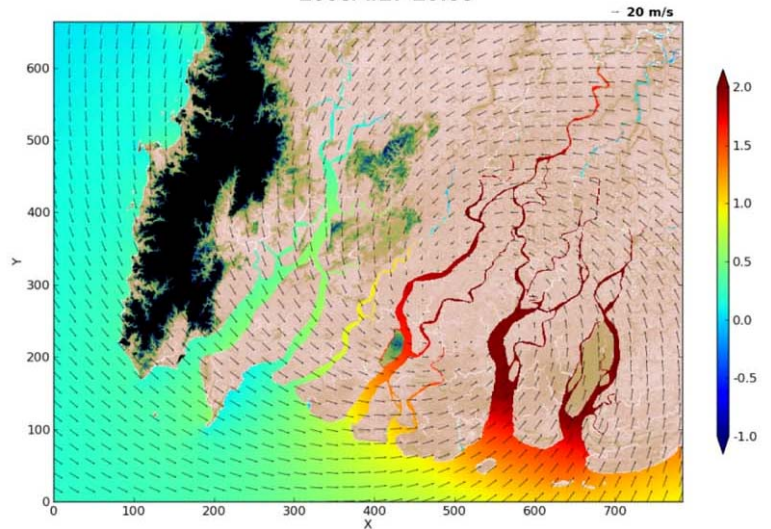
Figure 11.8.36 Deviation of Water Level and Wind Distribution



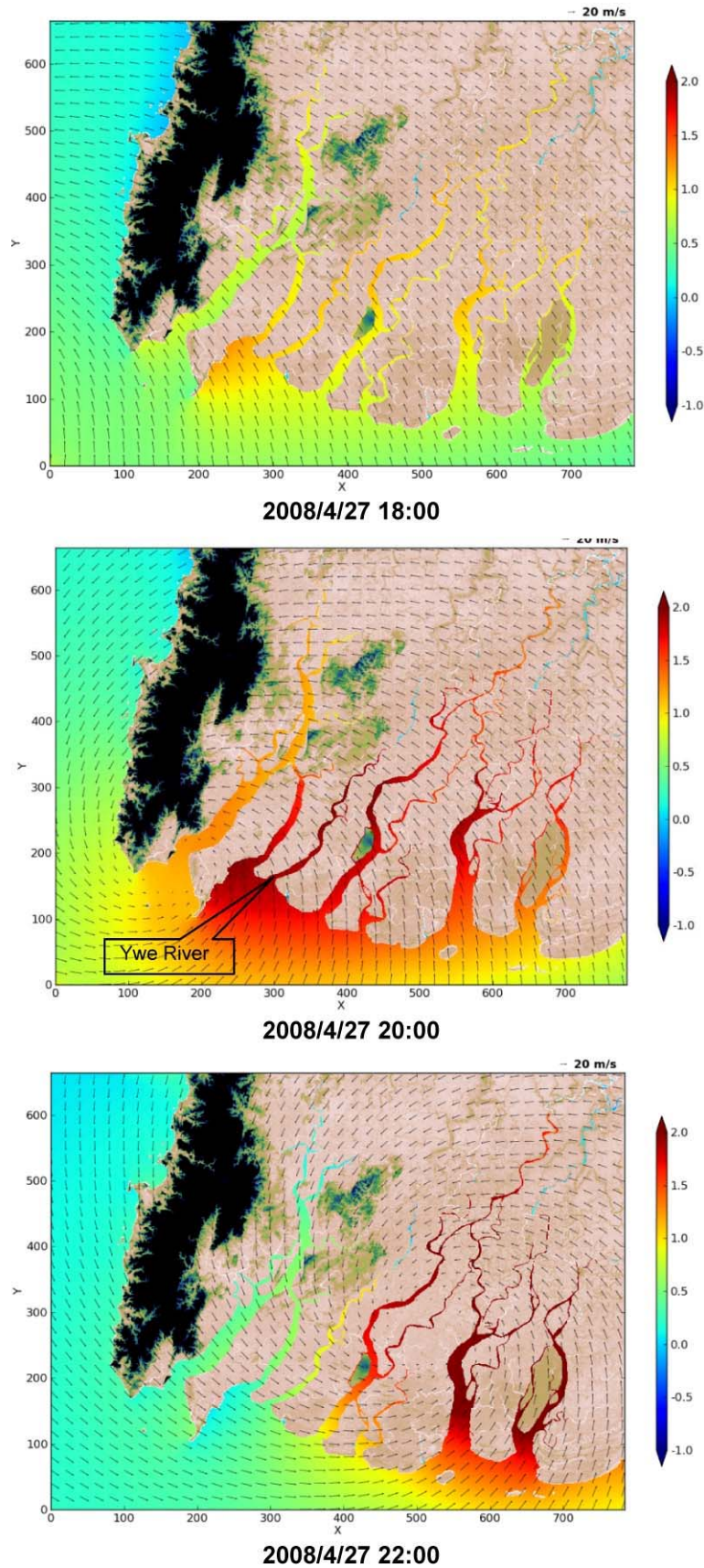
2008/4/27 18:00



2008/4/27 20:00



2008/4/27 22:00



Source: JICA Project Team

Figure 11.8.37 Deviation of Water Level and Wind Distribution (Cyclone Nargis)

11.8.8 CONDITION OF EARTHQUAKE AND TSUNAMI

(1) Target Level of Earthquake and Tsunami for Study

Port structures on the northern Pacific coast of Japan were destroyed by the 2011 Tohoku Earthquake and Tsunami. The Ministry of Land, Infrastructure, Transport and Tourism (MLIT) of Japan studied structural consideration on the effects of tsunami to port structures and published reports titled “The Policy for Tsunami-Resistant Design of Breakwaters” and “The Guideline for Tsunami-Resistant Design of Breakwaters”.

The Policy for Tsunami-Resistant Design of Breakwaters designated two levels of tsunamis by its magnitude and recurrence, which are L1 and L2 as described below and in Table 11.8.15.

- Level 1 (L1): L1 Tsunami is the tsunami that occurs frequently. The countermeasures to L1 Tsunami are “Disaster Prevention”. The Government of Japan makes efforts to protect human lives and properties by constructing tsunami-resistant structures as much as possible.
- Level 2 (L2): L2 Tsunami is the tsunami that rarely occurs but causes catastrophic damages. The countermeasures to L2 are “Disaster Mitigation”. The Government of Japan makes efforts to protect the lives at least, and to minimize the damages to properties.

Table 11.8.15 Design Level of Structures

Tsunami Level	Definition	Countermeasure
Level 1 (L1)	<ul style="list-style-type: none"> • High recurrence • Structure design level class 	<Disaster Prevention> <ul style="list-style-type: none"> • Coastal structure planning • Protecting tsunami wave by structures
Level 2 (L2)	<ul style="list-style-type: none"> • Low recurrence • Mega risk and huge damage • Maximum class 	<Disaster Mitigation> <ul style="list-style-type: none"> • Evacuation planning • Integrated tsunami disaster prevention planning

Source: JICA Project Team

“Disaster Mitigation” is the integrated countermeasure to tsunamis, consisting mainly of early evacuation. For example, the Tsunami Evacuation Tower (see Figure 11.8.38) was constructed instead of strengthening breakwaters in Nakatosa Town, Kochi, Japan, at high risk for a great tsunami. In addition, several soft measures such as enhancement of evacuation drills, increase of residents’ voluntary disaster mitigation organizations, and integrated actions of fire companies were introduced.

The delta area of Myanmar is a broad area. Disaster prevention countermeasures of breakwaters are not feasible considering cost-effectiveness. Therefore, tsunami countermeasures in the delta area should be devised in the manner of integrated mitigation measures considering damages resulting from L2 Tsunamis.

L2 Tsunami should be assumed as the largest tsunami in the study area, based on scientific studies consisting of tsunami sediment studies and topographic analysis of coastal areas. Thus, the fault model for tsunami simulation in the delta area shall be established.



Source: JICA Project Team

Figure 11.8.38 Tsunami Evacuation Tower in Nakatosa Town, Kochi, Japan

(2) Fault Model for Tsunami Simulation

In the study of Yangon Port in Section 11.7, the 2004 Indian Ocean Earthquake Tsunami (Segments 1, 2, and 3 in Figure 11.8.39) was simulated for the preparation of Maritime Disaster Prevention Programme. The Northern Part Structure Line (Segment 4 in Figure 11.8.39) was additionally considered. Eight cases of simulation were conducted, and Case 7, showing the maximum water level, was selected for damage analysis.

In the Northern Part Structure Line, only the south part of Segment 4 contains the aftershock area of the 2004 Indian Ocean Earthquake, illustrated as yellow circles in Figure 11.8.39. However, there were historically a lot of epicenters in Segments 4 and 5 as shown in Figure 11.8.40. In addition, the studies of topography and tsunami sediment dating technique identified four earthquakes in the last 3,000 years at a 900-year interval. From these evidences, the JICA Project Team estimated that the plate was active and there was a slight possibility of an occurrence of a mega-earthquake in this area within the next ___ years, which was linked to Segments 1, 2, and 3.

It is necessary to estimate the maximum tsunami (L2) with scientific studies for disaster prevention in the delta area. Therefore, the plate subduction in the west of Myanmar was considered as the fault model for the tsunami simulation. The fault model is shown in Figure 11.8.39.

Magnitude in this fault model was estimated with the equations described below:

$$M_0 = \mu u L W$$

Where: μ = modulus of rigidity
 u = fault slip amount
 L = fault segment length
 W = fault width

The modulus of rigidity was calculated from the equation below:

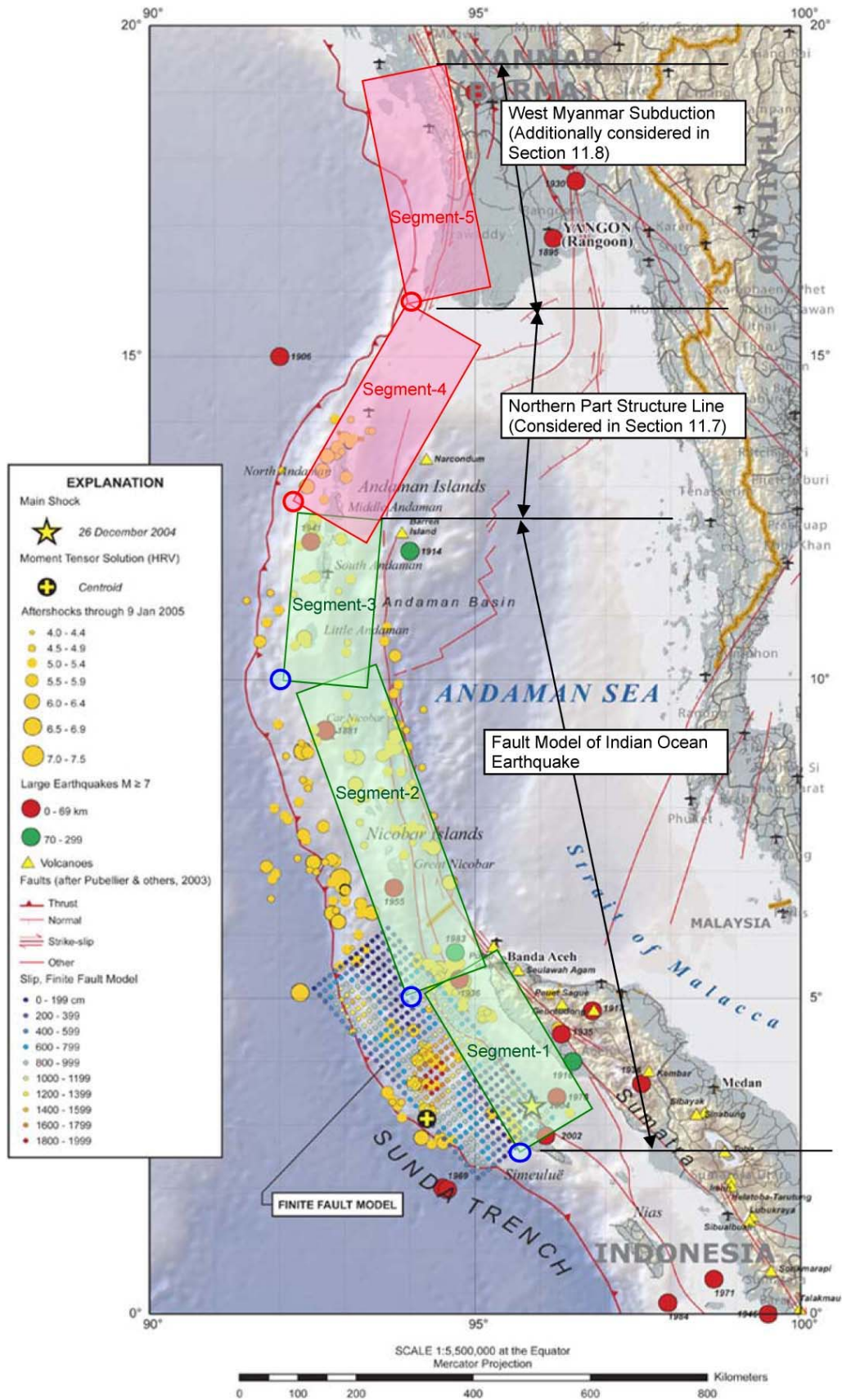
$$\mu = \rho V_s^2 = 4.48 \times 10^{10} \quad [N/m^2]$$

Where: ρ = crustal density (2.8 g/cm³)
VS = shear wave velocity (4.0 km/s)

$$\begin{aligned} M_0 &= \mu u L W \\ &= 4.48 \times 10^{10} \times 13 \times 2000 \times 10^3 \times 150 \times 10^3 \\ &= 1.75 \times 10^{23} \quad [N \cdot m] \end{aligned}$$

$$M_w = (\log M_0 - 9.1) / 1.5 = 9.428 \approx 9.4$$

Where: M_0 = seismic moment (N·m)
MW = moment magnitude



Source: USGS (<http://walrus.wr.usgs.gov/tsunami/sumatraEQ/seismo.html>), edited by the JICA Project Team

Figure 11.8.39 Fault Model for Tsunami Simulation in the Delta Area

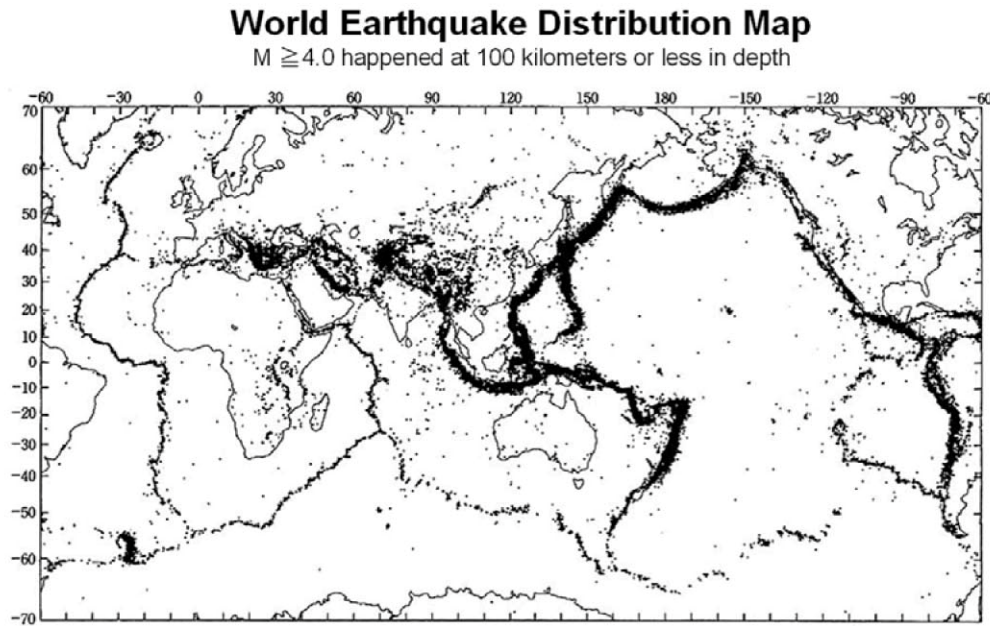
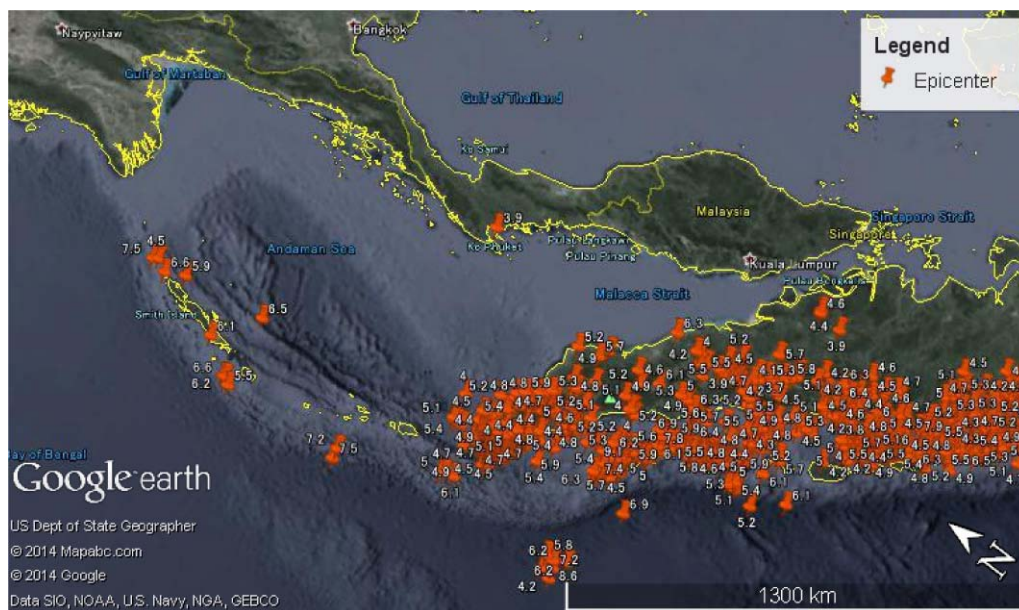


Figure 11.8.40 Distribution of Epicenter

(3) Probability of Occurrence of Model Earthquake

The probability of occurrence of model earthquake considered in the fault model in the previous subclause was estimated based on the historical earthquakes and frequency calculation by the Gutenberg-Richter Law. The Gutenberg-Richter Law calculates the inverse number of earthquakes per year from the counts of earthquakes in each size in the target data period, and estimates the probability of earthquakes in each size from the viewpoint of statistics.

The earthquake database of the United States Geological Survey (USGS) was applied. The historical earthquakes from 1973 to 2012 in the Indo-Australia/Eurasia Plate Boundary were extracted from the USGS database. The extracted epicentres are shown in Figure 11.8.41.



Source: JICA Project Team

Figure 11.8.41 Location of Epicenters in the Indo-Australia/Eurasia Plate Boundary

The relationship between the magnitude and the number of earthquakes were shown in Figure 11.8.42. The approximate coefficient of the Gutenberg-Richter Law is described below:

$$\text{Log}_{10}N(M) = a - b \cdot M$$

Where: N(M) = total number of earthquakes with magnitude equal or over M during the study period
a, b = constant number (approximate coefficient of N in Figure 11.8.42)

The probabilities of occurrence of earthquakes causing L1 and L2 Tsunamis were calculated as follows:

$$a = 6.33, \quad b = 0.71$$

The earthquake causing L1 Tsunami:

$$M = 9.0$$

Probability = 0.0217 times per year (return period = about 45 years)

The earthquake causing L2 Tsunami:

$$M = 9.4$$

Probability = 0.0113 times per year (return period = about 90 years)

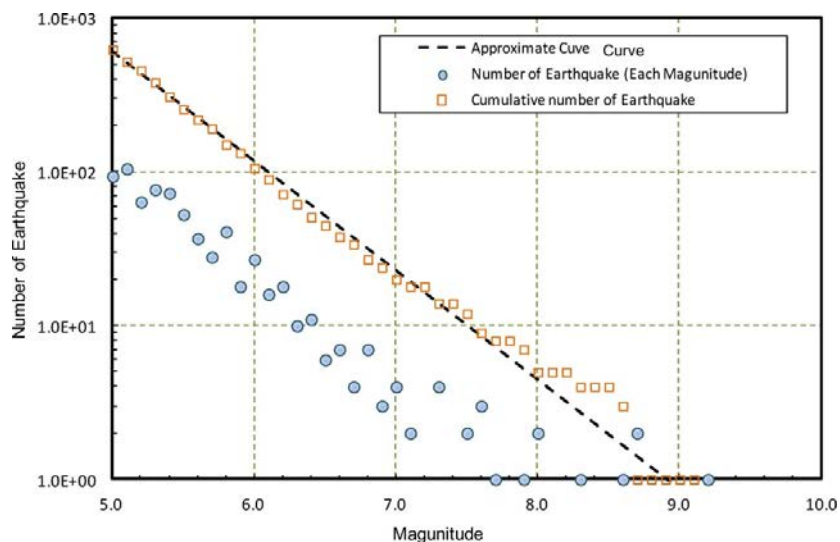
<Reference>

The Gutenberg - Richter Law based on the data around Japan is:

$$\text{Log}_{10}N(M) = 0.936(7.88 - M)$$

If, $M = 9.4$

Then, Probability = 0.0038 times per year (return period = about 265 years)



Source: JICA Project Team

Figure 11.8.42 Relationship between Magnitude and Number of Earthquakes

If the coefficient based on the data around Japan is applied, the return period of M9.4 earthquakes would be 265 years. On the other hand, if the coefficient based on the data of the Indo-Australia/Eurasia Plate Boundary is applied, the return period of the earthquake would be as short as 90 years. This short return period is due to active plate movements after the 2004 Indian Ocean Earthquake. Aftershocks of this mega-earthquake continue for several years, and gradually diminished. Therefore, the return period of a M9.4 earthquake would be longer than 90 years.

Nobuyuki Okamura¹ reported that “there is a subduction boundary in the west sea of the Myanmar, continuing from the source area of the 2004 Indian Ocean Earthquake. The latest global positioning satellite (GPS) observation estimated that the Indian Plate is moving towards the Eurasia Plate at a speed of 10 mm per year in a north-northeasterly direction in the subduction boundary of the west sea of Myanmar. It is estimated that ocean trench interplate earthquakes occur with a return period of several hundred years.”

The above survey is still ongoing to understand the plate movement precisely, and the observation is a tentative output. If the moving speed of 10 mm per year is applied, it would take 1000 years for the plate to move 10 m, which is the approximate length of the fault slip for the 2004 Indian Ocean Earthquake. From this consideration, the return period of M9.4 earthquakes is estimated to be 1000 years.

In conclusion, the return period of M9.4 earthquakes is estimated between 90 and 1000 years.

(4) Simulation Case

In total, two cases of tsunami simulation were conducted.

- Case-1: The 2004 Indian Ocean Earthquake Tsunami
Case 1 was for the validation of simulation model. The simulation outputs were compared with the flood marks.
- Case-2: The tsunami caused by the coupled faults model of the 2004 Indian Ocean Earthquake and west Myanmar subduction.
Case 2 was for the simulation of assumed maximum tsunami (L2).

11.8.9 RESULTS OF TSUNAMI SIMULATION

(1) Case 1: The 2004 Indian Ocean Earthquake Tsunami

The case of the 2004 Indian Ocean Earthquake Tsunami was conducted for the validation of tsunami simulation model.

1) Calculation Condition

The calculation condition for Case 1 is shown in Table 11.8.16.

Table 11.8.16 Calculation Condition (Case 1)

Item	Condition
Mesh size	Domain 1: 1800 m Domain 2: 600 m Domain 3: 200 m Domain 4: 50 m Domain 5: 10 m
Time step	1.0 second
Total simulation time	16 hours after the occurrence of an earthquake
Geo-reference system of mesh	WGS 1984
Projection of mesh	UTM 64 N
Fundamental equation and solver	Nonlinear long-wave theoretical formula, Leapfrog finite difference method
Seaside boundary	Free percolation
Connection boundary	Connection of water level and discharge
Run up boundary	Land: Kotani, <i>et al.</i> (1998) Others: Complete reflection
Fault model	2004 Indian Ocean Earthquake (Tohoku University)
Tide level	1.44 m (MSL=0 m)
Ground displacement	Subsidence: considered Upthrust: not considered
Bottom friction	Manning's roughness coefficient
Banking structure	Right bank of the Ywe River for Domains 3, 4, and 5

Source: JICA Project Team

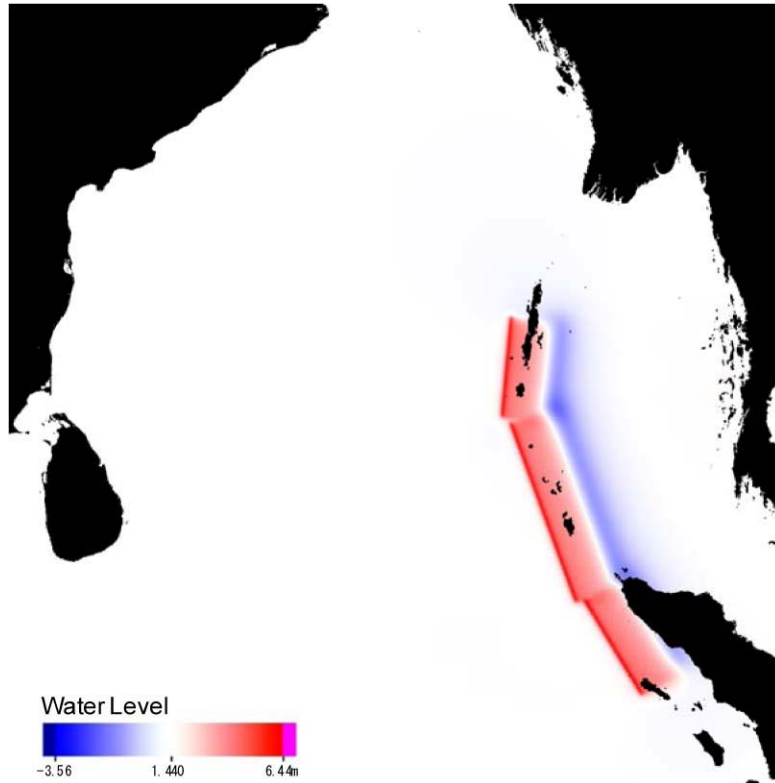
2) Parameters of Fault Model

The parameters of fault model are shown in Table 11.8.17. The Tohoku University model of the 2004 Indian Ocean Earthquake was applied. The visualized tsunami is shown in Figure 11.8.43. The maximum water level in the beginning of simulation was 6.33 m. The earthquake occurs immediately at the beginning of calculation.

Table 11.8.17 Parameter of Fault Model (Case 1)

Fault Slip Amount U (m)	Slip Direction θ (degree)	Depth d (m)	Angle of Slope δ (degree)	Angle of Slip λ (degree)
11	329	7,000	15	110
11	340	7,000	15	110
11	5	7,000	15	110
Length L (m)	Width W (m)	Latitude N (degree)	Longitude E (degree)	
330,000	150,000	2.5	95.75	
570,000	150,000	5.0	94.00	
300,000	150,000	10.0	92.00	

Source: JICA Project Team

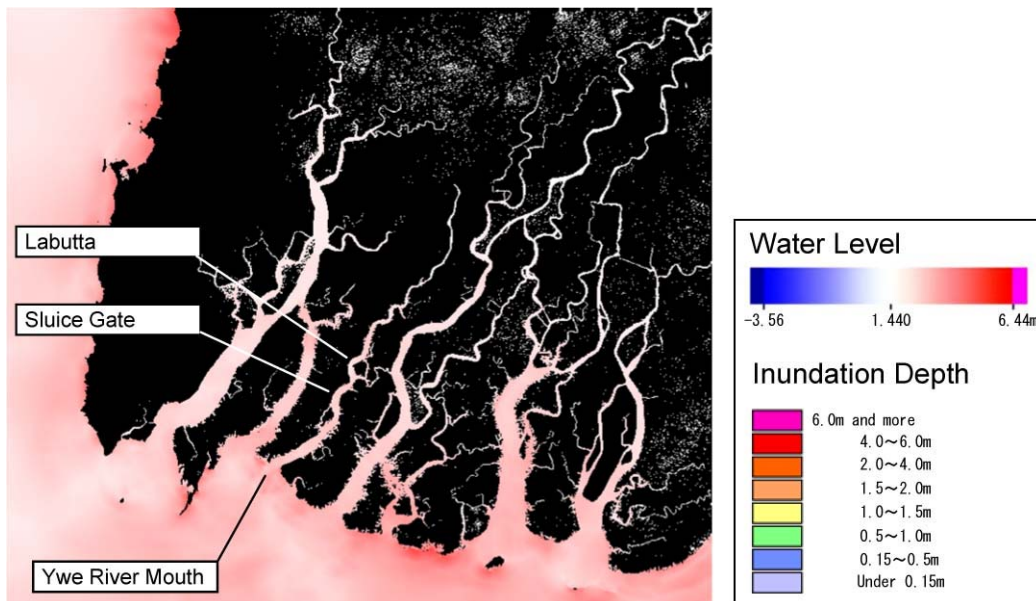


Source: JICA Project Team

Figure 11.8.43 Initial Condition of Tsunami Simulation for Case 1

3) Simulation Results

Enveloped maximum water levels are shown in Figure 11.8.44. Comparison of the flood marks and simulation outputs are shown in Table 11.8.18 and Figure 11.8.45. The simulation outputs were almost with the same as the flood marks.



Source: JICA Project Team

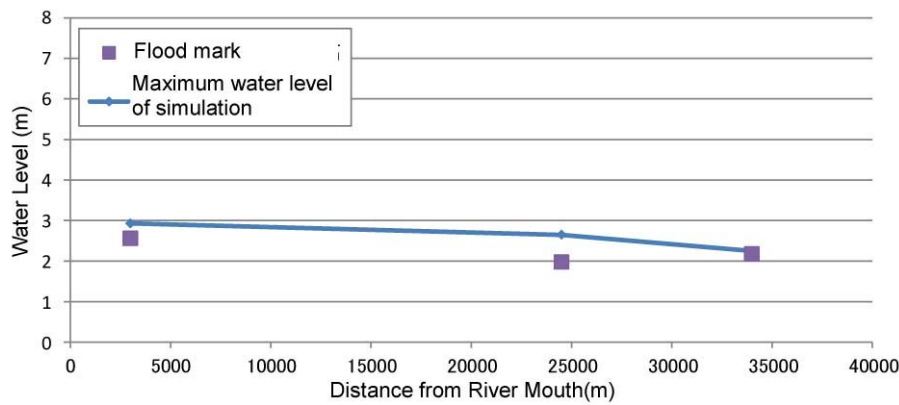
Figure 11.8.44 Enveloped Maximum Water Level in Domain 3 (200 m mesh) (Case 1)

Table 11.8.18 Comparison of Flood Mark and Simulation Output (Case 1)

No.	Distance from the River Mouth (m)	Point Name	Domain 4 (50 m mesh)			Domain 5 (10 m mesh)			Flood Mark
			Coordinate of Point		Water Level (m)	Coordinate of Point		Water Level (m)	Water Level (m)
			X	Y	Z	X	Y	Z	Z
1	3,000	River mouth	474	548	2.93	-	-	-	2.56
2	24,500	Sluice gate	721	254	2.65	-	-	-	1.98
3	34,000	Labutta jetty	807	109	2.22	345	364	2.25	2.17
Tide Level			-	-	1.44	-	-	1.44	1.44

Note: Coordinates of points are expressed in the coordinate space of calculation mesh, where the coordinate of the upper left corner is (X, Y) = (1, 1).

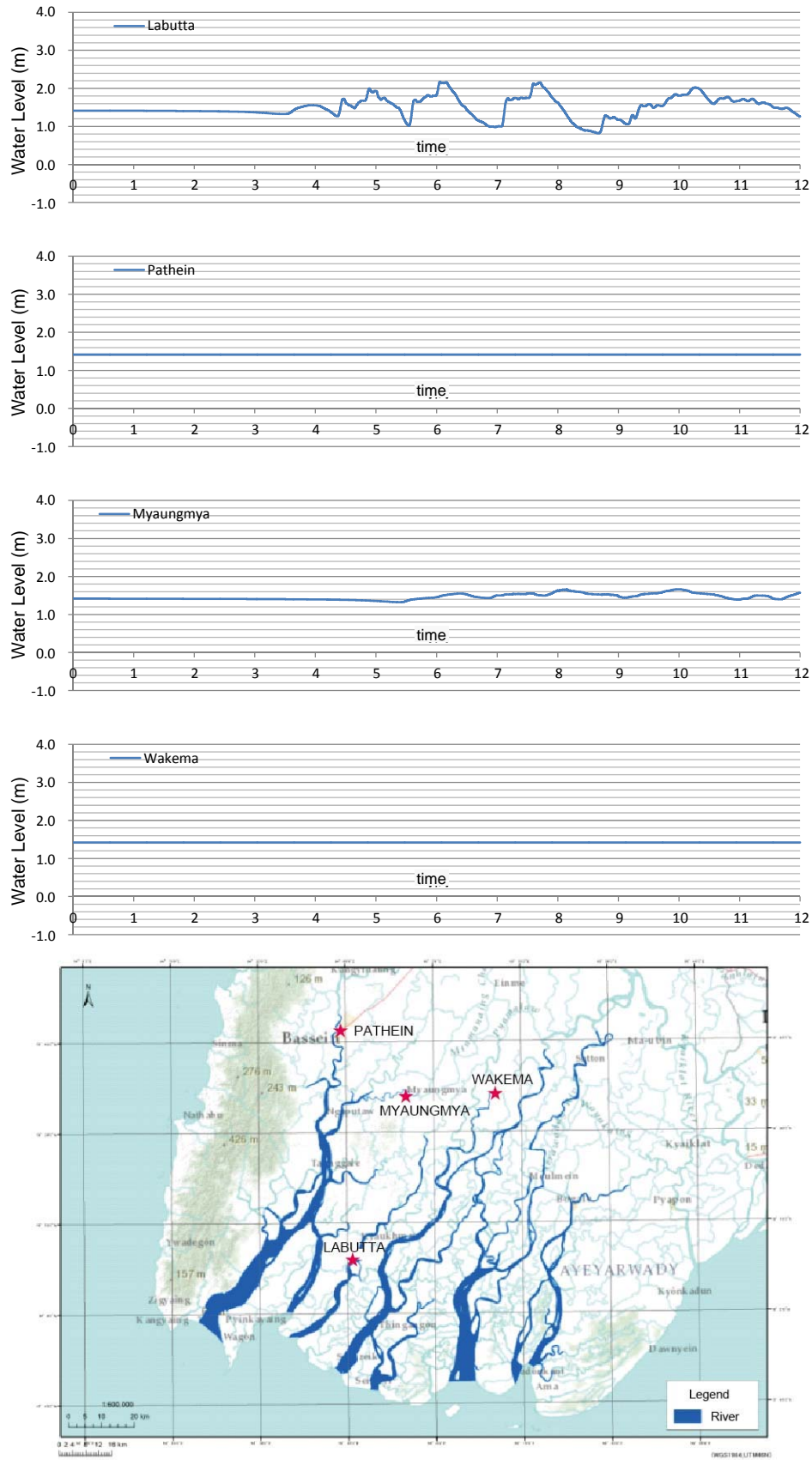
Source: JICA Project Team



Source: JICA Project Team

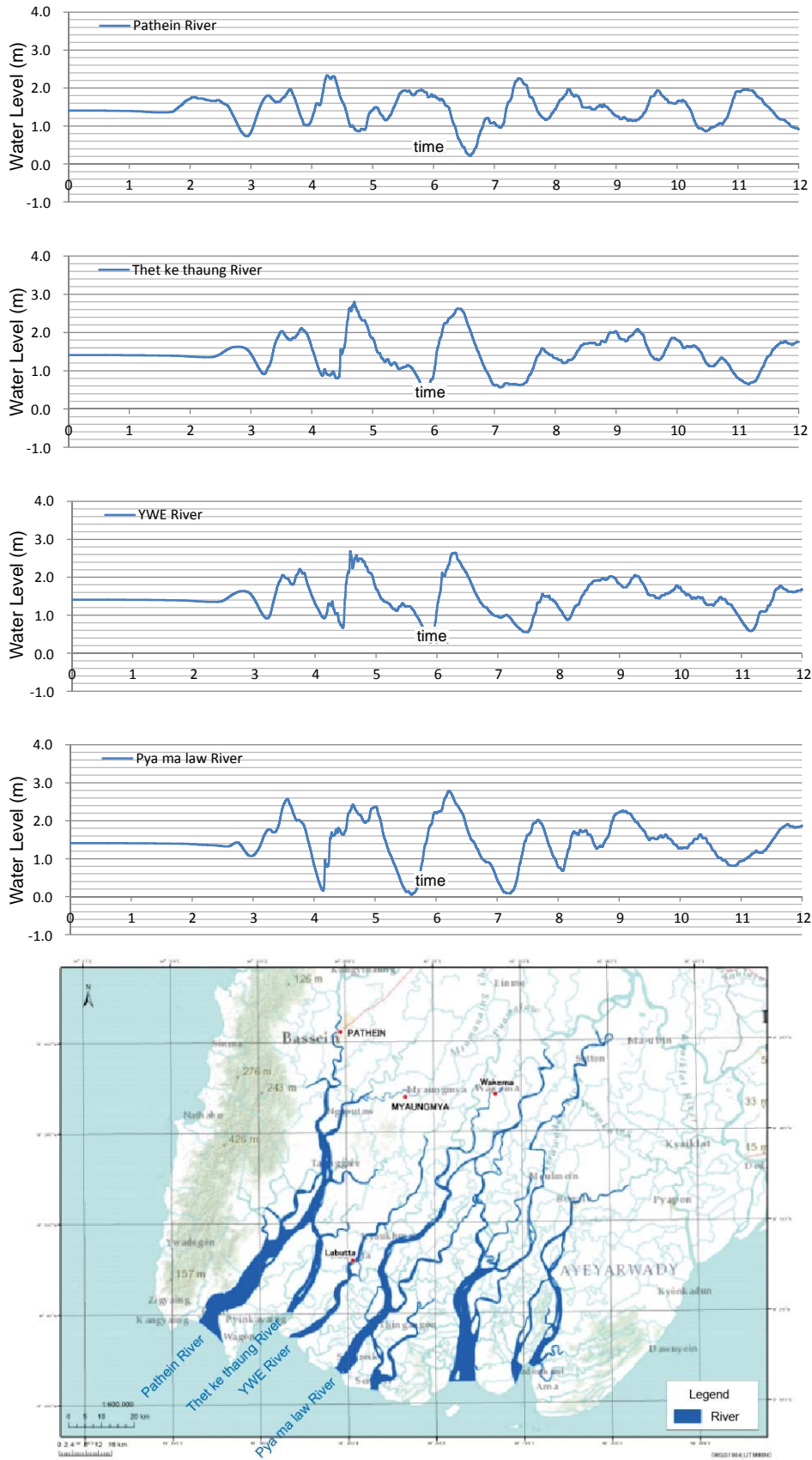
Figure 11.8.45 Longitudinal Profile of the Ywe River (Case 1)

The time series of simulated water levels in Labutta, Pathein, Myaungmya, and Wakema are shown in Figure 11.8.46. The time series of simulated water levels in the Pathein River, Thet ke thaung River, Ywe River, and Pya ma law River are shown in Figure 11.8.47. The time series of simulated water levels in the Payin za lu River, Ayeyawady River, Ka dou kani River, and Bogalay River are shown in Figure 11.8.48.



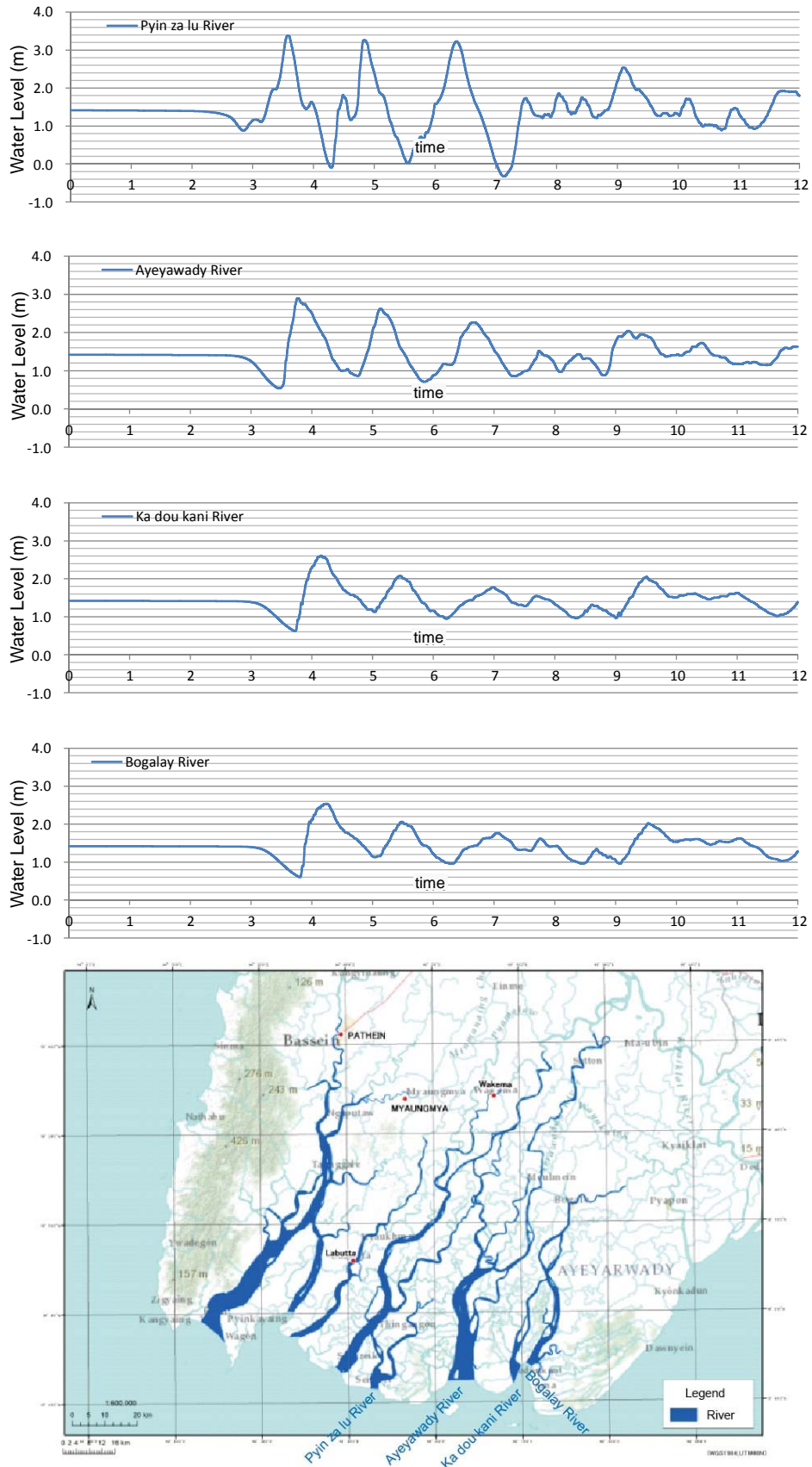
Source: JICA Project Team

Figure 11.8.46 Time Series of Simulated Water Level (Case 1) (1/3)



Source: JICA Project Team

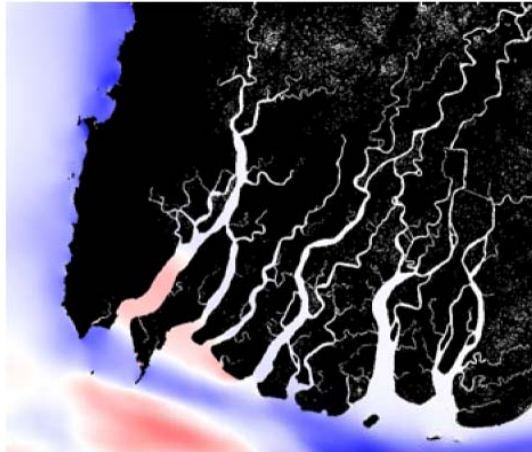
Figure 11.8.47 Time Series of Simulated Water Level (Case 1) (2/3)



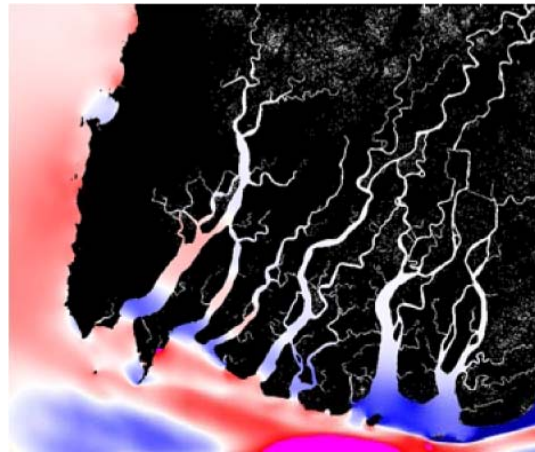
Source: JICA Project Team

Figure 11.8.48 Time Series of Simulated Water Level (Case 1) (3/3)

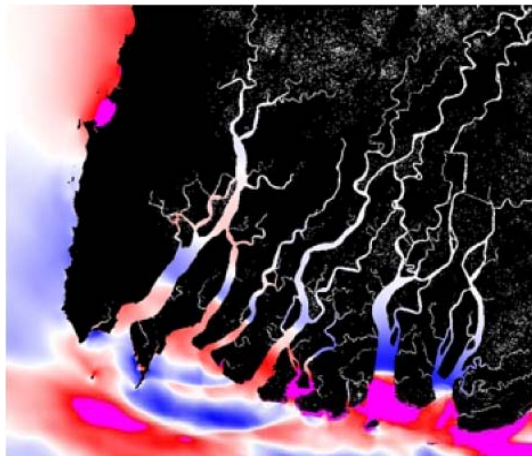
The time series of distribution of simulated water levels are shown in Figure 11.8.49.



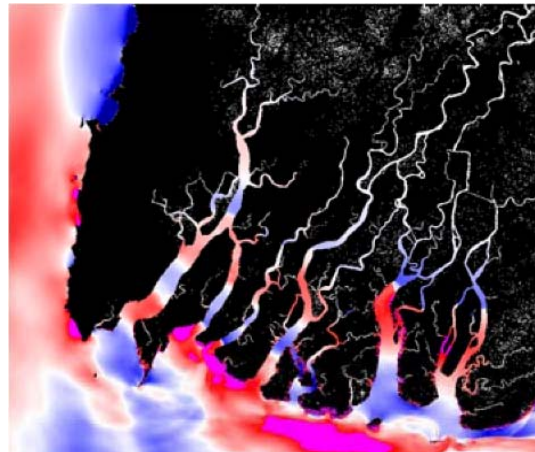
2 hours and 42 minutes after shock
The backwash is approaching to the coastline.



3 hours and 14 minutes after shock
The first wave is approaching to the coastline.



3 hours and 48 minutes after shock
The first wave is raising water levels at the river mouths.



4 hours and 38 minutes after shock
The second wave reached the river mouths.

Source: JICA Project Team

Figure 11.8.49 Time Series of Simulated Water Level Distribution (Case 1)

(2) Case 2: Tsunami Caused by Coupled Faults Model of 2004 Indian Ocean Earthquake and West Myanmar Subduction

The tsunami caused by the coupled faults model of the 2004 Indian Ocean Earthquake and West Myanmar subduction was simulated as the assumed maximum tsunami (L2) in the delta area.

1) Calculation Condition

The calculation condition for Case 2 is shown in Table 11.8.19.

Table 11.8.19 Calculation Condition (Case 2)

Item	Condition
Mesh size	Domain 1: 1800 m Domain 2: 600 m Domain 3: 200 m Domain 4: 50 m Domain 5: 10 m
Time step	1.0 second
Total simulation time	16 hours after the occurrence of an earthquake
Geo-reference system of mesh	WGS 1984
Projection of mesh	UTM 64 N
Fundamental equation and solver	Nonlinear long-wave theoretical formula, Leapfrog finite difference method
Seaside boundary	Free percolation
Connection boundary	Connection of water level and discharge
Run up boundary	Land: Kotani, <i>et al.</i> (1998) Others: Complete reflection
Fault model	Coupling of the 2004 Indian Ocean Earthquake and west Myanmar subduction
Tide level	1.998 m
Ground displacement	Subsidence: considered Upthrust: not considered
Bottom friction	Manning's roughness coefficient
Banking structure	Right bank of the Ywe River for Domains 3, 4, and 5

Source: JICA Project Team

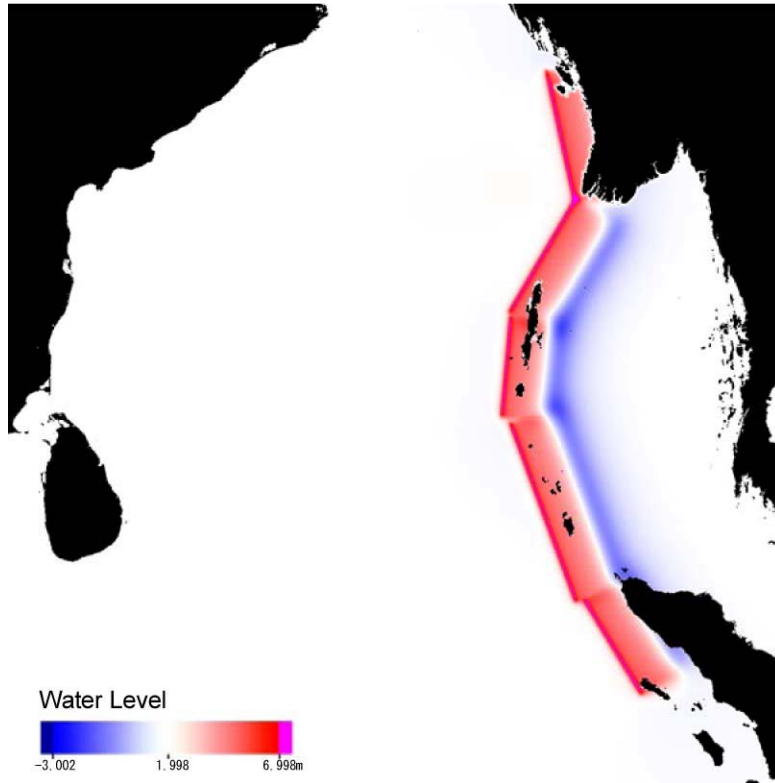
2) Parameters of Fault Model

The parameters of fault model are shown in Table 11.8.20. The visualized tsunami is shown in Figure 11.8.50. The maximum water level in the beginning of simulation was 11.04 m. The earthquake occurs immediately at the beginning of calculation.

Table 11.8.20 Parameter of Fault Model (Case 2)

Fault Slip Amount U (m)	Slip Direction θ (degree)	Depth d (m)	Angle of Slope δ (degree)	Angle of Slip λ (degree)
13	329	7,000	15	110
13	340	7,000	15	110
13	5	7,000	15	110
13	30	7,000	15	110
13	348	7,000	15	110
Length L (m)	Width W (m)	Latitude N (degree)	Longitude E (degree)	
330,000	150,000	2.5	95.75	
570,000	150,000	5.0	94.00	
300,000	150,000	10.0	92.00	
400,000	150,000	12.8	92.20	
400,000	150,000	15.8	94.00	

Source: JICA Project Team

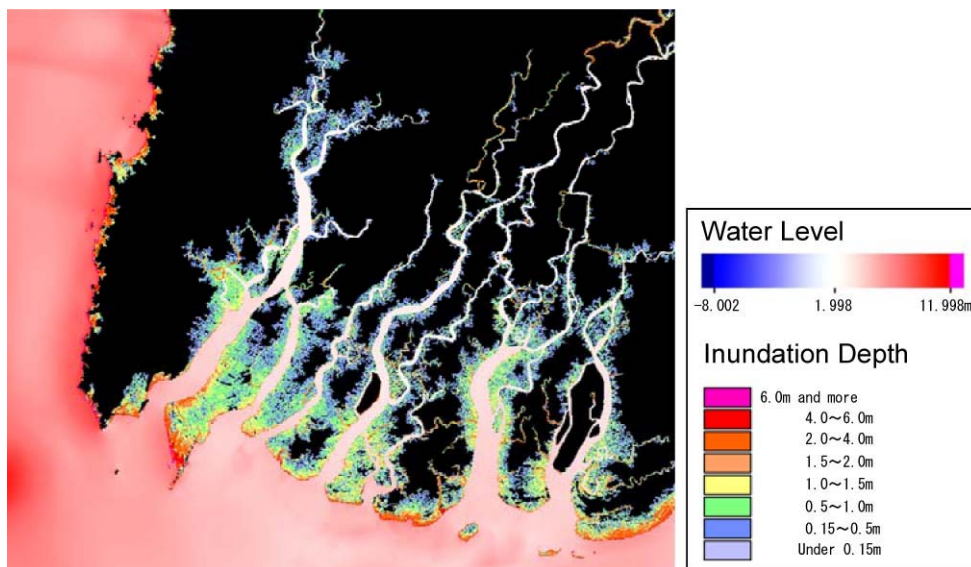


Source: JICA Project Team

Figure 11.8.50 Initial Condition of Tsunami Simulation for Case 2

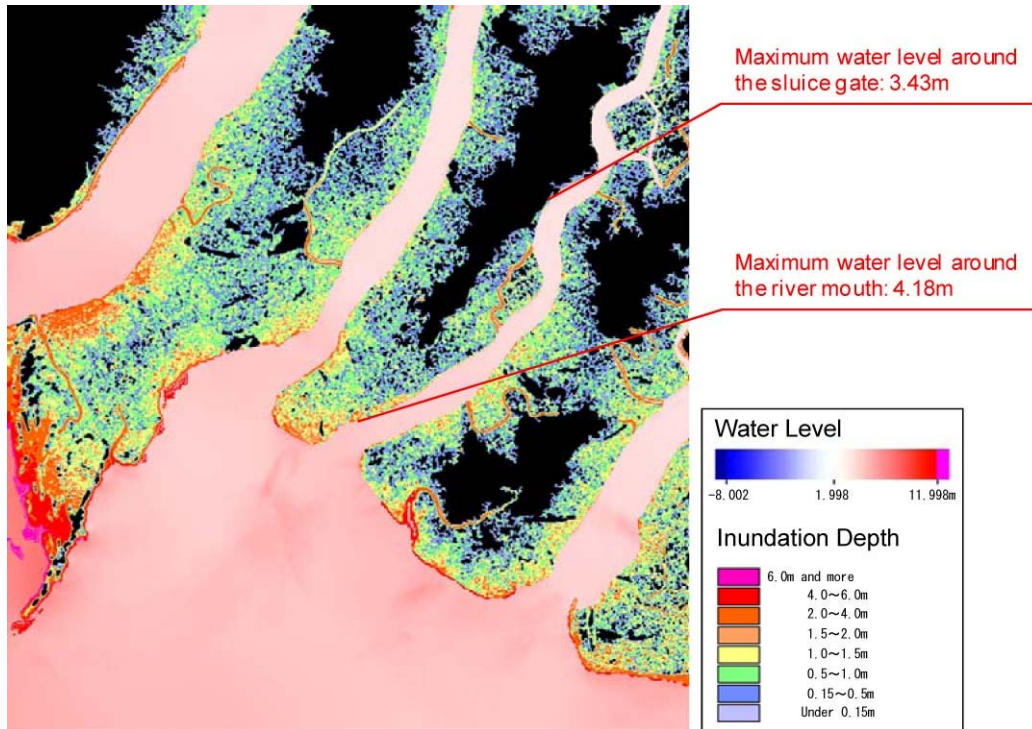
3) Simulation Results

Enveloped maximum water levels are shown in Figure 11.8.51, Figure 11.8.52, and Figure 11.8.53. The simulated water levels in the points of flood marks are shown in Table 11.8.21.



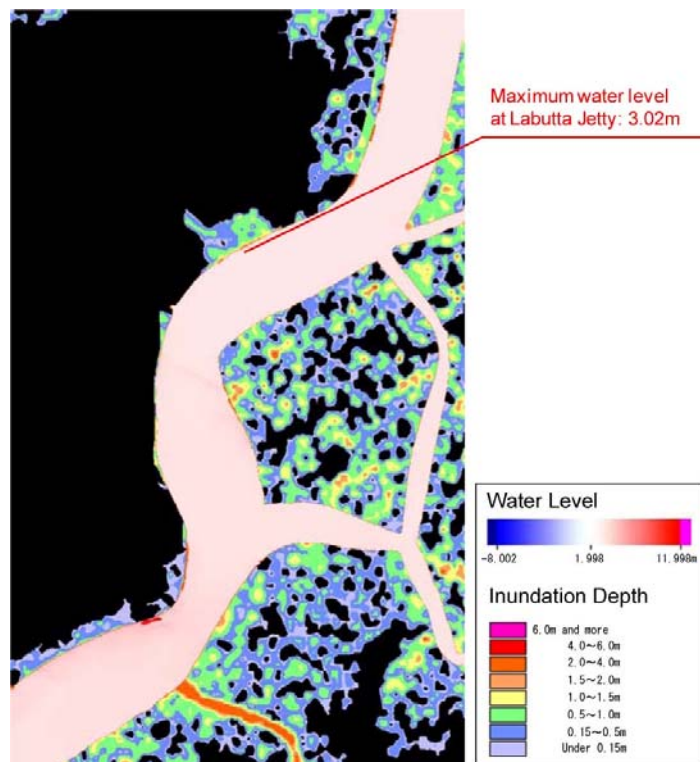
Source: JICA Project Team

Figure 11.8.51 Enveloped Maximum Water Level in Domain 3 (200 m mesh) (Case 2)



Source: JICA Project Team

Figure 11.8.52 Enveloped Maximum Water Level in Domain 4 (50 m mesh) (Case 2)



Source: JICA Project Team

Figure 11.8.53 Enveloped Maximum Water Level in Domain 5 (10 m mesh) (Case 2)

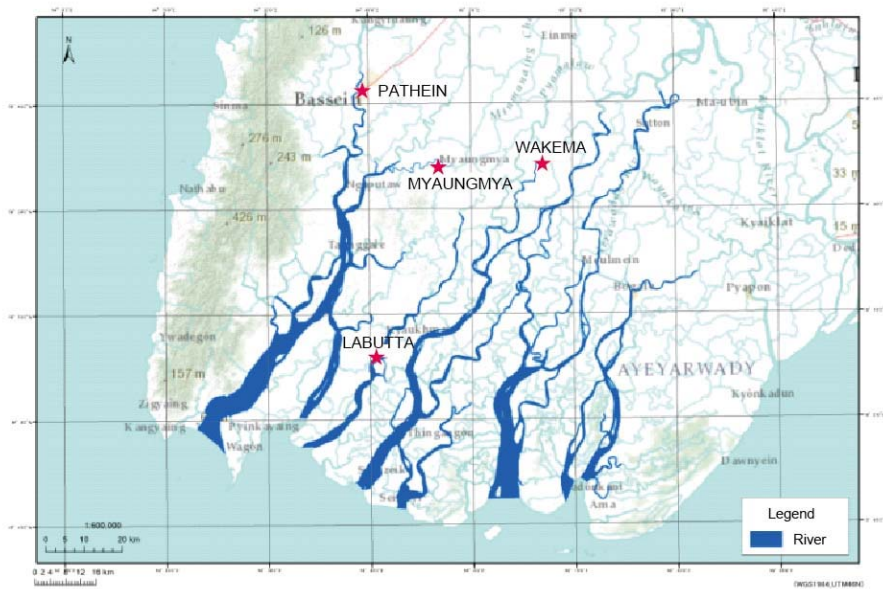
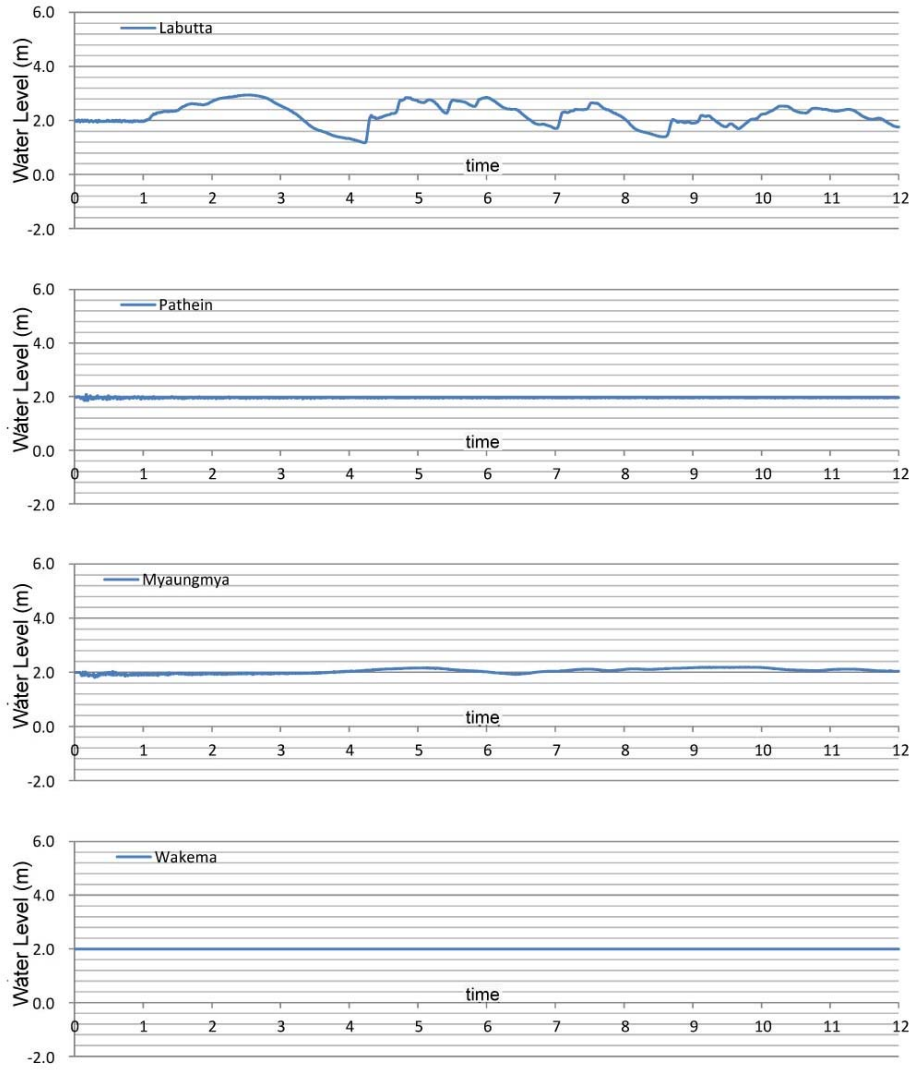
Table 11.8.21 Simulation Output in Point of Flood Mark (Case 2)

No.	Distance from the River Mouth (m)	Point Name	Domain 4 (50 m mesh)			Domain 5 (10 m mesh)			Flood Mark
			Coordinate of Point		Water Level (m)	Coordinate of Point		Water Level (m)	Water Level (m)
			X	Y	Z	X	Y	Z	Z
1	3,000	River mouth	474	548	4.18	-	-	-	-
2	24,500	Sluice gate	721	254	3.43	-	-	-	-
3	34,000	Labutta jetty	807	109	3.02	345	364	3.02	-
Tide Level			-	-	1.99	-	-	1.99	1.99

Note: Coordinates of points are expressed in the coordinate space of calculation mesh, where the coordinate of the upper left corner is (X, Y) = (1, 1).

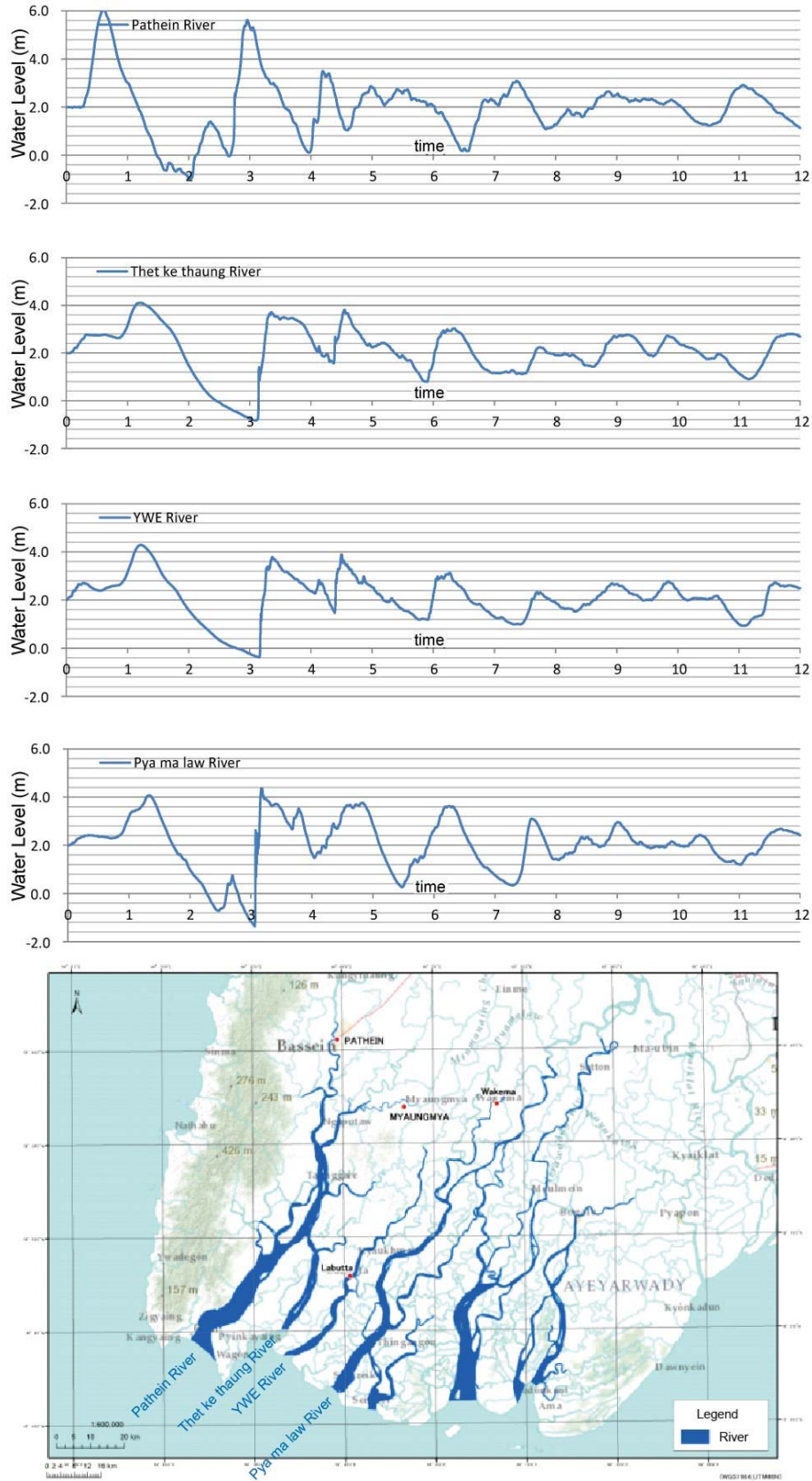
Source: JICA Project Team

The time series of simulated water levels in Labutta, Pathein, Myaungmya, and Wakema are shown in Figure 11.8.54. The time series of simulated water levels in the Pathein River, Thet ke thaung River, Ywe River, and Pya ma law River are shown in Figure 11.8.55. The time series of simulated water levels in the Payin za lu River, Ayeyawady River, Ka dou kani River, and Bogalay River are shown in Figure 11.8.54.



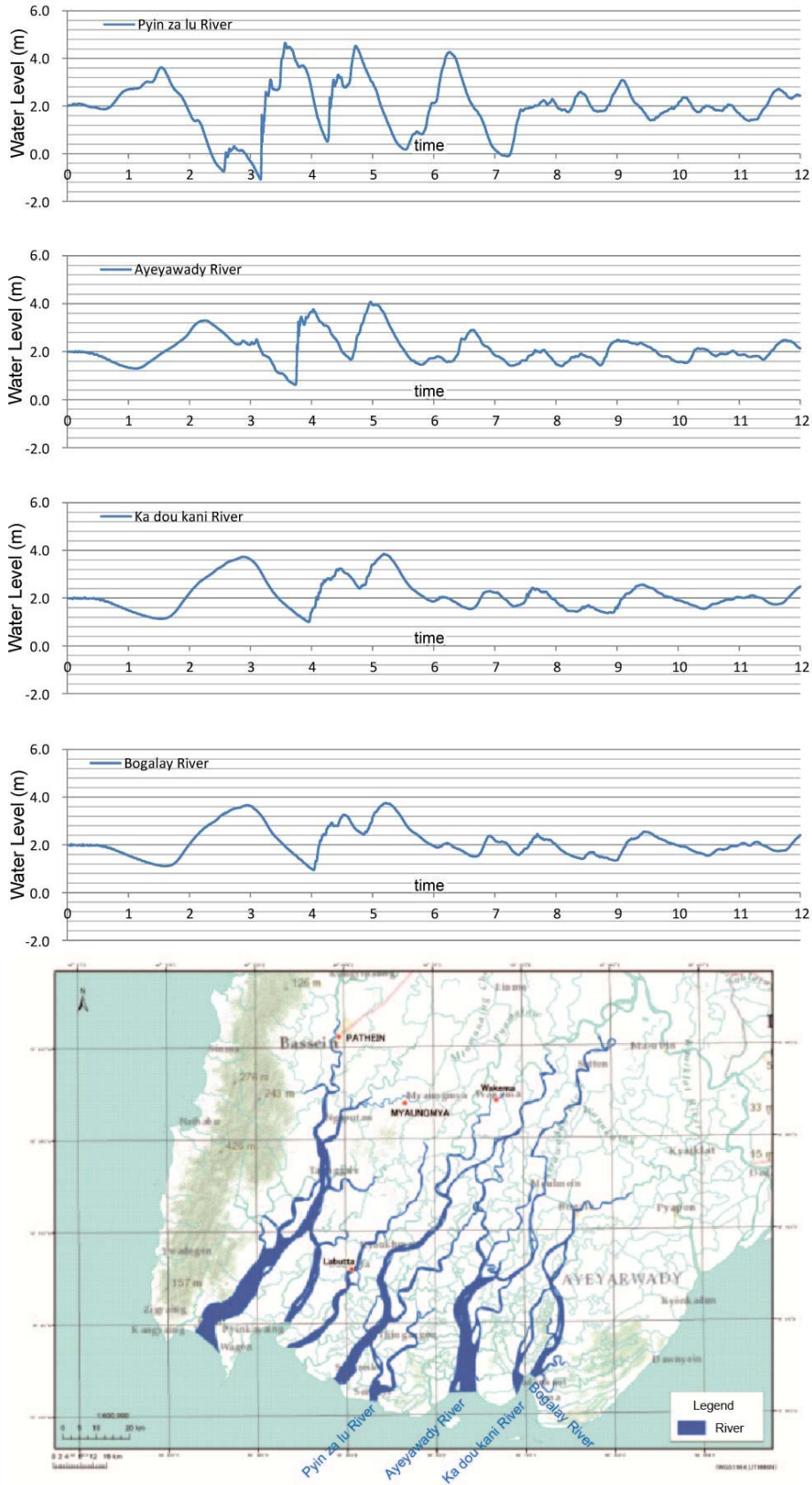
Source: JICA Project Team

Figure 11.8.54 Time Series of Simulated Water Level (Case 2) (1/3)



Source: JICA Project Team

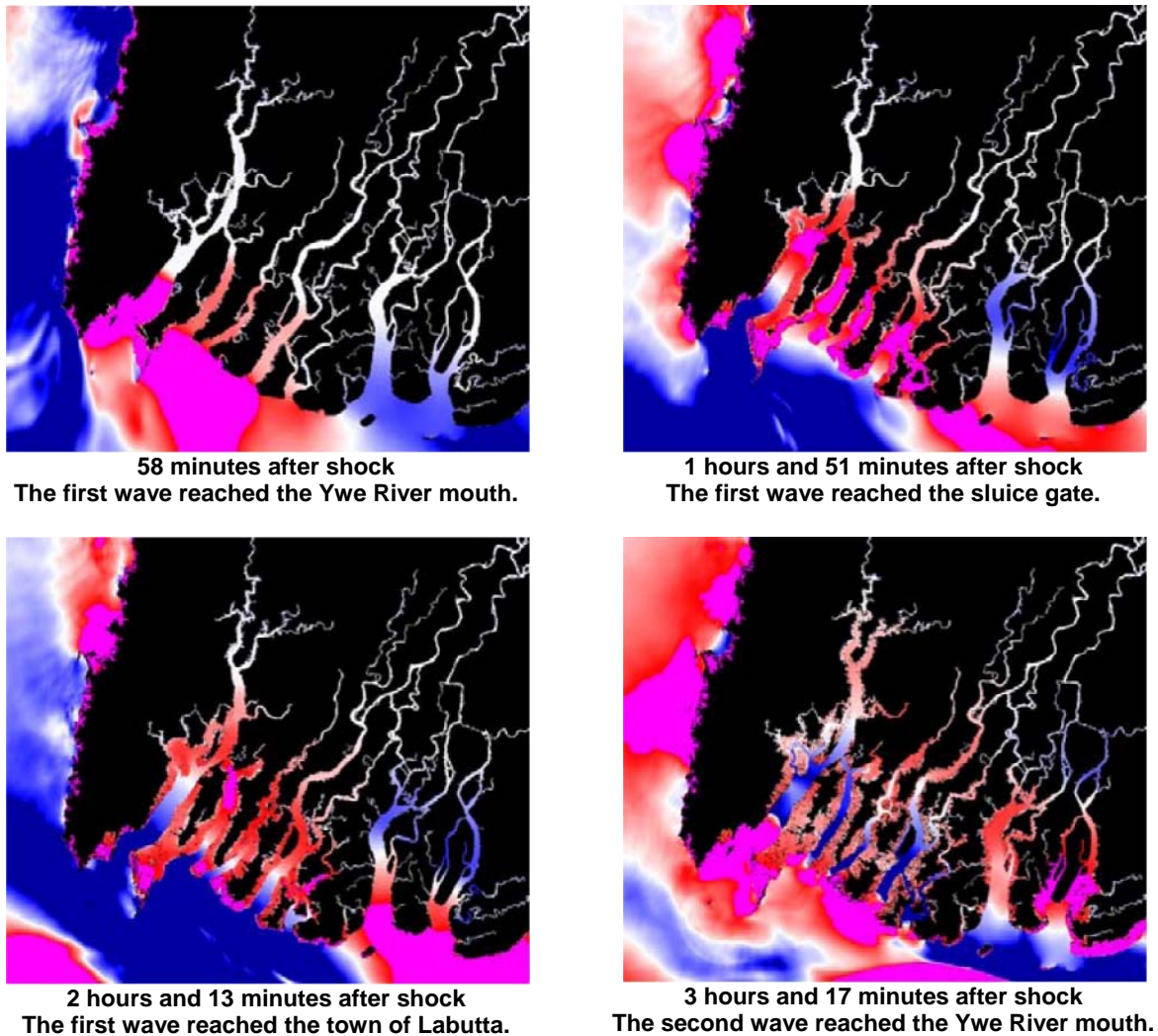
Figure 11.8.55 Time Series of Simulated Water Level (Case 2) (2/3)



Source: JICA Project Team

Figure 11.8.56 Time Series of Simulated Water Level (Case 2) (3/3)

The time series of distribution of simulated water levels are shown in Figure 11.8.57.



Source: JICA Project Team

Figure 11.8.57 Time Series of Simulated Water Level Distribution (Case 2)

11.8.10 EVALUATION OF EARTHQUAKE, TSUNAMI, AND STORM SURGE RISK IN THE DELTA AREA

(1) Evaluation of Storm Surge Risk

The risks of storm surges caused by cyclones were evaluated as described below:

- 1) The past and future cyclone data were analyzed. Cyclone Nargis in 2008 landed in the delta area for the longest duration. Approximately, 10% (four or five cyclones per year) of cyclones in the Bay of Bengal land around Myanmar.
- 2) The sensitivity analysis of cyclone traveling routes was conducted. The simulation case of Cyclone Nargis showed the highest water level deviation. The predicted lower pressure of cyclones will cause more severe storm surges.
- 3) Storm surges and tidal waves affect the delta area. Not only storm surges but both should be considered in the plan of countermeasures. The lead time of evacuation for storm surges

is longer than the one for tsunamis. Dissemination of meteorological information including cyclones is important.

(2) Evaluation of Earthquake and Tsunami Risks

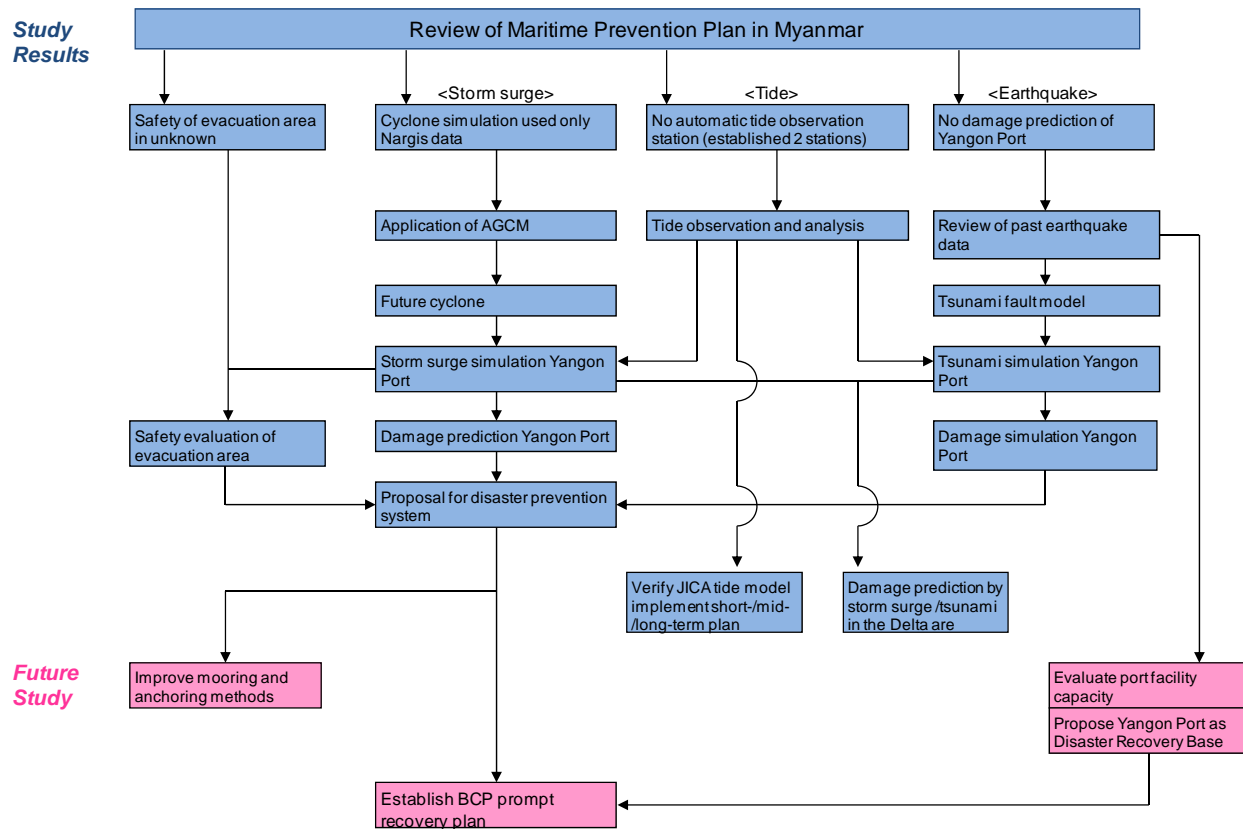
The risks of earthquakes and tsunamis were evaluated as described below:

- 1) There is a possibility of another coupled earthquake and tsunami in the fault of 2004 Indian Ocean Earthquake, Northern Part Structure Line, and West Myanmar Subduction in the Andaman Sea. The maximum strength of earthquakes in the study area was estimated at 9.4 in moment magnitude. The return period was estimated between 90 and 1000 years.
- 2) The tsunami caused by the assumed maximum earthquake was simulated in the delta area. The simulation showed a tsunami height of 4.3 m at the river mouth of the Ywe River, and 3.0 m around the town of Labutta. The tsunami reached the delta area in 30 mins at the earliest.
- 3) In conclusion, the ground floors of the buildings in the wide area of the delta will be inundated in case of assumed maximum tsunami, which will occur in several hundred years. The travel time of tsunami is very short. Early evacuation is necessary especially in the coastline. It is necessary to confirm if people can evacuate to a higher place within the given lead time.

11.9 RECOMMENDATIONS AND SUGGESTIONS TO MARITIME DISASTER PREVENTION PROGRAMME IN MYANMAR

11.9.1 RECOMMENDATIONS AND SUGGESTIONS TO MARITIME DISASTER PREVENTION AND PROGRAMME

The JICA Project Team has prepared recommendations and suggestions to the maritime disaster prevention and reduction in Myanmar which includes several focal points as discussed below. The disaster management system will be recommended.



Source: JICA Project Team

Figure 11.9.1 Study Flow and Recommendation

- It is a prerequisite to establish an appropriate and reliable observation/recording system of natural conditions to prepare countermeasures of disaster reduction based on the appropriate analysis and forecast of future possible disasters.
- It is advisable to add the simulation results and hazard maps of the JICA study into the maritime disaster prevention programme of Myanmar.
- It is necessary to develop knowledge of disaster risk management through reinforcement of soft component parts.

11.9.2 SEMINARS ON MARITIME DISASTER RISK MANAGEMENT

(1) First Seminar

- Date: Wednesday, 25 November 2009
- Place: Parkroyal Hotel, Yangon
- Participants: 80
 - 09:30~09:40: Welcome Address by MPA
 - 09:40~09:50: Welcome Address by IWT
 - 09:50~10:00: Opening Address by JICA-Myanmar
 - 10:00~10:20: Tea Break
 - 10:20~10:50: Basic Synopsis of Disaster Risk Management (Presenter: Mr. Kazuhisa Iwami)
 - 10:50~12:20: Disaster Risk Management in Japan

	(Presenter: Prof. Tetsuya Hiraishi)
12:20~13:30:	Lunch Break
13:30~14:30:	Storm Surge Simulation and Hazard Map for Yangon Port (Presenter: Dr. Masaaki Sakuraba)
14:30~14:50:	Tea Break
14:50~16:20:	Recommendations and Suggestions to Maritime Disaster Prevention Programme (Presenter: Mr. Kazuhisa Iwami)
16:20~16:30:	Closing Address by the JICA Project Team

(2) Second Seminar

- Date: 1st day, 25 January 2011
 - Place: Parkroyal Hotel, Yangon
 - Participants: 114
- | | |
|--------------|--|
| 10:00~10:10: | Welcome Address by MPA |
| 10:10~10:20: | Welcome Address by IWT |
| 10:20~10:30: | Opening Address by JICA-Myanmar |
| 10:30~10:45: | Tea Break |
| 10:45~11:15: | Seminar Summary (Presenter: Mr. K. Iwami) |
| 11:15~12:15: | Case Study of Disaster Risk Management in Japan
(Presenter: Prof. T. Hiraishi) |
| 12:15~13:15: | Lunch Break |
| 13:15~14:15: | Study of Cyclone and Storm Surge Simulation Myanmar
(Presenter: Dr. M. Sakuraba) |
| 14:15~14:45: | Evaluation of Safety Level of Ship Evacuation Area
(Presenter: Dr. M. Sakuraba) |
| 14:45~15:00: | Tea Break |
| 15:00~15:30: | Evaluation of Safety Level of Port Facility and Ships by Storm
Surge
(Presenter: Mr. H. Ushirooka) |
| 14:45~15:00: | Question and Answer Session |
- Date: 2nd day, 26 January 2011
- | | |
|--------------|--|
| 10:00~10:30: | Business Continuity Plan (Presenter: Mr. H. Ushirooka) |
| 10:30~11:00: | Earthquake and Tsunami (Presenter: Mr. S. Sato) |
| 11:00~11:15: | Tea Break |
| 11:15~11:45: | Study of Tsunami Characteristic in Myanmar
(Presenter: Dr. M. Sakuraba) |
| 11:45~12:15: | Damage Estimation by Tsunami (Presenter: Mr. H. Ushirooka) |
| 12:15~13:15: | Lunch Break |
| 13:15~13:45: | Enhancement of Tide Observation System
(Presenter: Mr. K. Iwami) |
| 13:45~14:45: | Case Study of Tide Observation System in Japan
(Presenter: Prof. T. Hiraishi) |

14:45~15:00:	Tea Break
15:00~15:30:	Study Results and Recommendation (Presenter: Mr. K. Iwami)
15:30~16:00:	Question and Answer Session

(3) Third Seminar

- Date: Monday, 15 September 2014
 - Place: Chatrium Hotel, Royal Lake Yangon
 - Participants: 138
- | | |
|--------------|---|
| 09:30~09:50: | Welcoming Address by MPA
Welcoming Address by IWT
Opening Address by JICA Myanmar |
| 09:50~10:10: | Tea Break |
| 10:10~10:40: | Opening Summary
(Presenter: Mr. Kazuhisa Iwami) |
| 10:40~11:25: | 2011 Tsunami in Japan
(Presenter: Prof. Tetsuya Hiraishi) |
| 11:25~12:10: | Future Mitigation for Mega-tsunami in Japan
(Presenter: Prof. Tetsuya Hiraishi) |
| 12:10~13:00: | Lunch Break |
| 13:00~13:30: | Tide Condition in Ayeyarwaddy Delta
(Presenter: Mr. Katsumi Aoki) |
| 13:30~14:00: | Earthquake and Tsunami in Myanmar
(Presenter: Mr. Seiichi Sato) |
| 14:00~14:15: | Tea Break |
| 14:15~14:55: | Tsunami Risk in Ayeyarwaddy Delta
(Presenter: Dr. Masaaki Sakuraba) |
| 14:55~15:35: | Cyclone and Storm Surge Risk in Ayeyarwaddy Delta
(Presenter: Dr. Masaaki Sakuraba) |
| 15:35~15:55: | Closing Summary
(Presenter: Mr. Kazuhisa Iwami) |
| 15:55~16:15: | Question and Answer Session |